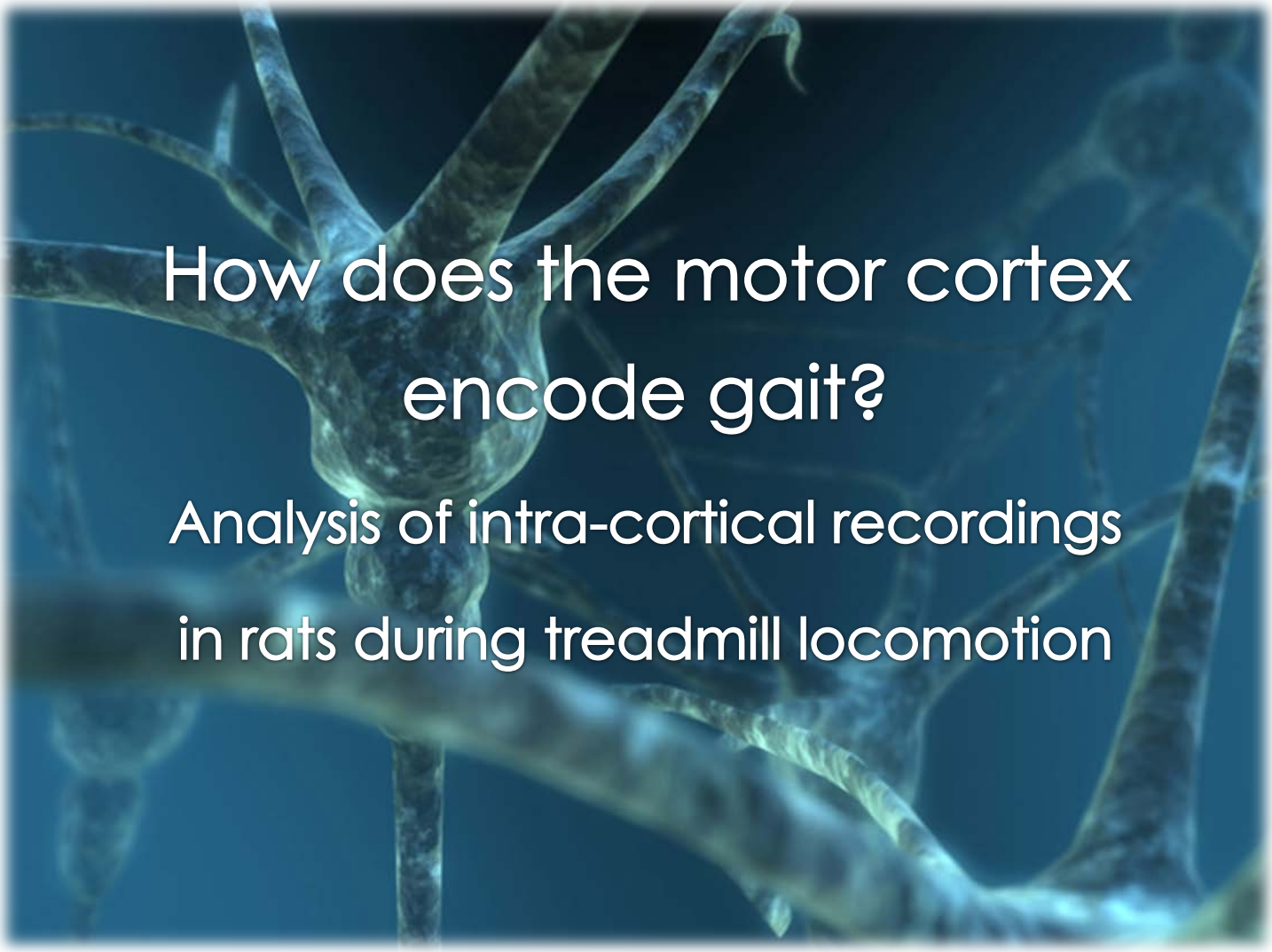

How does the motor cortex encode gait?

Analysis of intra-cortical recordings in rats during treadmill locomotion

Biomedical Engineering & Informatics

Master Thesis | Group 12gr1081

Spring Semester 2012

Jakob Skriver Routhe

Marko Joerg Niemeier

AALBORG UNIVERSITY

AALBORG UNIVERSITY

Department of Health Science & Technology
Frederik Bajers Vej 7D2
9220 Aalborg Ø
Telephone (+45) 9940 9940
Fax (+45) 9815 4008
http://www.hst.aau.dk

Title:
How does the motor cortex encode gait? Analysis of intra-cortical recordings in rats during treadmill locomotion

Theme:
Master Thesis

Project period:
Master Thesis, Spring 2012

Project group:
Group 12gr1081

Members:
Marko Joerg Niemeier
Jakob Skriver Routhe

Supervisor:
Winnie Jensen

No. printed Copies: 4

No. of Pages: 108

No. of Appendix Pages: 17

Completed: 1st of June 2012

Abstract:

Objective: The aim of the study was to investigate the role of the motor cortex in the initiation and end phase of locomotion and the influence of slope during walking.
Method: Ten Sprague-Dawley rats were enrolled in the experiment. In five rats a micro-wire 16 channel electrode array was chronically implanted in the primary motor cortex (M1) and a 4 channel intramuscular fine wire EMG electrode (bipolar) was implanted in the muscles vastus lateralis (VL) and biceps femoris (BF) of the right hindlimb. Over five days, intra-cortical signals (IC) and EMG data were recorded simultaneously with high-speed videography while the rat performed locomotion on a horizontal and inclined treadmill.
Results: The mean motor cortical cell discharge from one channel for all locomotor tasks showed similar shape demonstrating continuity between the curves for two rats. No increase was found in the firing rate between the different locomotor tasks. The EMG amplitude increased significantly in BF muscle during the inclined task compared to horizontal locomotion.
Conclusion: In conclusion, our study suggests that the M1 does not play a major role in the initiation and end phase of locomotion and during inclined locomotion. However, the applied protocol allows a temporal correlation of IC signals, EMG and kinematic parameters that can be used to investigate neuronal activity in relation to muscle activity during gait.

Preface

This report has been composed by the project group 12gr1081, fulfilling the 4^{th} semester of the Master of Science in Biomedical Engineering and Informatics with speciality in Medical Systems at the Institute for Health Science and Technology at Aalborg University, Denmark. This report was created in the period from February 1^{st} to June 1^{st} 2012.

The reference style used in the report is according to the Harvard method, ['Last name' 'Year']. The References are indicated before and after a full stop. If a reference is indicated before a full stop it refers only to the sentence, whereas if it stands after a full stop it refers to the entire section. The references listed in succession are stated in alphabetical order whereby references of the same author are set in chronological order starting with the oldest one: [Armstrong 1986, Drew 1988, Drew 2002]. Figures and tables are numbered with reference to the chapter for example figure 1 in chapter 2 is "figure 2.1". The captions are set below the figures and above the tables.

We would like to thank Jens Sørensen, Ole Sørensen, and Torben Madsen at Pathological Institute at Aalborg Hospital North for the assistance during the animal experiments conducted during the project period. Moreover, we would like to thank our supervisor Winnie Jensen for the technical assistance during the project.

This report is prepared by:

Aalborg University, June 2012.

Marko Joerg Niemeier

Jakob Skriver Routhe

Table Of Contents

Introduction 1

Motor disorders are a group of diseases that impair motor coordination and affect millions of people worldwide [WHO 2006]. The consequences and associated symptoms vary dependent on which part of the motor system is affected, such as primary motor cortex (M1), cerebellum, basal ganglia and spinal cord [Guyton & Hall 2005]. Some of the major pathological contributors of motor disorders are stroke, spinal cord injury and neurodegenerative brain diseases, for example Parkinson [DeLong & Wichmann 2007, Guyton & Hall 2005]. Motor disorders remain a therapeutic problem and improvements in the therapeutic methods are needed [Birbaumer 2006, Jaanis & Wolpaw 2008].

In particular, motor disorders that affect the person's ability to walk have a major impact on the quality of life and are therefore a core issue in the field of movement disorder research. Different rehabilitation strategies have attempted to address this problem, ranging from classical physiotherapy, neuromuscular stimulation methods, pharmacologic treatments and stem cell transplantation [Bahr 2006, Becker et al. 2003]. A relatively novel approach of rehabilitating motor disorders is the use of a brain-computer interface (BCI) which provides a link between the individual and an external device, see figure 1.1. By obtaining neurophysiological signals invasively or non-invasively from the motor cortex in the brain a BCI system can enable the control of for example a prostheses for walking restoration [Kennedy & Bakay 1998].

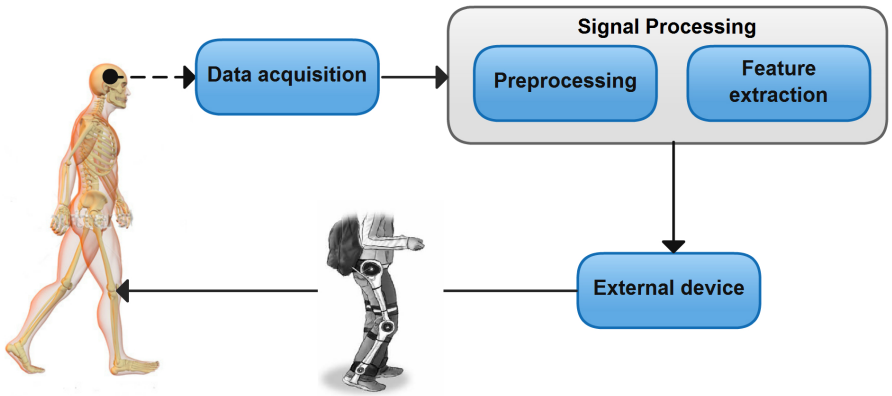

Figure 1.1. The approach of translating brain activity into commands for the control of an external walking device.

The motor cortex plays a crucial role in the planning and execution of voluntary movements [Guyton & Hall 2005]. A BCI system may be a useful tool for patients with paralysis or severe neuromuscular motor disorders because it can restore functionality by bypassing the damaged brain area. Cortical activity of planned voluntary movements can be detected even though natural output pathways of peripheral nerves and muscles are out of function [Wolpaw et al. 2002]. Today, intra-cortical (IC) recordings are one of the primary techniques used to investigate how the brain encodes information about the preparation and coordination of movement [Fitzsimmons et al. 2009, Jensen & Rousche 2005]. Based on single and multiple-unit recordings different studies have shown that the primary motor cortex (M1) is involved in alteration of movement parameters such as direction [Sergio & Kalaska 1997, Taylor et al. 2002] limb velocity [Reina et al. 2001], force [Boudreau & Smith 2001] and individual muscle activity [Kakei et al. 1999, Morrow & Miller 2003].

While different studies have shown the feasibility of BCI for restoring upper limb functionality such as reaching and grasping [Hochberg et al. 2006, Patil et al. 2004] it remains an open question whether a BCI can be used in restoring walking. For example by driving a leg prosthesis, using a exoskeleton or by the use of functional electrical stimulation (FES). One potential explanation for this discrepancy could be that the control of posture and locomotion is a more complex problem than the control of the upper limbs. The fact that the motor cortex is not assumed to play a major role during walking provides another explanation for the deficient research in that area. Walking is mainly accomplished by patterns of muscle activity which are stored in the spinal cord. Nevertheless, animal studies on cats have shown that the motor cortex is involved in the regulation of locomotion in situations which require precise limb control [Drew et al. 2002]. In order to further advance the use of BCI in restoring walking a better understanding of the cortical control regarding timing and coordination of muscle activation during locomotion is necessary. Studies on humans are difficult to accomplish due to ethical considerations and high costs. For this reason animal models are increasingly being used for research on motor disorders [LeDoux 2005]. Among the several potential species of animals such as higher-order primates, cats, mice and rats the majority of animal research has focused on small rodents [LeDoux 2005].

1.1 Initial problem formulation

The overall goal for this project is to obtain a better understanding about the contribution of the motor cortex during the regulation of gait. To achieve this goal the following initial problem needs to be addressed with a thorough literature review:

Understanding of the neurophysiology of gait control in humans and animals. Investigation of different assessment methods to analyse gait control and the use of animal models for research of gait control and motor disorders.

The report is divided into three major parts: I Problem analysis, II Problem solution and III Synthesis. The problem analysis will focus on answering the initial problem and is followed by a summary which is leading up to the project hypothesis. The problem solution contains the solution strategy and the implementation of the experimental protocol. Finally, in the synthesis methodological choices and results are discussed, followed by a conclusion.

PART

Problem Analysis

Neurophysiology of gait control 2

Locomotion is the ability of humans and animals to change location and occurs in different forms such as walking, trotting, galloping, swimming and flying. The motor system is able to perform three different types of motor tasks; rhythmic, reflex (involuntary) and voluntary. All forms of locomotion are characterized by some sort of rhythmic alternating activity of opposing limbs. Due to the simple repetition of the same movements, locomotion appears as an autonomous stereotyped action which does not involve higher brain structures. However, under natural conditions locomotion takes place in an environment with changing terrains and unexpected occurring events. Therefore permanently adjustment of the motor patterns to the actual surrounding is necessary. This chapter will focus on gait control which is defined as locomotion on solid substrate. Today most of the information about walking is based on animal studies rather than on human studies. In order to understand the neurophysiology of gait control the analysis is divided in cortical, spinal and peripheral level, see figure 2.1. [Kandel et al. 2000, Rosenbaum 1991]

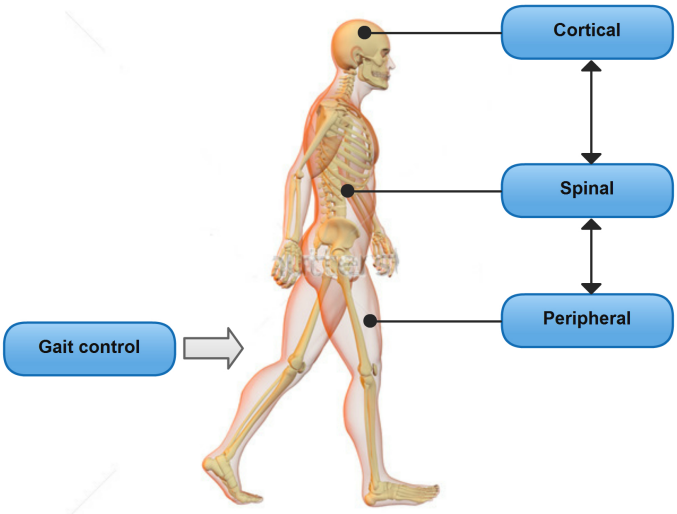

Figure 2.1. Overview of the parts of the motor system that are involved in gait control; cortical level, spinal level and the peripheral level.

2.1 The gait cycle

The implementation of gait is a complex process which involves time dependent activation and deactivation of different muscles in the leg. The terminology used to describe the various phases and footfall patterns in the gait cycle varies in the literature and is different between species. However, in principle the gait cycle can be divided into two main phases; swing phase and stance phase. The stance phase occurs when the foot is in contact with the ground and corresponds to around 60 % of the total gait cycle duration. The swing phase occurs at the time the foot is lifted from the ground and corresponds to around 40 % of the total gait cycle duration. [Kandel et al. 2000]. The gait cycle of quadrupeds and humans is very similar and can be subdivided into the following four phases (Figure 2.2):

- **Flexion (F):** Initially, the swing phase starts with a flexion at the hip, knee, and ankle.
- **1st extension (E_1):** About half way through the swing phase the ankle and the knee extend although the hip is still flexed. Subsequently, due to the extension at the ankle and the knee the foot is actually moved ahead of the body, thereby preparing the leg for the upcoming weight as soon as the foot hits the ground.
- **2nd extension (E_2):** When the foot gets ground contact weight of the body is transferred to the leg causing a combination of flexion in the knee and the ankle joints, and strong contraction of the extensor muscles occurs. Latter mentioned muscles show yielding properties in this early phase of stance which is important to allow the body a smooth and efficient gait.
- **3^{ed} extension (E_3):** The forward movement of the body is established during the late phase of stance by producing a propulsive force through mutual extension of the hip, knee, and ankle.

[Kandel et al. 2000]

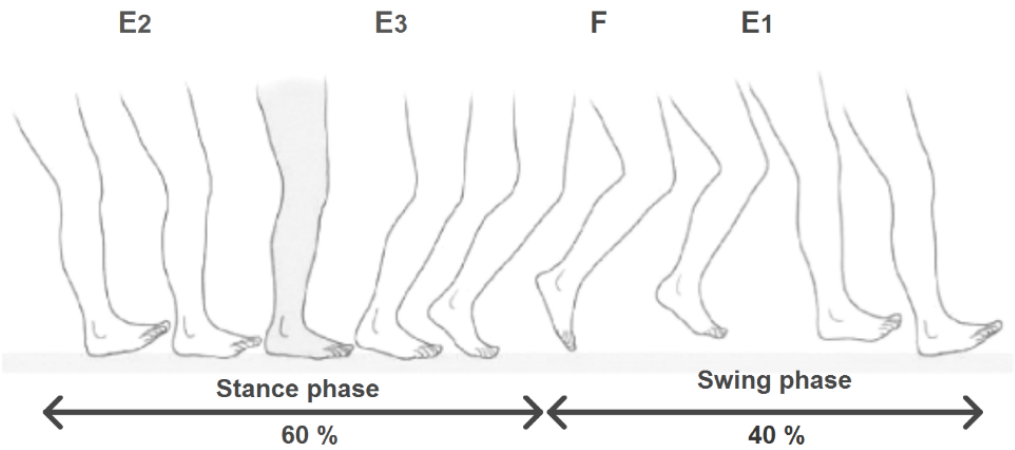

Figure 2.2. Phase E_2 and E_3 happen during the time the foot is in contact with the ground (stance phase) when leg is pushed down in order to actuate the body. The phases F and E_1 occur during the time the foot is off the ground (swing phase) when the leg is retracted and pulled in moving direction toward the next footfall. [Kandel et al. 2000]

2.2 Gait control at the spinal level

Several different animal studies have been conducted in the past in order to explain the control of stepping in mammals. One of the first investigators in that field was Charles Sherrington who found out that cats are still able to produce rhythmic movements with their legs when the spinal cord is severed [Sherrington 1906]. T. Graham Brown went a step further than Sherrington [1906] by cutting also the dorsal root of the spinal cord which implies the elimination of any sensory feedback from the muscles to the spinal cord. Even after this fatal spinal cord injury rhythmic bursts of reciprocal activity in flexor and extensor motor neurons of the hind legs could be produced [Brown 1911]. However, it could also be observed that the total speed of locomotion decreases in animals whose spinal cord has been separated from the brain [Carew 1985]. A study by Taub & Berman [1968] on monkeys with deafferented limbs on both sides suggests that sensory feedback might not be necessary for locomotion, but it is appropriate for accurate movement execution. In humans, it is known that people suffering from tabes dorsalis, a disease which affects the dorsal roots of the cortex, have difficulties in walking normally [Kalat 1980].
These observations lead to the following conclusions:

- No input is needed from the brain for producing stereotyped actions like walking.
- The basic rhythm for walking is produced by neural circuits located in low levels of the nervous system, e.g. the spinal cord.
- No sensory input is needed for the production of rhythmical gait patterns.
- Sensory information from peripheral receptors is necessary to modify motor patterns for locomotion movements with respect to environmental conditions.

[Kandel et al. 2000]

The production of motor patterns

In accordance with his observations Brown [1911] suggested the existence of two systems of neuron types, called half-centers, which each control the contraction of either flexor or extensor muscles. The half-centers have the property of mutually inhibiting each other depended on fatigue in the inhibitory connections which results in rhythmic changes of activity.
Following studies with cats, using different excitatory drugs alone or in combination with electrical stimulation supported Brown [1911] half-centres hypothesis. Bursts of activity were found either in flexor or extensor motor neurons or as short sequences in a rhythmic reciprocal manner.
Unfortunately, concrete information about neural circuitry and principles of the rhythm generating system in the mammalian spinal cord is missing because of the high complexity of this nervous system. However, more is known about the principles of rhythm generators in invertebrates and lower vertebrates as the lamprey. The neural networks which are responsible for the production of rhythmic motor patterns even when sensory feedback is missing, are named central pattern generators (CPG).[Kandel et al. 2000]

Central Pattern Generators (CPG)

CPGs have been detected in several rhythmic motor systems such as walking, swimming and respiration. The generation of rhythmic motor activity in absent of sensory input depends on three points: (1) cellular characteristics of each nerve cell within the network, (2) characteristics of the synaptic junctions between neurons, and (3) the structure of interconnection between neurons.
Basic components of a CPG are endogenous bursters. These spontaneously active bursters can be a motor neuron by itself or a drive for motor neurons. Endogenous bursters exist in locomotor systems but they need to be controlled in some way in order to be affective in this sequential working system. This task belongs to so called neuromodulators, which also modify the cell behaviour for instance in matters of depolarization time. They can vary from short depolarization (bursts) over to maintained depolarization (plateau potential).
Besides the firing duration of neurons, the production of rhythmic patterns requires also time-dependent processes of increased or decreased activity within the neuronal network. An example of a time-dependent process is synaptic depression which describes a delay in excitation after a depolarization occurred.
Several CPG's are also able to produce complex temporal patterns of activity of various groups of motor neurons. Two simple forms of sequential controlled motor patterns are mutual inhibition, where neurons fire out of phase with each other and mutual excitation which implies synchronous firing of neurons. [Kandel et al. 2000]

2.3 Gait control at the peripheral level

Sensory input from peripheral receptors is necessary to adapt gait pattern to the current terrain or spontaneous occurring events. Thereby, three kinds of information sources can be distinguished: somatosensory input from muscle and skin receptors, vestibular input from the apparatus which controls the balance and visual input. According to Sherrington [1906] somatosensory input is provided from proprioceptors, located in muscles and joints and exteroceptors, located in the skin. Proprioceptive feedback is associated to body movements and comes from Golgi tendon organs and muscle spindles in extensor and flexor muscles. There are three known excitatory pathways which send signals from extensor sensory fibres to extensor motor neurons: a monosynaptic pathway from Ia fibres, a disynaptic pathway from Ia and Ib fibres and a polysynaptic pathway which includes the extensor half-centers of the CPGs. The latter pathway controls besides the grade of activity also the length of the stance period (On figure 2.3 the descending motor pathways are illustrated).
Exteroceptors are associated to the adjustment of gait according to external stimuli for instance to overcome obstacles. The stumbling-corrective reaction in cats displays a well-studied example concerning these kinds of receptors. An interesting feature of this example is that the same stimulus (touching dorsal part of the paw with a rod) applied at different phases during the gait cycle evokes different reactions. A flexion movement is evoked when the paw is touched during the swing phase but a extension movement is evoked when the same stimulus is applied during the stance phase. The stumbling-corrective reaction is phase-dependent meaning that identical stimuli excite different groups of motor neurons in relation to the time [Forssberg et al. 1975]. Interestingly, similar observations have been made in humans during walking or standing [Nashner et al. 1979].

2.4 Gait control at the cortical level

After reading the previous sections the question arises which role the brain plays for the control of walking. The involvement of the human brain during posture was investigated in an experiment in which subjects were asked to stand on a platform which could perform different forms of displacement [Nashner et al. 1979, Nashner & McColluma 1985]. Two different reflex responses could be elicited, one inducing destabilization in posture and the other one stabilization in posture. It was found that reflexes which led to a destabilization in posture were somehow attenuated. This observation might be due to an regulation process controlled by the brain because patients with damage to the cerebellum or the vestibular system are less able suppressing reflexes. Furthermore, the correction of posture due to disturbances requires the activation of muscle groups, also called muscle synergies. Muscle synergies have been shown to be activatable under experimental conditions by electrical stimulation of the motor cortex [Humphrey 1968].
It has been shown that neurons in different brain regions like the motor cortex, the brain stem and cerebellum are rhythmically active during locomotor activity. However, it seems that each region is responsible for different tasks in the modification of locomotor function (On figure 2.3 the descending motor pathways are illustrated).

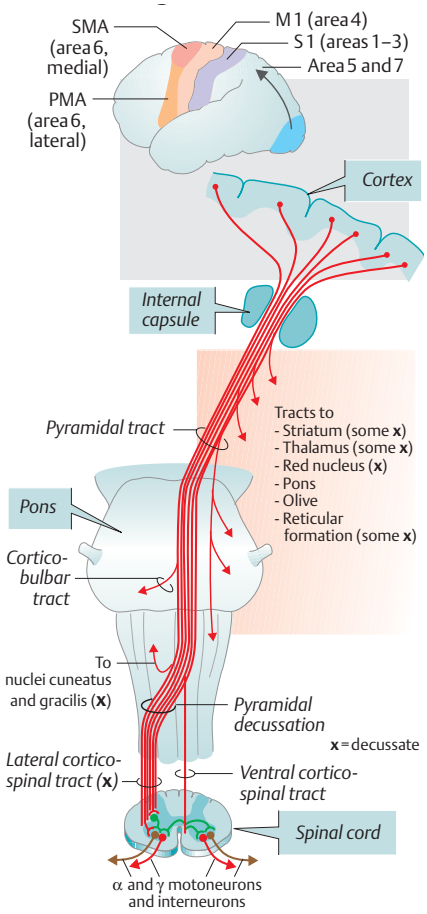

Figure 2.3. The descending motor pathways. Showing the supplementary motor area (SMA), premotor cortex (PMA), the primary motor cortex (M1), the primary somato-sensory cortex (S1). [Despopoulos & Silbernagl 2003]

Kandel et al. [2000] distinguishes three locomotor systems that needs to be controlled: (1)initiation of locomotion and regulation of speed, (2) adjustment of motor patterns with respect to sensory feedback and (3) modification of limb movements in response to visual input.
In cats it was shown by Shik et al. [1966] that the initiation of walking and walking speed can be controlled by applying tonic electrical stimulation to the mesencephalic locomotor region. Interestingly, the pattern of locomotor activity is not related to the pattern of the electrical stimulus but rather to its intensity. With higher stimulation strength and increasing speed of the treadmill the gait pattern changes from walking to trotting over to galloping. Shifts in gait patterns are most likely controlled by local circuits in the spine because they were also observed in animals whose spine was transected at lower thoracic level.[Shik et al. 1966]

The same principle of adoptable gait pattern can also be observed in humans. While normal walking implies that both feet are on the ground, during running one foot has ground contact [Alexander 1984].
Resent conclusions about identifying the descending pathways which are responsible for the initiation of locomotor activity come from studies in the lamprey and neonatal rat. Locomotion could be initiated by delivering glutamate receptors agonists. Also in the decerebrate cat the application of agonists that bind to glutamate receptors in the spinal cord evoke an initiation of gate. However, no locomotor activity was seen when glutamate receptor antagonists were delivered and the mesencephalic locomotor region was stimulated. [Kandel et al. 2000]
In rats the control of posture is indicated by the amount of dopamine in the caudate nucleus. Dopamine is produced in the substantia nigra, a brain structure located in the midbrain. An dysfunction of the substantia nigra can cause Parkinson symptoms. The amount of dopamine increases or decreases depending on the level of lateral and vertical curvature of the treadmill. [Freed & Yamamoto 1985]

The role of the motor cortex during gait

Several studies exist on cats investigating the role of the motor cortex during locomotion by recording activity from pyramidal tract neurones (PTN) with chronically implanted micro-wire electrodes [Armstrong & Drew 1984, Armstrong 1986, Widajewicz et al. 1994]. In general all do agree on the fact that the motor cortex plays a facultative rather than an obligatory role during locomotion. However, it seems to be important in the control of precise walking, for example on a horizontal ladder [Armstrong 1986].
Armstrong & Drew [1984] identified 93 PTNs in a total amount of 165 single neurones. When walking on a treadmill with modest speed (50 cm/s) more than half of the single identified cells (56 %) showed an increased discharge frequency than at rest. Further, about 80 % demonstrated a time-locked modulating behaviour in accordance to the step-cycle. [Armstrong & Drew 1984]
Another study by Widajewicz et al. [1994] carried out on cats indicated that the motor cortex influences the control of hindlimb trajectory when overcoming obstacles attached on a treadmill belt, see figure 2.4. 63 from 72 identified PTN in the M1 were found to be representative for the hindlimb area. 67 % of them turned out to have significantly increased characteristic discharge patterns correlated to hindlimb trajectory during voluntary adjustments of the locomotion cycle. Discharge patterns were different whether the corresponding hindlimb was leading or trailing when stepping over the obstacle but also

during the stance phase and swing phase.[Widajewicz et al. 1994]

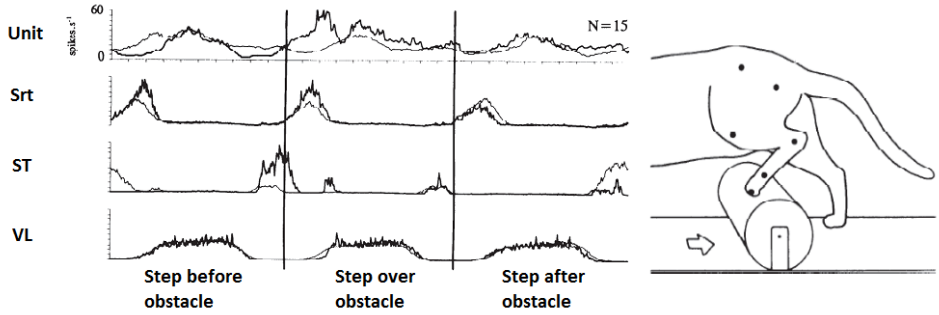

Figure 2.4. Averaged neuronal activity (N = 15) and EMG activity from the three hindlimb muscles flexor sartorius (Srt), semitendinous (St) and vastus lateralis (VL). The thinner line indicates signals from normal treadmill walking while the thicker line indicates when the cat is stepping over the obstacle. [Widajewicz et al. 1994]

A potential explanation of the increased discharge frequency could be that the motor cortex is involved in visuomotor coordination. The visual perception of an upcoming obstacle is supposed to cause modulation in the activity of motor cortex neurons. Studies investigating experimental lesion of the motor cortex have shown that walking is impaired in tasks that require visuomotor coordination such as stepping over obstacles or walking on rungs of a ladder.[Kandel et al. 2000]

The activity of PTNs was also shown to be dependently active during postural control while standing and walking on an inclined plane. In both motor tasks the cat was placed on a treadmill which was either standing still or moved (speed: 50 cm/s). The treadmill was periodically tilted between ± 15° to the left or to the right side, see figure 2.5.

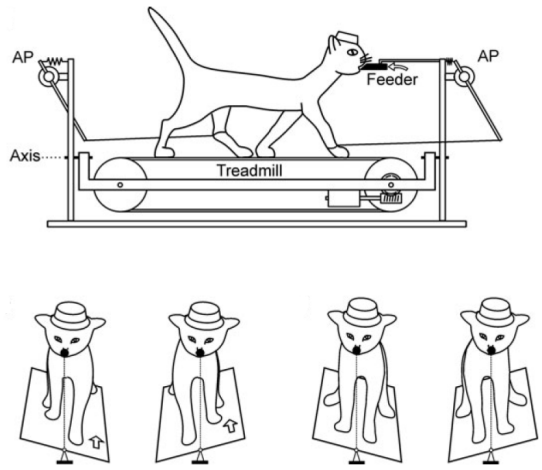

Figure 2.5. Experimental design of the cat walking on a moving treadmill belt inclined to the right or to the left [Karayannidou et al. 2009].

From 121 identified hindlimb PTN's 47 % showed a static response to tilt during standing and 63 % showed a positional response to tilt during walking. The observed increase in magnitude of activity suggests that about half of the identified PTN's contribute to the participation in

the maintenance of postural during standing or adaptation of walking on an inclined surface. [Karayannidou et al. 2009]

A recently published study of Fitzsimmons et al. [2009] has shown that neural activity modulates in relationship to the gait cycle in both M1 and S1. The study was conducted on monkeys which were trained to walk bipedally, see figure 2.6. Based on IC recordings obtained from multiple micro-wire arrays it was observed that the firing rate for each neuron peaked at a particular phase of the gait cycle. It was possible to extract bipedal walking patterns which in turn could be used to predict leg kinematic and EMG. Fitzsimmons et al. [2009] concluded that the observed involvement of the cerebral cortex during gait is due to a higher demand on the walking task, in this case bipedal walking, which is in agreement with Armstrong [1986]. As a long term goal it is proposed that IC recordings from M1 and S1 may be utilized for BMI application to restore walking in people suffering from paralysis.

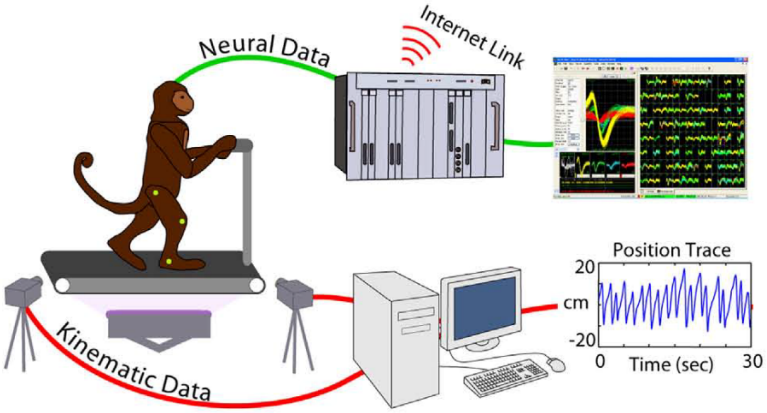

Figure 2.6. Illustration of the the bipedal walking setup conducted on monkeys, consisting of a custom modified, hydraulically driven treadmill; wireless, 2-camera tracking of kinematics; and a MAP neural acquisition system.[Fitzsimmons et al. 2009]

Methods for assessment of gait 3

Various methods exist to assess gait in humans and animals, see figure 3.1. This chapter will focus on methods for measuring cortical activity, muscle activity, kinetics and kinematics of movement.

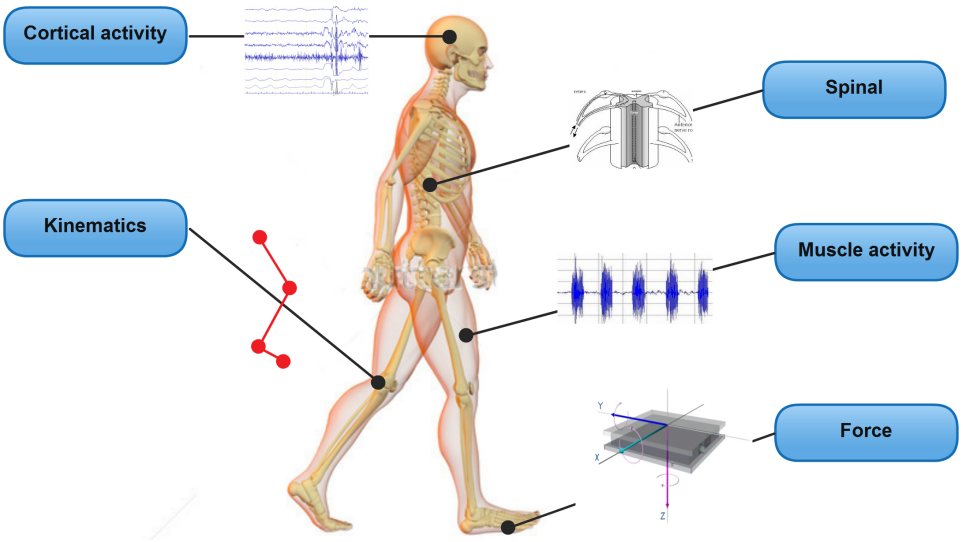

Figure 3.1. Overview of the various methods to assess gait.

3.1 Cortical activity

The neuronal task of transmitting information is mainly realized by synapses and action potentials, revealed as electrical activity. The receptor activation may have either an excitatory or inhibitory effect on the membrane site, thus excitatory or inhibitory postsynaptic potentials, depending on what ions they increase the permeability to. These potentials are the most representative electrical activity that can be recorded from the scalp.

Electroencephalography (EEG)

Electroencephalography (EEG) is a medical imaging technique that reads electrical activity from the scalp generated by large neural populations. This makes it feasible to detect voluntary

intention, visual stimuli and alteration in brain activity correlated to cognitive states [Lebedev & Nicolelis 2006]. The obtained electrical activity is a summation of excitatory and inhibitory postsynaptic potentials, coming from neurons situated in the most superficial areas of the cerebral cortex [Misulis & Head 2003].
A typical adult human (age 20-60) EEG signal is about 10 μV to 90 μV in amplitude and range between 6 to 13 Hz when measured from the scalp [Aurlien et al. 2004]. Measuring EEG is a completely non-invasive procedure that can be applied repeatedly to patients, normal adults, and children with virtually no risk or limitation. Typically clinical use of EEG are to diagnose epilepsy, brain death, encephalopathy or monitor anaesthesia. In research EEG is used in neuroscience, psychophysiological research and cognitive science and psychology. However, the technique provides only a low spatial and temporal resolution compared to invasive recordings due to an overlap of information coming from multiple cortical areas. Further, the electrical signals coming from deeper regions like basal nuclei cannot be distinguished due to their small amplitude compared to the ones generated by the most superficial layers. [Misulis & Head 2003]

Electrocorticography (ECoG)

Electrocorticography (ECoG) also known as intracranial EEG (iEEG) is a method to record electrical activity using electrodes placed directly on the exposed surface of the cortex. In order to do so a craniotomy has to be performed to assess the brain surface and place the electrode grid. Compared to EEG, ECoG has the advantages of being far less contaminated by noise and more spatially specific because of smaller electrodes. Further the frequency resolution is better due to its proximity to the neural tissue.[Sanchez & Principe 2007]

Intra-cortical brain signals (IC)

Cortical signals can also be obtained with invasive techniques. By implanting single electrodes or electrode arrays directly in the cortex, neural activity can be recorded from single neurons, one at a time or simultaneously from multiple neurons. Due to the direct interface between electrode and cortex the signals provide a high spatial resolution and the use of micro-wire electrode arrays allow to monitor the activity of large populations of neurons distributed over various cortical areas. However, the necessity of the invasive surgical procedure leaves a risk of infections, making the technique not as practical as EEG. Electrode arrays allow the collection of a big amount of data in short period of time and reveal temporal dynamics between neural populations when looking [Churchland et al. 2007]. Jensen & Rousche [2005] used a 16-channel tungsten micro-wire array (50 μm diameter, spacing approx. 500 μm blunt tips) directly placed in the M1 of a rat to measure neuronal activity from multiple units in the forelimb area during a paddle press task. The array was embedded to a depth of approx. 1.7-1.8 mm in order to hit Layer V and VI. [Jensen & Rousche 2005]

Fitzsimmons et al. [2009] have demonstrated that kinematics of bipedal walking rhesus macaques can be predicted from IC recordings obtained from chronically implanted micro-wire arrays. Multiple micro-wire arrays were implanted differently in two monkeys in various cortical areas based on previous mapping studies. The size of the arrays ranged from 32 to 64 electrodes. The stainless steel micro-wires were spaced 1 mm apart from each other ranging in diameter from 40 to 60 μm. Further, double-layer implants were used whereby one layer was 300 μm deeper

than the other, see figure 3.2.

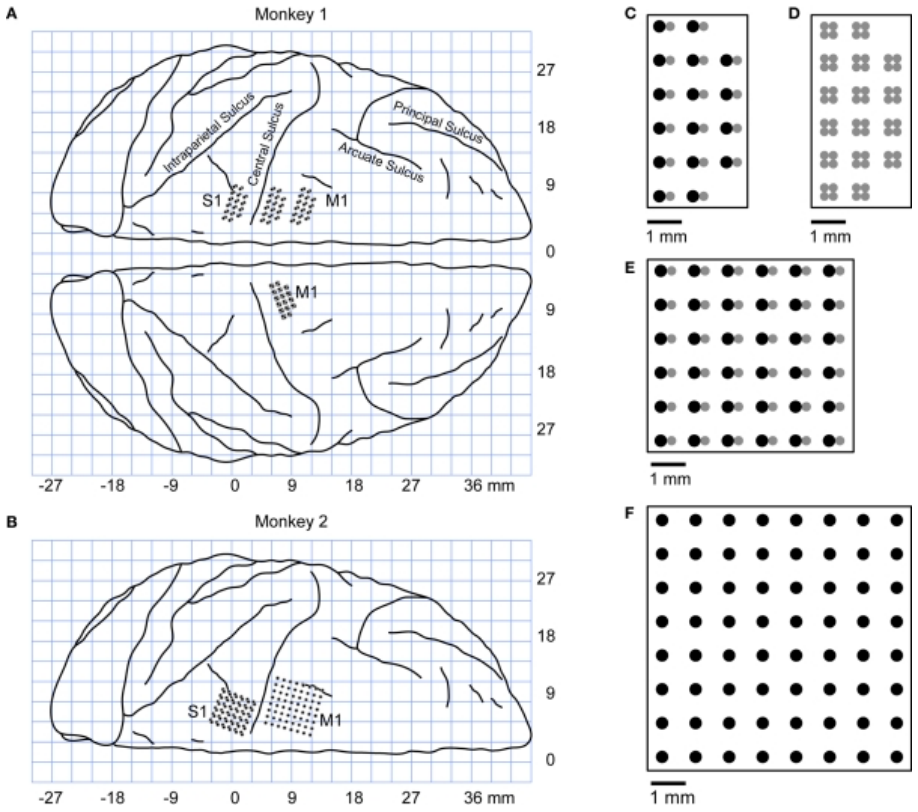

Figure 3.2. Outline of the locations of the implants and the used micro-wire arrays. **(A)**: In monkey 1 micro-wire arrays were implanted in both hemisphere, in the left M1 and S1 and in the right M1. **(B)**: In monkey 2 micro-wire arrays were implanted only in one hemisphere in M1 and S1. The different colours of the arrays **(C-F)** indicate multi-layer configurations whereby each shaft consisted of two **(C,E)** or four **(D)** micro-wires with different lengths (layer difference: 300 μm). [Fitzsimmons et al. 2009]

A drawback of micro-wire electrode arrays for measuring single- or multi-neuronal activity is their stability in recording from the same population of neurons over a period of time. Muthuswamy et al. [2005] have developed a three channel microactuated micro-wire electrode array which allows precise bi-directional positioning (step resolution 8,8 μm) of each individual electrode within the brain tissue after implantation. The used thermal microactuators enable the array to move linearly up to 5 mm linear in a direction. Single unit recordings were acquired from the somatosensory cortex from an adult rat over a time period of three days demonstrating that the technology is feasible to be applied in deep brain structures of rodents.

3.2 Muscle activity

In the human motor system the contraction of muscles is hierarchically controlled by the central motor system and the principle of the motor unit (MU). In voluntary contraction, force is modified by a combination of MU recruitment and changes in MU activation frequency. For instance for a long muscle contraction, active MUs will increase their rate of firing and previously inactive MUs will be recruited [John W. Clark & Neuman 1998]. Besides the force also the speed of contraction is dependent on MU recruitment and firing frequency. When MUs with a low threshold are recruited the muscle contraction is characterized by low force-generating capabilities and high fatigue resistance. On the other hand if a movement requires greater force and/ or faster contraction MUs with a high threshold are recruited. [Moritani et al. 2004]

Electromyography (EMG)

Electromyography (EMG) is a recording of electrical signals produced by muscle contraction which means that these signals can be measured with the use of transducers that convert an ionic current to a current of electrons [John W. Clark & Neuman 1998]. The amount of the recruited MU and their average firing frequency define the electrically activity in a muscle which at the same time are the relevant factors for the exerted muscle force. This suggests a direct relation between the measured EMG signal and the exerted force. [Moritani et al. 2004] Measured EMG signals are normally in the range from less than 50 μV up to 20-30 mV depending on the muscle under observation. The firing rate of the MUs is about 6-30 Hz. EMG can be measured by using intramuscular and surface electrodes which are explained in the following. [John W. Clark & Neuman 1998]

Surface EMG (sEMG)

Surface electrodes give an overview of activation during a task from superficial muscles. This implies that they are sensitive to electrical activity over a wide area so that the recordings can be somewhat affected by crosstalk but also the movement of the electrode. Crosstalk is an interference of unwanted signals coming from nearby muscles and can to some extend be reduced by filtering. Nevertheless, this can be difficult and it may distort and affect the quality of the EMG signal. To achieve a good signal transmission, the stratum corneum can be removed which is the outer-most layer of the skin and consists mostly of dead skin cells. This layer works as a semipermeable membrane to ions, which means that there will be a difference in the ionic concentration across the membrane and a difference in potential. Therefore, if the effect of this layer can be reduced, the connection to the electrode will be more stable. To further improve the electrical contact between the electrode and the skin an electrolytic gel is used to maintain proper electrical contact. This means, there are two interfaces; an electrode-electrolyte interface and a skin-electrolyte interface. A way of bypassing one of these interfaces is to implant the electrodes directly on the muscle under the skin. This has been demonstrated by Schumann et al. [2006] which used two subcutaneous arrays to investigate the myoelectrical activity in the vastus lateralis (VL) and the biceps femoris (BF) of the healthy mouse. By using two arrays with four monopolar EMG channel each, it was possible to clearly characterize the activity patterns and thereby the function of each muscles during normal gait, see picture 3.3. [John W. Clark & Neuman 1998]

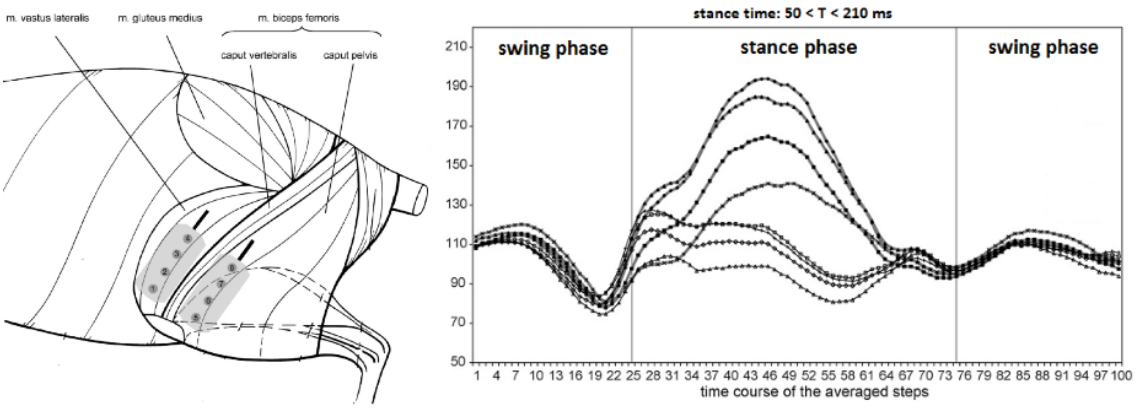

Figure 3.3. Averaged time course of the monopolar EMG-activity (RMS - root mean square) of 1985 normalized gait cycles. The vertical line at marker 25 and 75 indicates touch down and lift off, respectively. Vastus lateralis muscle - fat grey lines (in the top during stance phase); biceps femoris muscle - black thin lines (in the bottom during stance. [Schumann et al. 2006]

Intramuscular EMG (iEMG)

Intramuscular EMG (iEMG) is used to record local activity from only a few muscle fibres deeper in the muscle as opposed to the overall information when using sEMG. This means that crosstalk is avoided but the overall picture of the behaviour of the muscle is lost. iEMG electrodes have the advantage that they do not have to contend with electrolyte-skin interface as it is the case for sEMG. Instead, the behaviour of the electrode is only determined by the electrode-electrolyte interface. The present extracellular fluid surrounding the electrode maintains this interface. Different studies have demonstrated the feasibility of implanting stainless steel micro-wire electrodes in the hindlimb of mice to record appropriate EMG signals, see figure 3.4 [Gillis & Biewener 2001, Pearson et al. 2005]. The micro-wire leads have also the advantage of minimizing the surgical damage to the muscles and the mechanical influence on the gait pattern. [Pearson et al. 2005]

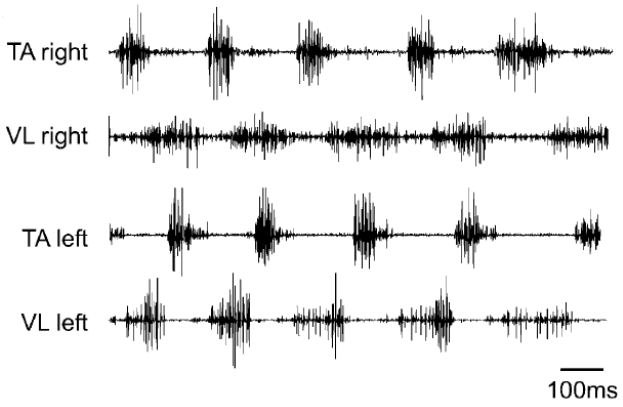

Figure 3.4. Examples of intramuscular EMG recordings from hind leg muscles tibialis anterior (TA) and Vastus Lateralis (VL) in mice [Pearson et al. 2005].

3.3 Kinematics and kinetics

When analysing gait by looking at the limb kinematics or measuring force dynamics no biological signals are obtained directly from the individual. Thus, no physical device does necessarily have to be in contact with the individual for signal transmission thereby minimizing the behavioural influence.

Video Kinematics

The most common way to analyse gait is with the use of video capture technology. Depending on the dimension that is needed videos can be recorded by either 2-D or 3-D analysis [Thota et al. 2005]. 3-D analysis is more complex since more than one camera is needed. In animal studies with rodents a transparent encapsulation of treadmills is most commonly used. The placement of the camera depends on the required information. Cameras can be positioned lateral to the encapsulation or under the encapsulation (2-D analysis). Joint measures are captured from lateral view with markers placed on the joints. Using automatic detection software the position and joint angles can be calculated for each video frame [Pearson et al. 2005, Thota et al. 2005].

Kinetics - Pressure recordings

Gait analysis can also be assisted by the measurement of force dynamics (e.g. velocity, coordination, duration, vertical reaction forces) of the individual paw stance phases [Schumann et al. 2006]. This can be achieved for instance by the use of a CatWalk analysis system (Noldus Information Technology) [Technology 2012]. The apparatus consists of a glass plate (walkway) and an encased fluorescent tube placed alongside the distal long edge of the glass. The tube is placed so that the light enters into the glass from the edge and thereby will be completely internally reflected in the glass. When the rat walks on the glass plate the light leaves the glass and illuminates the paw instead, making the places of contact visible, see figure 3.5. In a darkened environment the images of the paw prints can be recorded with a video camera located under the walkway. The intensity of the illumination is related to pressure/ weight support. [Hamers et al. 2006, Neumann et al. 2009]

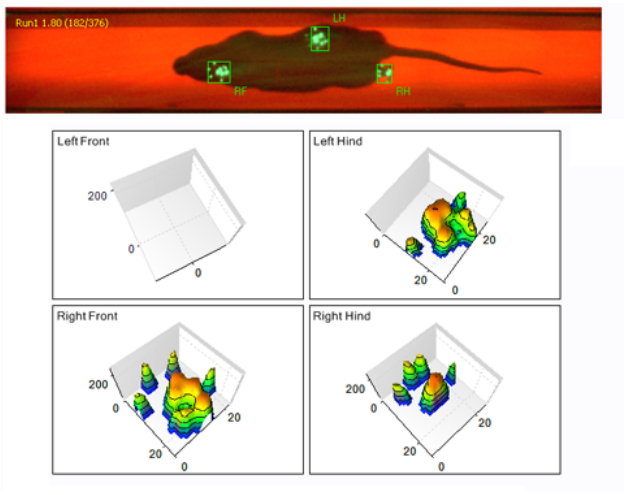

Figure 3.5. Gait analysis with CatWalk system (Noldus Information Technology). [Technology 2012]

The rat as a model of human gait 4

Animals are commonly used in scientific research for the investigation of pathological conditions in humans due to the risk of causing harm to an actual human and other ethical issues. Choosing an appropriate animal model describes a trade-off between high resemblance to the human and simplification of its complexity. Therefore, the individuals can range from higher-order primates over to rats and even worms. The judgement of the choice of model is traditionally also done by the two criteria reliability and validity, see table 4.1.
The laboratory rat (Rattus norvegicus) though has been used over the years in many experimental studies because it shows similarities with the human regarding anatomy and physiology which will be explained in the following sections. Further, these kinds of rodents have fairly homogenous strains and are easy to monitor during experiments making them in general less expensive. [Kolb & Tees 1990, LeDoux 2005]

Table 4.1. Criteria for judging animal models. [LeDoux 2005]

Criteria	Definition
Reliability:	Refers to the ability of the model to provide consistent results under different conditions.
Validity:	Refers to the conceptual framework underlying the model. • **Face validity:** The model exhibits a motor syndrome that meets typical criteria used to define the syndrome in humans. • **Etiologic validity:** The model was derived from a cause known to cause the motor syndrome in humans • **Predictive validity:** The model predicts a key feature of the human motor syndrome, such as response to treatment

4.1 Cortical structure of the motor cortex

The organisation of the motor system in humans and rats have some differences and cannot directly be compared, see figure 4.1. When looking at the human motor cortex three main components can be distinguished: primary motor area (M1), premotor area (PMA) and supplementary motor area (SMA). In comparison rodents have two cerebral regions which are related to motor function: the rostral forelimb area (RFA) and the caudal forelimb area (CFA). A comparison study between rodents and primates identified the RFA as analogue to M1 and

showed resemblance of the CFA to PMA and SMA. [Kolb & Tees 1990, Nudo 2007]

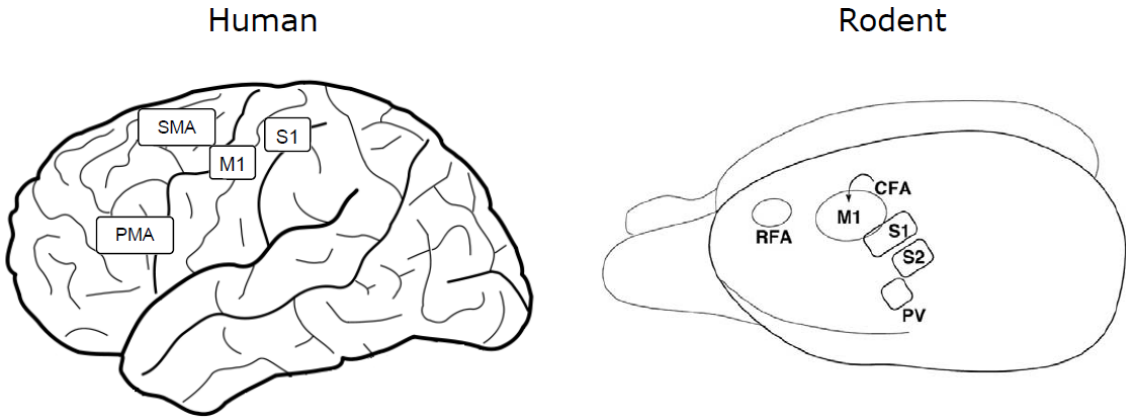

Figure 4.1. Brain of a human and a rodent. Human cortex with primary somatosensory cortex (S1) and primary motor cortex (M1), premotor area (PMA) and supplementary motor area (SMA). Rodent cortex with the motor areas RFA and CFA and the primary (S1) and secondary (S2) somatosensory areas and the parietal ventral somatosensory area (PV). Modified from [Neafsey et al. 1986].

It is well known that the human M1 has a somatotopic organization which implies that each parts of the body is represented within a specific location, see figure 4.2. Starting with the leg in the most medial location followed by the hand and finally the face in the most lateral location.

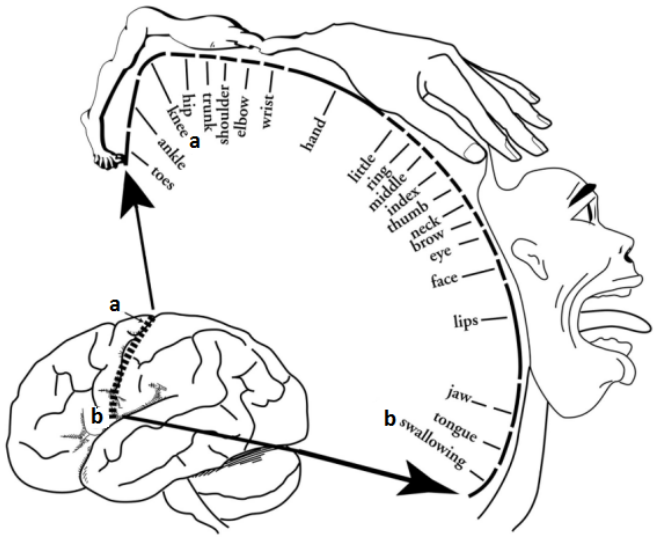

Figure 4.2. Somatotopic organization of the primary motor cortex (M1). Each part of the body is represented within a specific location.[Guyton & Hall 2005]

However, in rats not such a clear discrimination of the distinct body party was found [Neafsey et al. 1986]. One problem is that the mapping results differ between the individual rats, see figure 4.3. On the other hand one problem is that parts of the motor cortex and the primary somatosensory cortex (S1) overlap [Giovanni & Lamarche 1985]. This applies in particular for the hindlimb representations and partially for the forelimb representations [Neafsey et al.

1986]. Despite this the cortical structure of rats seems to be simpler than that of humans which makes it appropriate for neuroscience research.

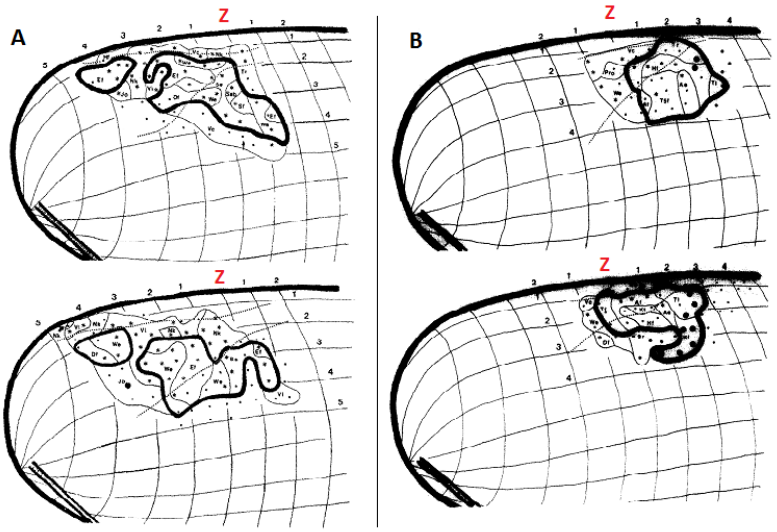

Figure 4.3. Somatotopic organization of the motor cortex for the forelimb and the hindlimb (heavy lines) in two different rats. **A**: Forelimb representation, **B**: Hindlimb representation. Each square grid equals 1mm in square, the red *Z* denotes bregma. [Neafsey et al. 1986]

4.2 Anatomy of the corticospinal tract

The corticospinal tract is the main pathway in both humans and rodents which transmits motor signals directly from the cerebral cortex to spinal cord motor neurons (See figure 2.3). In both species the corticospinal tract originates from layer V pyramidal cells in the cerebral cortex. The majority of corticospinal neurons are located in a large contiguous area of frontoparietal cortex associated with M1 and S1. However, a comparison study has shown that the total number of corticospinal fibers per unit brain weight or body weight is substantially greater in primates in relation to rodents indicating a greater volume of white matter. Further, in primates the exact origin of corticospinal neurons is located in the ventral PMA while it is the RFA in rodents. [Nudo 2007]

4.3 Gait control

The coordination of posture and gait in vertebrates like humans and rodents is supraspinal controlled by the CPG in the spinal cord. The supraspinal network of quadrupeds is preserved in humans but further developed to bipedalism [Jahn et al. 2008]. Therefore the gait cycle of both rats and humans can be divided in four phases (Flexion, Extension 1-3), see section 2.1. Due to these similarities several studies have investigated patterns of muscle activation by comparing locomotion of cats and humans [Kandel et al. 2000]. The main difference regarding skilled movements between rats and humans are the sensory control. Humans direct movements resting on visual inputs, whereas rats primarily use olfactory organs, audition, and vibrissae palpation [Whishaw 2003].

4.4 Anatomy of the rats hindlimb

The structure, anatomy and functionality of the rats hindlimb and the human leg, are also comparable. The limbs are comprised of similar muscles and bones and the skilled movements of the rat is comparable to humans [Whishaw 2003]. The muscles composing the rats hindlimb propagate along the knee joints and the hip making the rat able to exert movement of the hindlimb and thigh at the same time. Common muscles in the human leg and the hindlimb of the rat are listed in table 4.2 and illustrated in figure 4.4.

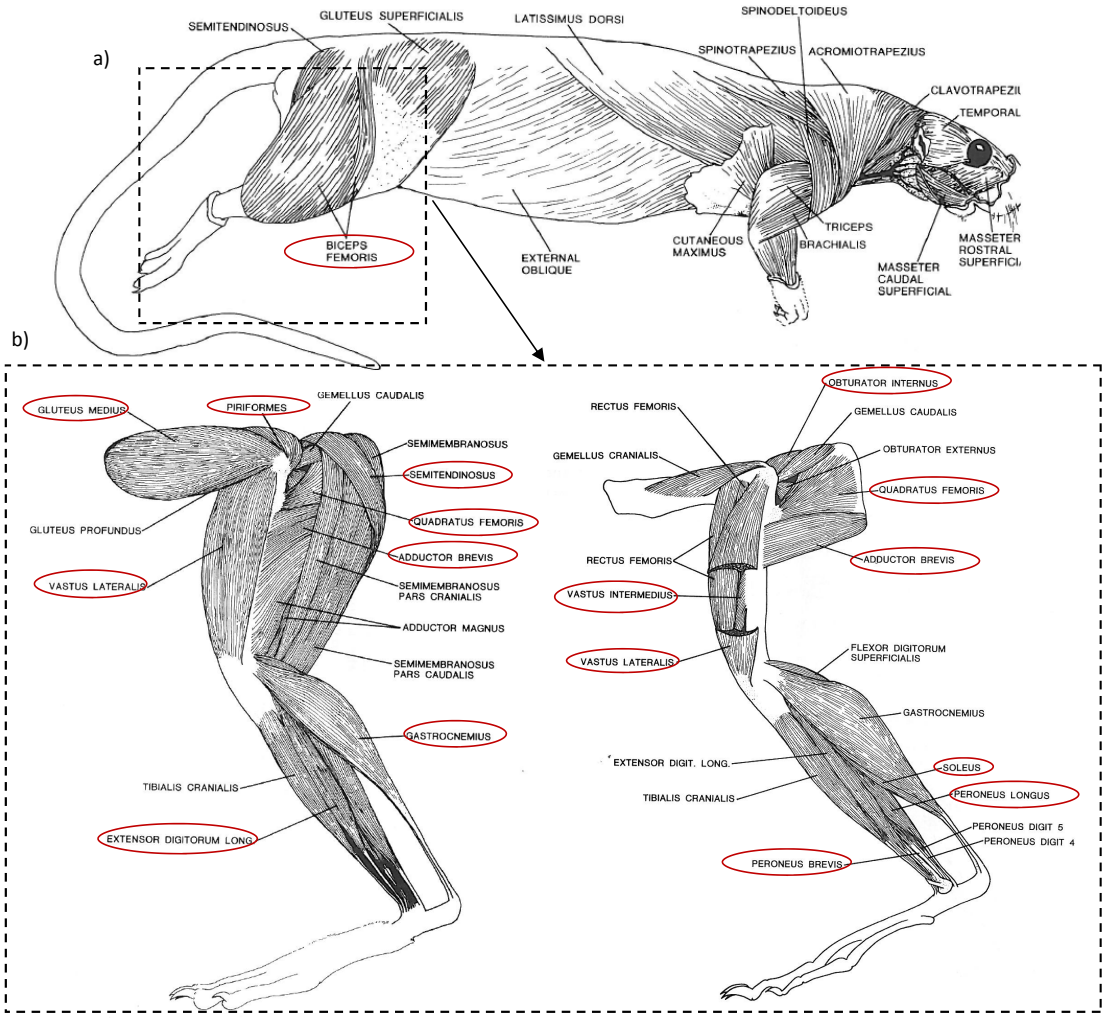

Figure 4.4. a) Lateral view of the superficial musculature of the rat. b) The muscles of the hindlimb (biceps femoris removed). Muscles with the same function in humans and rats are marked with a red circle. [Chiasson 1994]

Table 4.2. Common muscles in the human leg and the hindlimb of the rat. [Chiasson 1994]

Movement	Common muscles
Movement of the foot	
	Dorsiflexion:
	Extensor digitorum longus and Extensor digitorum brevis
	Plantarflexion:
	Peroneus longus, Peroneus brevis and Flexor digitorum longus
Movement of the knee	
	Flexion:
	Biceps femoris, Semitendinosus
	Extension:
	Vastus lateralis, Vastus intermedius and Vastus medialis
Movement of the hip	
	Rotation:
	Quadratus femoris and Obdurator externus
	Extension:
	Semimembranosus
	Abduction:
	Glutus medius, Piriformis and Obdurator internus
	Adduction:
	Adductor magnus, Adductor longus, Adductor brevis and Pectineus

Project hypothesis 5

In this chapter a short summary of the problem analysis will be presented. Furthermore, we will outline the hypothesis of this study.

Summary

Motor disorders are affecting millions of people worldwide, depriving the ability of producing controlled movements. The human motor system is highly complex and the smallest disruption in the system can cause the intentional movement to become abnormal or impossible. Motor disorders affecting walking are of great interest, yet being a complex problem to solve. One approach is to create a BCI system to restore functionality in persons with motor disorders. To address the problem of restoring walking the investigation of processes in the motor system under normal conditions provides a fertile ground for future research in BCI systems.

There are various methods to assess gait in humans and animals ranging from measuring cortical activity, muscle activity and body kinematics. The use of micro-wire electrodes have shown to be a promising method to record IC activity from the motor cortex. The method makes it possible to record the discharge frequency of neurons in the motor cortex with high temporal and spatial resolution. When investigating gait a high amount of gait cycles (at least several hundred) need to be analysed in order to obtain high statistical reliability. The use of treadmills is a preferred tool because it allows the subject of investigation to perform repetitive locomotor movements with different velocities and inclination without claiming much space. In combination with high speed videography and reflective markers placed on strategically important locations on the subject it is possible to analyse kinematics of a high number of gait cycles. Off-line tracking of the individual marker position allows the calculation of joint angles which in turn are usable to detect recurring events in the gait cycle. Event detection is also necessary to correlate a certain movement to, for instance parallel recorded IC signals. To assess muscle activity in rodents different methods have been developed. Recording of iEMG using fine wire electrodes have shown to produce precise EMG recordings with minimal surgical damage to the individual.

The rat has become a preferred animal model in research of locomotion to obtain a better understanding of the motor system and pathological conditions. It has a number of qualities making it feasible for animal studies. In particular rats have compared to other rodents the

advantage of being large enough for procedures such as chronic neural recordings and surgical intervention on major organ systems and muscles, making it suitable for most physiological studies relevant to human diseases. Furthermore, the use of rats implies a low economic burden and has greater acceptability from ethical perspectives. Although the rats motor system is not entirely comparable with the humans, studies indicate that the motor system related to the control of locomotion shows resemblance between humans and rats.

To date, there exist several animal studies which have focused on either the cortical activity of the motor cortex or on patterns of muscle activity related to movements. However, only a few studies have investigated both IC recordings of the motor cortex and iEMG of the hindlimbs in relation to each other. It is assumed that the combination of both recording methods will further improve characterisation of timing and coordination of muscle activation. Most studies on rodents have focused on gait analysis on a horizontal surface but have rather investigated how the neural activity in the motor cortex changes during uphill and downhill locomotion. However, based on findings from previous studies with cats it is assumed that motor cortex activity is modulated when locomotion differs from normal walking, especially in situations where precise movement control is required. Further, it remains unclear to what extent the motor cortex is involved in the initiation and ending phase of locomotion. These phases could be seen as a voluntary movement which is known to be controlled by the motor cortex. A better understanding of the role of the motor cortex during gait would be important in the development of a BCI system for walking restoration. The findings could be of practical relevance regarding control, activation and stopping of a future walking assist and to control different walking patterns.

The overall goal for this project is to obtain a better understanding about the contribution of the motor cortex during the regulation of gait. This will be achieved by implanting a micro-wire electrode array in the hindlimb area of the M1 and correlate the obtained IC signals with the activation of the hindlimb muscles. In order to characterise the timing and coordination of muscle activity iEMG will be recorded together with high-speed videography of the kinematics. The aim of the study is to get a better understanding of how the primary motor cortex contributes to the control of gait for different inclination angles during treadmill locomotion (Horizontal, uphill and downhill) and investigate what role the motor cortex have in the initiation phase and end phase of gait. It is presumed that the neuronal firing rate in the M1 will vary under different inclination angles and in the initiation phase and end phase of locomotion compared to continuous horizontal locomotion.

Hypothesis

The hypothesis of this project is therefore:

The cortical cell discharge increases in the primary motor cortex during the initiation and ending phase of locomotion as well as during locomotion on an inclined surface compared to continuous horizontal locomotion.

PART

Problem solution

Solution Strategy 6

In this chapter, we will present the solution strategy to the project in order to answer the project hypothesis.

6.1 Strategy for obtaining the data

Figure 6.1 illustrates the solution strategy for the project. A pilot experiment was conducted on three rats in order to approve the feasibility and the design of the full-scale experiment. The pilot experiment will not be further documented.

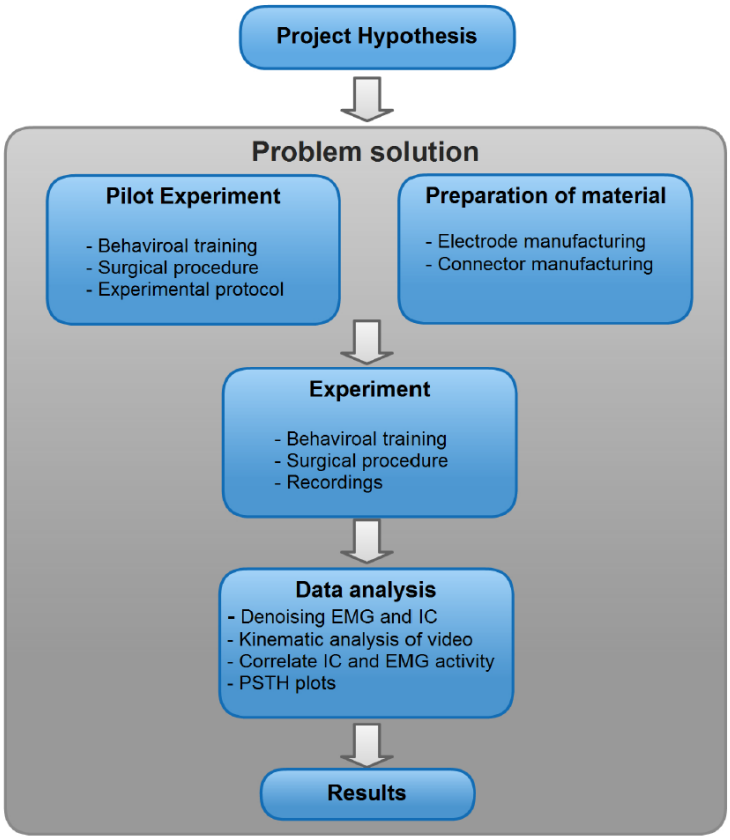

Figure 6.1. Overview of the main parts of the solution strategy and strategy for obtaining data.

Before the surgical procedure the animals were trained in walking steadily on a treadmill. Animals that fulfilled this criterion were chosen for further use. Alongside the pilot experiment electrodes and connectors for recording iEMG and IC signals were manufactured (see appendix A and B for more information about electrode design and manufacturing). After the behavioural training was accomplished the full-scale experiment was started and IC signals, iEMG and video kinematics were recorded from the animals. Finally, the obtained data was analysed. The IC and iEMG data was filtered and the video kinematics were analysed in order to correlate the data. The problem solution ends up with the results to support or reject the project hypothesis.

6.2 Methodological choices

To address the project hypothesis, a large amount of data was obtained. In order to do this the following methodological choices were considered as cornerstones in the experimental design.

Animal species

Ten male Sprague-Dawley rats were chosen to be used for the experiment. This type of rat is extensively used in other similar studies investigating IC signals [Jensen & Rousche 2005, Jensen et al. 2006]. Furthermore, they are relatively cheap and easy to take care of.
The criteria to perform the surgery on the rats was that the animal was minimum 12 weeks old and had a body weight above 350 g on the day of the surgery to make sure the skull of the rat was fully developed before the implantation process.

Cortical activity

A large number of studies have demonstrated the possibility of recording single neuronal activity in the motor cortex and related it to the control of voluntary movements. The studies have shown that neurons in the motor cortex modulate their discharge frequency during the production of voluntary movements [Georgopoulos et al. 1983, Jensen et al. 2006, Porter & Lemon 1993].
To assess the cortical activity in the brain it was decided to record IC signals using a 16-channel tungsten micro-wire array electrode (A-M systems, Catalog number: 795500). This type of electrode was chosen because it provides IC signals from a large area of the primary motor cortex. Previous studies using this type of electrode in rat experiments have shown satisfying results [Jensen & Rousche 2005, Jensen et al. 2006].

Kinematic assessment

In order to detect the event times of the gait cycles 2-D high speed videography was selected to assess the kinematic data from the rats joints. The placement of markers on the hindlimb of the rat makes it possible to calculate the joint angles of the rat with video tracking software and thereby detect certain events in the gait cycle [Pearson et al. 2005].

Muscle activity

In order to correlate the cortical activity with the muscle activity iEMG was recorded from the rats hindlimb. The electrode configuration for recording iEMG was conducted using a

method developed in a study by Pearson et al. [2005]. The advantages of this method are that appropriate EMG recordings can be obtained with minimum surgical damage to the muscles and the implanted leads have only a modest restriction on the locomotion (16 % reduction in knee movement range after 6 days of recovery) [Pearson et al. 2005]. The electrodes were made using multi-stranded, Teflon coated annealed stainless steel wire (A-M systems, Catalog Number 793200). These type of wires have been shown to be easy to work with in the manufacturing process and are suitable for long-term recordings (stable signal for up to 16 days) [Pearson et al. 2005]. Bipolar electrode configuration was chosen compared to monopolar electrode configuration because of its reduced noise sensitivity [Schumann et al. 2006].

Hindlimb muscles

iEMG electrodes were surgically implanted into two superficial muscles (VL and BF) of the hindlimb of the rat. These two muscles have successfully been used in a large number of locomotion studies to record EMG in rodents [Pearson et al. 2005, Scholle et al. 2005, Schumann et al. 2006, Thota et al. 2005]. As largest muscle of the hind limb, the BF is located laterally in the thigh and is involved in multiple actions such as thigh abduction, hip extension and knee flexion [Gillis & Biewener 2001]. Although, its main function is to stabilize the hind leg during stance phase [Schumann et al. 2006]. The VL is the largest muscle of the quadriceps and a major extensor of the knee [Gillis & Biewener 2001]. This muscle plays a primary role in supporting the weight of the rat during stance phase [Schumann et al. 2006].

Experimental tasks

The experimental task for the rats involved locomotion on a treadmill. In the first part of the experiment the rat was walking on a horizontal treadmill and an inclined treadmill (15 deg). Assuming that locomotion on an inclined surface implies a higher demand in limb coordination compared to horizontal locomotion, we believe this will result in a increased involvement of the motor cortex during the control of gait [Armstrong 1986]. To investigate the initiation and ending phase of locomotion the treadmill was alternately started and stopped, making the rat walking only for a short period of time. Thereby the focus lays on the first steps after the treadmill was started and before the treadmill was stopped. The task was motivated by the fact that cortical areas are less active during continuous locomotion, but mostly involved in the adaptation of gait due to environmental changes [Drew et al. 2002, Widajewicz et al. 1994].

Treadmill speed

The velocity of the treadmill belt was chosen to 29 cm/s to obtain a sufficient number of gait cycles from the rat. A study by Clarke & Parker [1986] investigated normal locomotion in the rat and found the mean value of velocity to be 24 cm/s for the walking phase in rats [Clarke & Parker 1986]. In a study by Hattori et al. [1994] it was shown that a treadmill velocity of 30 cm/s is sufficient to familiarize almost all rats with walking on the treadmill after only two trainings sessions (20 min/day). In another study which investigated different walking pattern at Sprague Dawley rats, it was observed that the animals walk at speeds of 17-48 cm/s, trot at speeds of 59-71 cm/s and gallop at speeds of 60-122 cm/s [Gillis & Biewener 2001].

Experimental protocol 7

The following chapter leads through the experimental protocol of the study by describing the used materials, experimental setup, surgical procedure and the experimental tasks.

7.1 Aim

The aim of the study was to investigate the role of the primary motor cortex in the initiation and end phase of locomotion and the influence of slope during walking compared to horizontal locomotion in healthy rats.

7.2 Materials

The following materials were used to conduct the experiment.

TDT System

- RX5 Pentusa Base Station (Tucker-Davis Technology, Alachua, USA)
- RA16PA 16-channel medusa pre-amplifier for IC
- RA16CH 16-channel chronic headstage for IC
- IC electrode array with custom made adaptor
- RA4PA 4-channel medusa pre-amplifier for EMG
- RA4LI 4-channel headstage for EMG
- EMG electrodes with custom made adaptor

Camera

- Camera (Basler A602fc-2)
- 2 x 400W telescope work lamp (SARTANO)
- Black painted markers
- The camera software is only compatible with Windows XP SP2

Computer

- DT340 card (PCI bus digital I/O and counter/timer board)

- Video recording and processing software Vicon Motus 9.2 (Vicon Systems, Oxford, Great Britain)
- Real-time Processor Visual Design Studio (RPvdsEx) software
- Windows XP SP2

Treadmill

- Motor-driven treadmill enclosed in Plexiglas (Letica Scientific Instruments AUC Institute 8 no. 33558)
- Mini lifting jack
- Voltmeter
- 100 Ω potentiometer
- 12 V Battery (MFD by YUASA corp. for ENERSYS inc.)

Other

- Grass stimulator (Model: SD9J, S/N: 99A0543G)
- Grass Photoelectric stimulus isolation unit (Model: PSI06, S/N: 03K01026)
- Shaver
- Tape

7.3 Experimental setup

The experimental setup consisted of four main components which can be seen in figure 7.1 below. For the experimental task the rat was walking on a motor-driven treadmill. Kinematic data were obtained from a high-speed camera, and iEMG and IC signals were recorded with a Tucker-Davis Technologies (TDT) system (Tucker-Davis Technology, Alachua, USA). The collected data from the camera and the TDT system were stored on a computer and an external hard-drive.

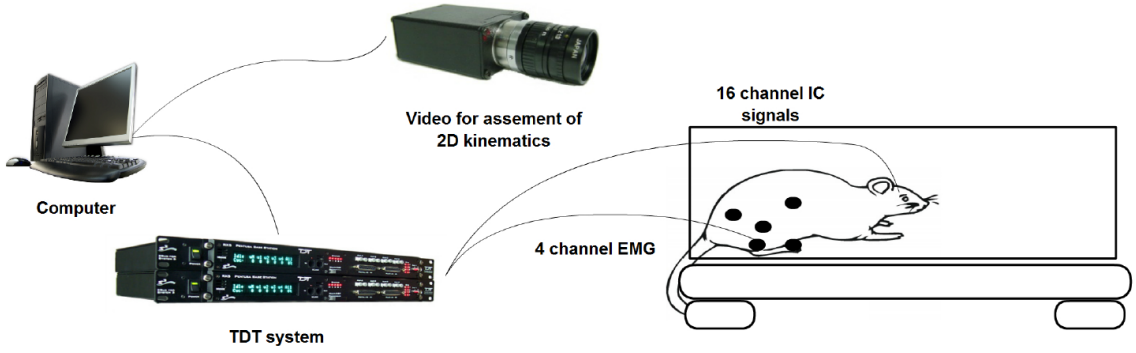

Figure 7.1. Experimental setup showing the equipment used for simultaneous analysis of high-speed video, IC signals and iEMG in rats while performing locomotion on a motor-driven treadmill.

Treadmill setup

The motor-driven treadmill was enclosed in a Plexiglas cover to prevent escape. Adjustable barriers were used to provide a running surface of 30 cm length and 10 cm width. The incline

of 15 deg was adjusted manually by using a mini lifting jack to lift the treadmill and the angle was measured with a protractor. The treadmill was powered by a 12 V battery whereby the velocity of the treadmill belt was adjusted for each task by modifying the input power. The desired velocity of 29 cm/s was achieved by the use of different resistors, based on results from a treadmill velocity test which was performed prior the experiment (see appendix D)

Camera setup

The high-speed camera (Basler A602fc-2) was placed laterally to the right hindlimb of the rat to record video (height 10 cm; length 20 cm). In order to track the locomotive movement adherent black markers were placed on intrinsic anatomical locations of the hindlimb (toe, heel, knee and hip) of the rat, see figure 7.6. Vicon Motus 9.2 motion analysis system (Vicon Systems, Oxford, Great Britain) software was used to track the position of the markers and process kinematic movements of the hindlimb. A telescope work lamp was installed behind the camera in order to increase the contrast of the markers for the later video analysis. The frame rate of the camera was set to 100 Hz. The camera was connected to the computer with a 10 pin RJ-45 jack and an IEEE 1394 socket. To clock the camera externally another cable was used between the RJ.45 jack and a DT340 card. [Basler 2005]

Tucker-Davis Technologies (TDT) setup

The TDT system was used to record IC signals and EMG signals continuously while the rat was walking on the treadmill. The IC electrode array was connected to the RA16PA pre-amplifier through the RA16CH headstage with a custom made adaptor for the IC electrode array. The pre-amplifier was connected through fibre-optics to the RX5 Pentusa Base Station. The iEMG electrodes were connected to the RA4PA pre-amplifier through the RA4LI headstage with a custom made adaptor for the iEMG electrodes. Data were stored on a computer equipped with a DT340 card (PCI bus digital I/O and counter/timer board) for offline processing. [Tucker-Davis Technologies Inc 2012]

Computer and software setup

Real-time Processor Visual Design Studio (RPvdsEx) running on a computer with Windows XP Professional (32-bit version Service Pack 2) was used to communicate with the RX5 Pentusa Base Station (TDT system). The Vicon Motus 9.2 (Vicon Systems, Oxford, Great Britain) software was used to store the video data on the computer. Peripherals setup consisted of an external hard-drive connected through USB 2.0 interface to the computer. The IC, iEMG and the video recording will be synchronised by using the Vicon clock signal that is send to the TDT system during video recording.

7.4 Animals and behavioural training

Animals

Ten male Sprague-Dawley rats were trained for two weeks and the best five performing rats were chosen for implantation for the experiment. The five rats were weighing between 348 g and 431 g (mean 368 g ± 35) at the day of surgery. The rats were individually caged and placed in a temperature-controlled room with a 12/12-hour light/dark cycle after implantation. They had free access to food and water during the whole experiment. The inclusion criteria for electrode implantation was the ability of the rat to walk steadily on the treadmill for at least 30 s at the velocity of 29 cm/s to insure sufficient data would be obtained under the recordings. The body mass of the rats had to be above 350 g on the day of the surgery to make sure that the skulls of the rats were fully developed for before implementing the IC electrode. The experiment was carried out with approval from the Danish Committee for the ethical use of animals.

Hand and treadmill training

The rats were hand trained the first two days after arrival to the animal lab in order to get them accustomed to the handling by the human operators during the recording sessions. Besides hand training each rat was trained on the treadmill for two weeks. For the initial training session the rat was placed on the treadmill for about 10 minutes to get familiar with the new environment. The first time the rat had to walk on the treadmill the velocity was set very low at 23 cm/s to get the rat used to walk on the treadmill. A training session on the treadmill consisted of 4-6 trials, each 60 s long, with a break of 2 min in between. In case the rats received two training sessions per day a break of at least one hour was left between both sessions. If the rat performed good at a velocity of 23 cm/s during the first training session the velocity was increased by 1-2 cm/s in the next session. This was done until a velocity of 29 cm/s was reached. In order to motivate the rats they were given treats in form of sugar pellets (NOYES Precision Pellets) after each or several trials. The rats were trained for two weeks with 20 training sessions in total (2 sessions/ day). After the first week of training rats which failed to run steadily (frequent immobility, uplifting of the forelimbs, stressful behaviour) were excluded from the experiment. The different training tasks consisted of the following:

- Locomotion on the horizontal treadmill with velocities from 23 cm/s to 29 cm/s.
- Locomotion on the treadmill with inclination (uphill and downhill) of 15 ° with velocities ranging from 23 cm/s to 29 cm/s.
- Locomotion on the treadmill with focus on initiation and end phase of locomotion.

It was important that the rat showed steady locomotion to assure appropriate video kinematic recordings. This was evaluated by noting down the following parameters at each trial:

- Time in seconds of steady running performance.
- A grade from 0 to 6 was given to the rat for each trail reflecting the performance. The grade 6 was given for best performance and the grade 0 was given if the rat was not able to run at all.

7.5 Surgical procedure

The surgical procedure performed on the rats was subdivided in two parts: First two bipolar iEMG electrodes were implanted in two different muscles of the right hind limb and secondly a 16 channel electrode array was implanted in the corresponding hind limb area in the M1 of the rat. The materials and surgery tools used to perform the surgical procedure are listed in appendix C.

Preparation

To perform the surgery two persons were required; a sterile surgeon and a non-sterile assistant, see figure 7.2. The time duration of one surgery was between 2-3 hours. The room was equipped with two tables, one of them being sterile. All surgical tools were steam sterilized in the autoclave (Tools at 121°C for 3min/3min and towels/clothes 121°C for 10min/10min). Bone screws and rubber bands were put into silver trays. The IC electrode and the iEMG electrode were put in sterilization pouches before they got sterilized with gamma emission. The microscope was covered with a sterile t-shirt, fastened by rubber bands and connected to an external screen so that other non-sterile persons could follow the surgery.

Figure 7.2. Figure showing the surgical setup with the sterile surgeon and the non-sterile assistant.

Anesthesia and preparation of the rat

The surgical procedure was performed under deep anaesthesia of the rat. The animals were anaesthetized with an injection of a mixture of Hypnorm and Dormicum. The stock solution was 1 ml Hypnorm (Fentanyl citrate 0.315 mg/ml) and 1 ml Dormicum (Midazolam hydrochloride 1mg/ml) in 2 ml of sterile water. A dose of 0.2 ml per 100 gram was given for the first hour and supplemented periodically during the surgery. After the rat was anaesthetized the head and hindlimb of the animal were shaved and prepared for the surgery using a 1% iodine brush. In order to prevent the eyes of the rat to dry out a layer of Vaseline was applied on the eyes.

Implantation of iEMG electrode

The electrode configuration for recording the iEMG was conducted using a method developed in a study by Pearson et al. [2005]. The design and manufacturing of the iEMG electrodes can be found in appendix B. The four channel bipolar iEMG electrodes were surgically implanted into two superficial muscles of the hindlimb of the rats, the VL and BF. The BF is superficial located in the thigh and VL is located just below a superficial layer which makes the muscles accessible. The surgery was started by making an incision of about 4 cm length at the skull in caudal direction to the neck. This was followed by a second approximately 2 cm long incision at the hindlimb. The skin at the hindlimb area was separated from the muscles by using a blunt scissor. A long forceps was used to establish a tunnel from the neck where the connector was located to the hindlimb. The electrodes wires were pulled from the head down to the hindlimb of the rat with a long forceps. Two electrodes for bipolary recordings were inserted in VL and BF (The BF electrode was marked with an extra wire loop) with an eyelet needle (size 5.0) attached to a suture wired loop. After insertion at the distal end two knots were made on the wire. The remaining slack of the electrode was looped and sutured to a muscle in the hindlimb area, see figure 7.3. Two wires (Cooner AS 631) attached on the electrode were used as ground and placed in the established tunnel from the rat's head to the hindlimb. After the electrode was implanted the incision at the hindlimb was sutured together and closed with surgical glue (LiquiBand Surgical S).

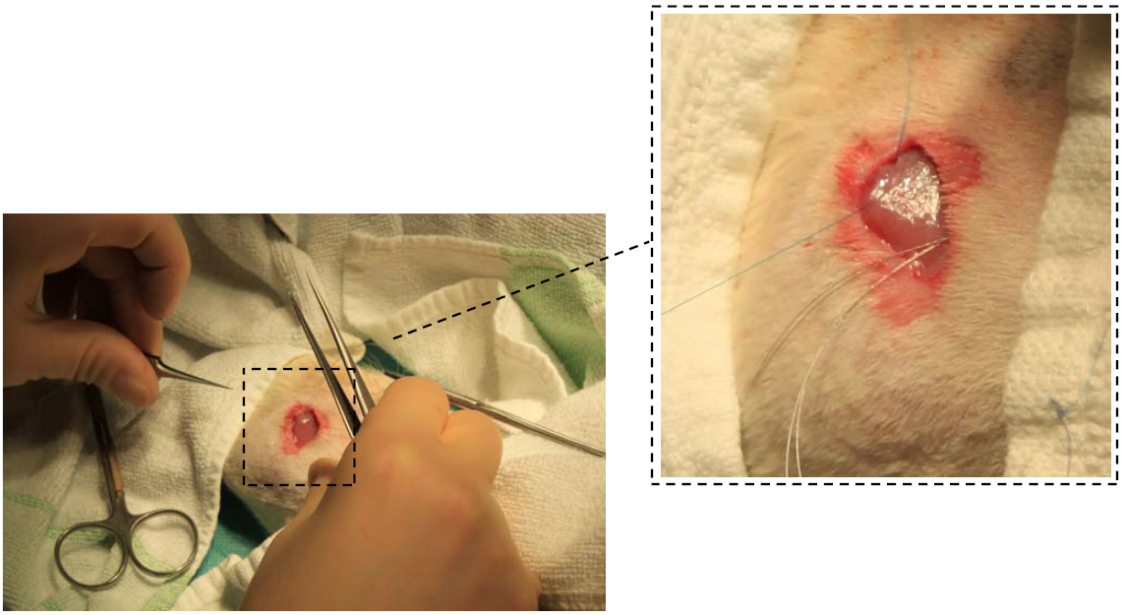

Figure 7.3. Implantation procedure of the iEMG electrode in the VL and BF of the right hindlimb of the rat.

Implantation of intra-cortical electrode

The design and manufacturing of the IC electrodes can be found in appendix A.
Before starting the implantation of the IC electrode the head of the rat was fixed in a stereotaxic frame, see figure 7.5 (a). Local anesthetic (Lidocaine) was applied to the ear bars and skin of incision and vaseline was applied to the eyes for the second time. A craniectomy was performed at the M1 area corresponding to the right hindlimb, meaning that the surgery was

performed on the left side of the brain. The area was identified by stereostactic coordinates regarding to the midline and bregma of the skull [Kolb & Tees 1990], see figure 7.4. After the area of the craniectomy has been located, four holes were drilled in the skull with a 2 mm hand drill; two holes for ground wires, one hole for fixation and one hole for exposing the cortex to implant the IC electrode, see figure 7.5 (c,d). A rongeur was used to expand the screw hole to a size that fitted the IC electrode (approximately 2 mm x 2 mm), see figure 7.5 (d,e). Three bone screws were screwed in the other holes turning the screwdriver 2 to 2.5 rounds. Before inserting the IC electrode, the dura as the the outermost layer which covers the brain surface was removed, see figure 7.5 (g).

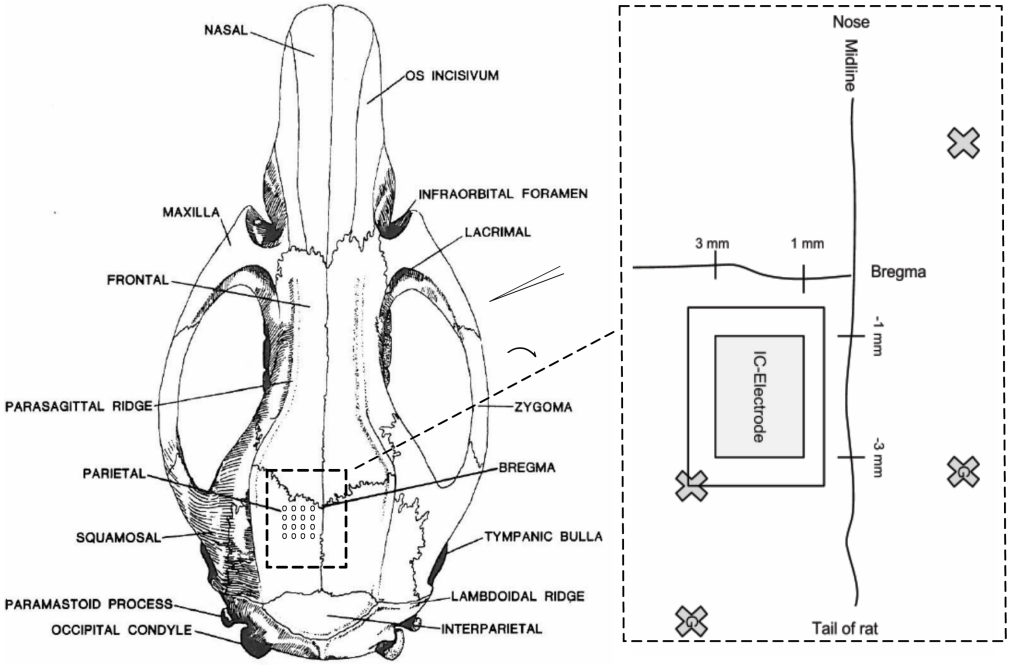

Figure 7.4. The recording site and coordinates for the implantation of the IC electrode. The drilled holes for the craniectomy and the bonescrews for ground(G) are visualized with a cross.

A dummy socket was placed on top of the IC electrode to get a better view when inserting the electrode. The electrode which was fixed in a manually operated micromanipulator of the stereotaxis had to be lowered to a depth of 1.7 mm into the brain. To obtain this the electrode was quickly lowered 2.0 mm to penetrate the brain tissue and then elevated 0.3 mm to reach the correct height. Dental acrylic (Heraeus Kulzer Paladur, Germany) was used to fixate the IC and the iEMG electrode to the skull and to cover the area around the electrodes. Before applying the dental acrylic small pieces of absorbable haemostatic gelatin sponge (Spongostan TM) was inserted around the exposed part of the cortex in order to keep the dental acrylic from the cortex. As the last part of the surgical procedure the skin was closed with suture posterior and anterior of the electrodes.

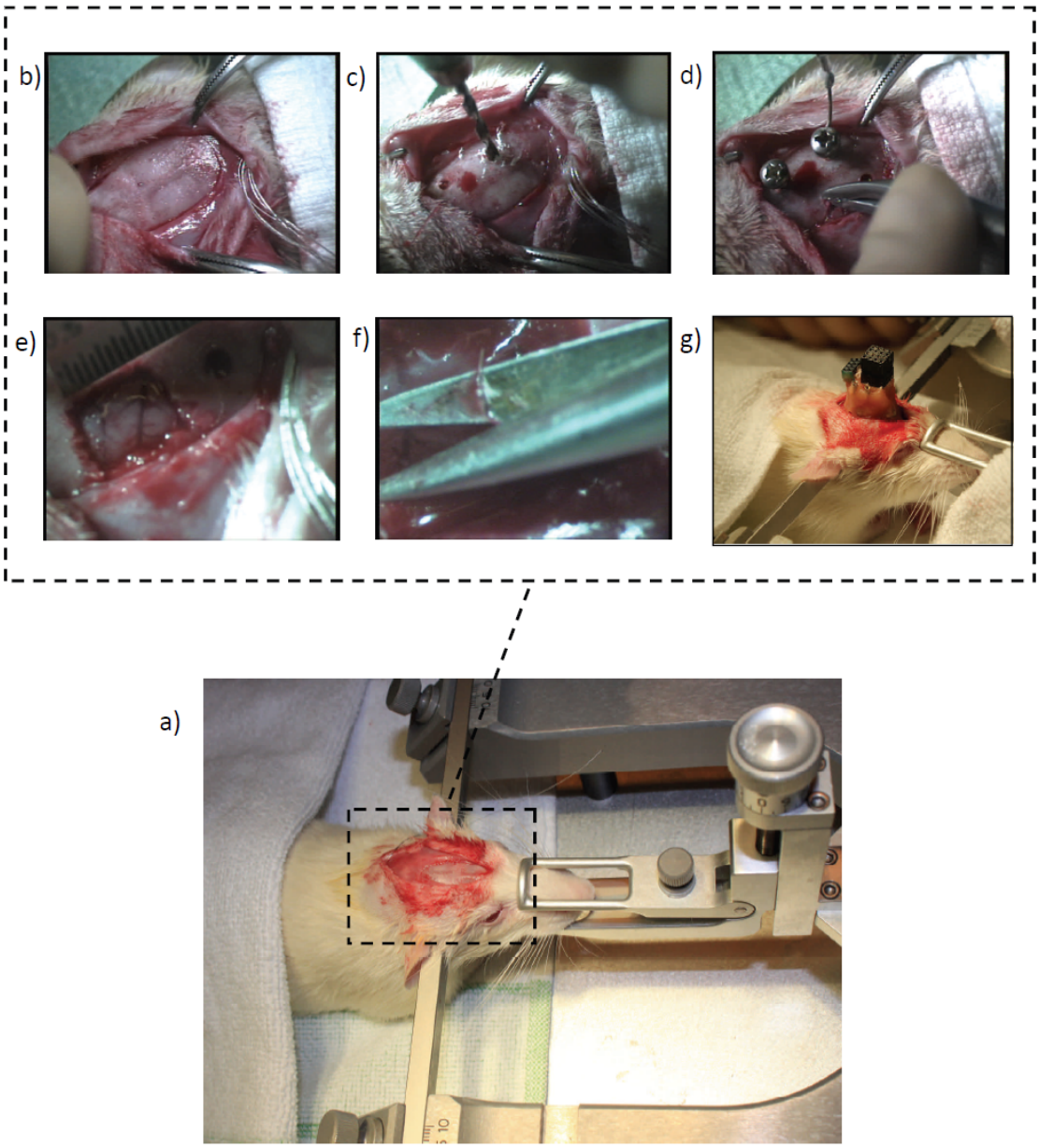

Figure 7.5. Steps for implanting the IC electrode into the motor cortex of the rat. **a)** The rat was fixated in a stereotaxis frame **b)** A scalpel was used to make an incision of about 4 cm length at the skull **c)** Four holes were drilled in the skull with a 2 mm hand drill **d)** Three bone screws were screwed in the other holes turning the screwdriver 2 to 2.5 rounds. **e)** The craniectomy was performed **f)** The dura covering the brain surface was removed **g)** The electrode was fixed in a manually operated micromanipulator of the stereotaxis and lowered into the motor cortex.

7.6 The experimental tasks

All experimental tasks were performed on the treadmill, see figure 7.6. Before the experiment micro-stimulation were applied on the rats and control recordings were recorded from each rat prior the surgery. Each task was performed while IC signal, iEMG and video kinematics were recorded. The first recording from each rat were made 2-3 days after the surgery. All tasks

consisted of trials of 30 s walking on the treadmill with velocity set to 29 cm/s. Between each trial the rat were given a break of 2 min to recover while the recorded data was exported.

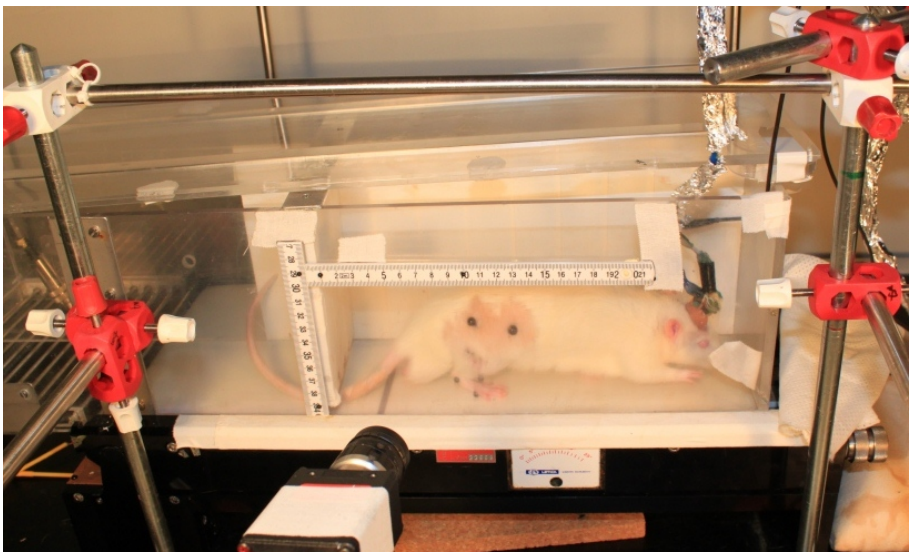

Figure 7.6. Treadmill setup with the rat during horizontal locomotion. The position of the black markers on the joints of the rats right hindlimb are also visualised (hip, knee, heel and toe).

Control recordings

In order to determine whether the implantation of the iEMG electrodes in the hindlimb affects the gait cycle of the rat a control video recording was done before the surgical procedure. For the control recording the rat was walking on the horizontal treadmill for 30 s at the velocity of 29 cm/s.

IC micro stimulation

Two days after the surgery micro stimulation were applied to all 16 channels of the implanted electrode array. The aim of the micro stimulation was functional cortical mapping in order to estimate which channels correspond to the hindlimb motor area. This was done by comparing the stimulated channel with observed motor response of the hindlimb. The micro stimulation was started at 100 μA and was gradually increased to 500 μA in steps of 100 μA until a response was observed. If a response was observed, the stimulation current was decreased by 50 μA and stimulation was applied again. The threshold current was defined as the lowest current at which consistent responses were visible. [Neafsey et al. 1986, Jensen & Rousche 2005]

Locomotion on the horizontal treadmill

The rat had to walk on the horizontal treadmill for 30 s at the velocity of 29 cm/s. This was repeated four times for each recording day in order to obtain a high number of gait cycles from each rat.

Locomotion on the inclined treadmill

The rat had to walk uphill and downhill on the treadmill for 30 s on an inclination of 15° at the velocity of 29 cm/s. This was repeated four times for both uphill and downhill walking for each recording day in order to obtain a high number of gait cycles from the rat.

Locomotion on the horizontal treadmill with focus on initiation and end phase

In this task, the focus lay on the beginning of the locomotion (initiation to move) and the end phase of the locomotion of the rat in a period of 4 s. Therefore, the treadmill was started and stopped alternately in short time periods of 30 s. The start and end phases were chosen as the following on figure 7.7 and the task was repeated eight times for each recording day:

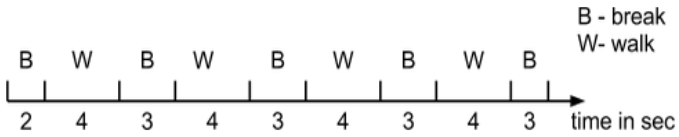

Figure 7.7. Procedure for the task where the focus was on the initiation and end phase of locomotion.

Experiment recording schedule

The recordings were conducted over five days and was divided in two sessions with a break of at least one hour in between the sessions.

Table 7.1. Recording schedule for each of the five recording days where each day was divided into two session with a break of one hour in between the sessions.

Task	Time	Gait cycles/day	Gait cycles 5 days
1st session			
Preparation	15		
Horizontal running	2 min(4x30s)	200	1000
Uphill running	2 min (4x30s)	200	1000
Downhill running	2 min (4x30s)	200	1000
Exporting time	36 min		
Total for session	63 min	600	3000
2nd session			
Preparation	15 min		
Initiation and end	4 min(8x30 s)	2x32	160
Exporting time	24 min		
Total for session	43 min	2x32	160
Total for each rat	106 min	696	3480

7.7 Data acquisition and recording procedures

Prior recording

Before the recording session was started the rats right hindlimb were shaved and marked with anatomical markers for the kinematics recordings, see figure 7.6. The markers were placed at the toe, heel, knee and hip on the right hindlimb, and one marker was placed on the side of the rat as reference for the locomotive analysis. Afterwards, iEMG and IC headstages were connected carefully to the implant. The preamplifier was then turned on and the quality of the EMG and IC signals were examined visually and by the use of speakers from the TDT which made the neural firing audible. Before the recording was started a threshold was set each IC channel with a the auto-thresholding function ($RMS \cdot 1.2$), implemented in the software. The used sampling frequency and filter settings for the IC, EMG and video kinematics are explained in the following sections.

IC recording

IC signals were measured with a 16 channel micro-wire array electrode from the motor cortex area which represents the hind limb control of the rat. The IC signals were sampled at 24.414 kHz and bandpass filtered (LP: 8000 Hz, HP: 800 Hz) and contained snippets with 22 samples of spike activity.

iEMG

iEMG was recorded in a biploar configuration from chronic implanted wires in the VL and BF of the right hind limb, in total 4 channels. Two ground wires were connected to the connector. The continuous EMG signal was sampled at 4882.8 Hz and bandpass filtered (LP: 2500 Hz, HP: 20 Hz).

Video kinematics

Video recordings of rat kinematics were recorded with the Basler A602fc-2 high speed camera with a frame rate of 100 Hz and stored as Audio Video Interleaved (AVI) multimedia container format. The joint kinematics of the rat were obtained by the use of highspeed video recording and tracking software to synchronize the gait cycles with the IC signal and EMG signal.

During recording

The TDT system was first set to Preview mode and thresholds were set to all IC channels while the rat was resting on the table. The rat was then placed on the treadmill and the treadmill was started. Afterwards the recording software of the TDT system was started together with the video recording software of the Vicon system. After 30 s the TDT system, the Vicon system and the treadmill were stopped. The recorded IC signals were saved on the computer and the video files were exported to an external hard drive. Two persons were present under recording. One person monitored the rat and regulated the treadmill, while the other person was operating the recording equipment.

Data analysis 8

The data analysis is separated into three parts; analysis of video recordings, IC recordings and EMG recordings. However, the different recordings have to be seen in relation to each other since the IC and the EMG recordings were synchronized to gait cycles events, detected in the video recordings. Further, the analysis of all parts have in common that the duration of the individual gait cycles were presented in percentage to allow simultaneous comparison between the three types of recording over several gait cycles.

8.1 Analysis of video recordings

The video recordings were used to obtain certain events in the hindlimb kinematics. Therefore the positions of the joint markers were determined in the video data either by using Vicon Motus 9.2 automatic tracking software (Vicon Systems, Oxford, Great Britain) or by manual inspection. The obtained marker coordinates were further processed with MATLAB (MathWorks, Natick, USA) to calculate joint angles for toe, heel and knee and to detect the gait cycle events foot lift off and foot touch down.

Event definition

A single gait cycle was defined as the point in time when the foot was lifted off from the treadmill belt until the recurrence of the same event. The event between two lift off's when the foot was set back on the treadmill belt was defined as touch down, see figure 8.1. The events lift off and touch down were defined as events of interest:

- **Lift off** - Time when the foot is lifted from the ground. Indicates the beginning of the swing phase and the end of the stance phase.
- **Touch down** - Time when the foot touch the ground. Indicates the beginning of the stance phase and the end of the swing phase.

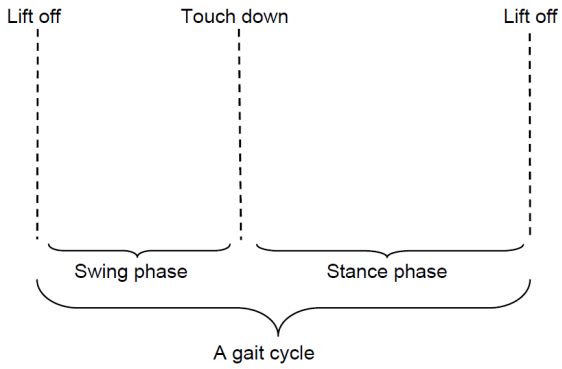

Figure 8.1. Phases of one gait cycle: starting with the lift off (beginning of swing phase), followed by touch down of the foot (beginning of stance phase) and finally another lift off which represents the end of the gait cycle.

Event detection

Video recordings used to investigate the initiation and end phase of locomotion were analysed manually. The manual tracking was faster compared to the automatic tracking because the events of interest were only needed for the first and last gait cycles after the treadmill was started and stopped, respectively. Vicon Motus 9.2 automatic tracking software was used to track the joint marker positions in video recordings when the rat was walking constantly for 30 s on the horizontal and inclined treadmill, see figure 8.2.

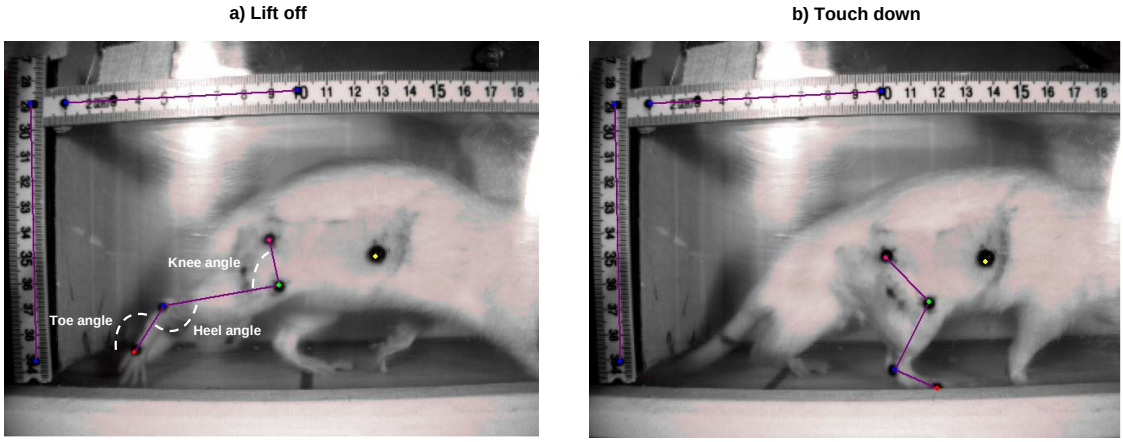

Figure 8.2. Illustration of the events of interest in the gait cycle tracked with the Vicon Motus software. a) The lift off indicates the beginning of the swing phase. b) The touch down indicates the beginning of the stance phase.

In order to determine the events lift off and touch down from the automatically tracked marker position the joint kinematics were calculated in MATLAB and visualized in graphic plots. From the plotted graphs a characteristic pattern was observed in the toe angle occurring during each gait cycle, see figure 8.3. By comparing the video and the graphs it was observed that the plotted toe angle contained spiky fluctuations that are suitable to detect the lift off events of the right hindlimb. In particular, lift off was detected by finding the maximum of the toe angles. The

touch down event was detected as the maximum x-coordinate of the toe marker between two detected lift off events.

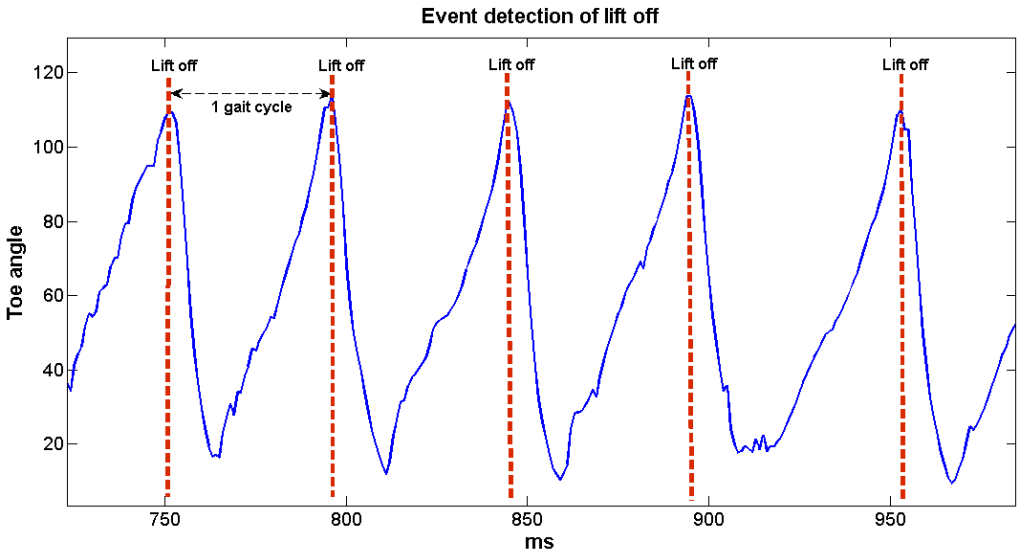

Figure 8.3. Event detection of the foot lift off. The maximum values of the toe angle corresponds to the lift off for the right hindlimb illustrated with the dashed red line.

Exclusion criteria for gait cycles

Only gait cycles which were similar in their kinematic movement and gait duration were utilized for further analysis. Therefore gait cycles where the rat was hitting the treadmill cover, taking very long or short steps or ran out of the camera focus needed to be excluded. In order to get an indication of the average gait cycle duration video recordings were analysed manually. For each rat, day and task the mean gait cycle duration was calculated from ten appropriate gait cycles. Gait cycles with duration shorter or longer than ± 100 ms from the mean duration were removed. Further, only heel angles between 65°-120° were included [Gillis & Biewener 2001, Pearson et al. 2005].

Normalization in gait duration

The kinematic data of the individual gait cycle were normalized in time whereby the duration of one gait cycle corresponded to 100 %.

8.2 Analysis of intra-cortical recordings

The analysis of the IC recordings was done in relation to the gait cycle events and thus indirectly related to muscle activation. This means that the IC recording were separated in time windows, each corresponding to a gait cycle. In order to do so, the IC recordings needed to be synchronized to the initial trigger signal of the Vicon system when the video recording was started. Afterwards the neural firing rate within the motor cortex was estimated and visualized by the use of a Peristimulus Time Histogram (PSTH) generated in MATLAB (MathWorks, Natick, USA). To detect significant modulations in the firing rate, 95% confidence limits were calculated.

Peristimulus Time Histogram (PSTH)

Peristimulus Time Histogram (PSTH) is a commonly used tool in neurophysiology for investigating nerve cell behaviour. The method allows the capturing of time dependent neuronal firing rates in correlation to a event trigger. The PSTH is generated by dividing time or percentage into contiguous intervals (bins) in which the discharge trains of neural impulses are summed up over a high number of trials. The shape of a PSTH is largely dependent on the selected size of the bin, see figure 8.4. If the selected bin size is too large, the time-dependent spike rate information is not visualised (larger probability for a neuron would fire within that bin). With a bin size too small, the PSTH fluctuates greatly making it difficult to read the underlying spike rate pattern. [Shimazaki & Shinomoto 2007]

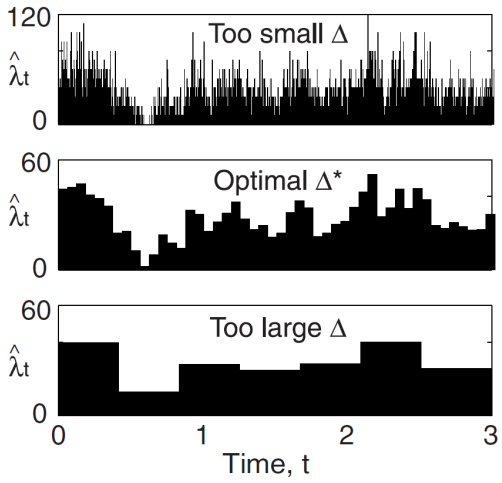

Figure 8.4. Peristimulus Time Histogram (PSTH) with bin sizes: too small, optimal, and too large.[Shimazaki & Shinomoto 2007]

In this study PSTH were generated for each of the sixteen IC channels as percentage of the individual gait cycle duration. Thus, the gait cycle duration was divided into equally sized intervals (bins) of 1% whereby 0 % and 100 % corresponded to two subsequent lift off events, see figure 8.5. At least 100 gait cycles were used to create a PSTH whereby each bin contained the total number of action potential of the neurons firing rate within this bin-size, quantified as spikes/s. To obtain the mean firing rate, each bin was divided by the total number of gait cycles used to create the PSTH. Afterwards the mean was calculated and subtracted from the PSTH to minimize the influence from different threshold settings and signal-to-noise ratio for the different recording days. Finally, a moving average filter was applied, smoothing the normalized PSTH in order to reveal the inhibitory and excitatory behaviour of the mean spike firing rate.

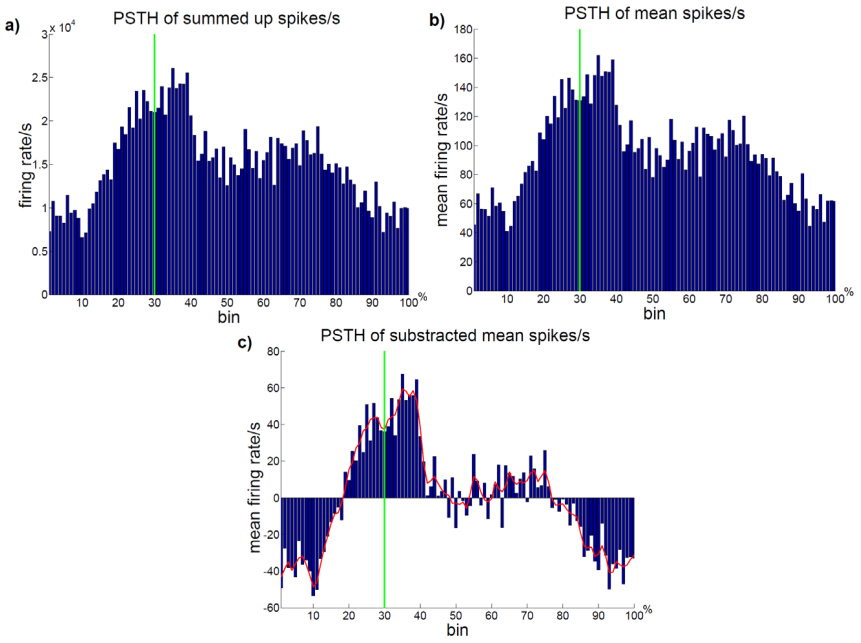

Figure 8.5. Example of the processing steps for the PSTH. a) Firing rate from 161 gait cycles summed up in 100 bins (100 % = individual gait cycles duration). b) Mean firing rate c) Firing rate when mean subtracted, smoothed firing rate (red graph).

Confidence Interval

In order to indicate significant changes in the firing rate the 95 % confidence interval was calculated, assuming that the null hypothesis is that the neural firing rate behaves like an independent Poisson point process. Further this implies that the cell firing rate has a constant average λ and is independent from previous firing events, stimuli or firing from adjacent cells [Abeles 1982]. The expected firing rate within each bin can be calculated as:

$$n = \lambda \cdot N \cdot \Delta t \tag{8.1}$$

where n is the expected mean firing rate, Δt is the bin size and N represents the number of gait cycle duration substractedused to generate the PSTH.

Consequently, the Poisson distribution can be calculated as:

$$P(m;n) = \frac{e^{-x} \cdot n^m}{m!} \tag{8.2}$$

where $P(m;n)$ describes the probability of finding m spikes within a bin that is part of a PSTH window having the expected firing rate n. An example of a Poisson distribution with an expected mean firing rate n = 10.5 is shown in figure 8.6.

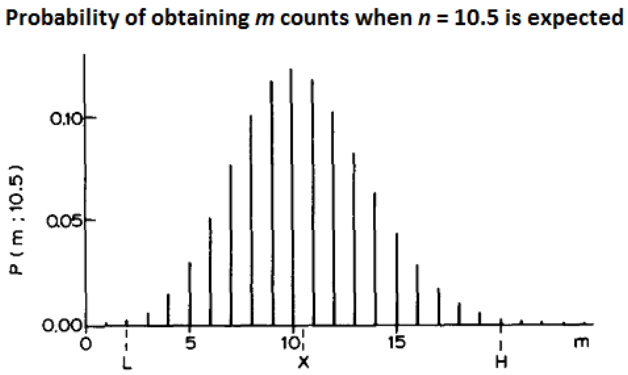

Figure 8.6. Poisson distribution. The graph shows the probability of obtaining m counts in a bin if the expected firing rate is 10.5. L and H represent the lower and upper limits of the 95% confidence interval. [Abeles 1982]

The lower and upper confidence limits can then be obtained by finding m spikes, where $P(m;n) < 0.025$ (lower confidence limit) and $P(m;n) > 0.975$ (upper confidence limit). For cases $n < 30$ an approximation of the Poisson distribution has shown to be accurate enough for a 95% confidence interval [Abeles 1982]. Assuming a normal distribution with an average of n and a standard deviation of $\sqrt{n}$ the lower (L) and upper (H) confidence limits can be approximated as:

$$L = x - 2.58\sqrt{x} \tag{8.3}$$

$$H = x + 2.58\sqrt{x} \tag{8.4}$$

If the firing rate of a channel exceeded the 95% confidence interval in three out of five days the channel was chosen to be used for further analysis given that it was related to hindlimb activity. In figure 8.7 an example is shown for channel 8 from rat 3.

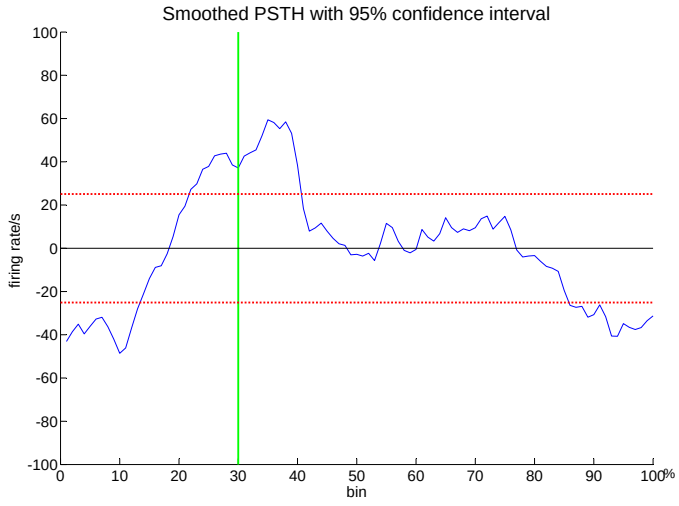

Figure 8.7. Application example of the 95% confidence interval in order to detect significant modulations in the IC signals.

Analysis of intra-cortical micro-stimulation

The data from the IC micro-stimulation was analysed qualitatively in order to document the channels related to the right hindlimb. A color mapping of all 16 channels was used to represent the different movement registered when stimulating on each single channel.

8.3 Analysis of iEMG

Each of the four monopolar EMG channel was digitally band-pass filtered (50-300 Hz) to remove artefacts and a band-stop filter (49.5-50.5 Hz) was applied to remove 50 Hz noise. Subsequently the signals from two different recording sites within the same muscle were subtracted from each other to obtain the actual bipolar EMG signal. Further, to translate the filtered EMG signal to a single positive polarity the signal was rectified. Similar to the IC recording the rectified EMG was analysed in relation to the gait cycle events which means that it was separated in time windows which correspond to a full gait cycle. In order to do so the EMG was synchronized to the initial trigger signal of the Vicon system when the video recording was started. The average muscle activity was calculated according to the amount of gait cycles used to create the corresponding PSTH.

Normalization in gait duration

Similar to the kinematic data EMG recordings for each gait cycle duration were normalized to percentage whereby 100 % corresponds to the individual gait cycle duration. p

Results 9

The following chapter presents the results from the experimental recordings. Four out of the five rats which underwent surgery were included in the experimental sessions, because one rat was not able to walk on the treadmill after the surgical procedure. The results contain data from two rats (rat 1 and rat 3), which was due to various problems with the video recordings and the iEMG data from the remaining two rats. The stated results are preliminary and therefore can only give an indication about the activity of the motor cortex during locomotion. The applied statistical calculations are applied on means of a high number of gait cycles. Results were considered statistically significant at $p < 0.05$.

9.1 Intra-cortical micro-stimulation

The results from two IC micro-stimulation of rat 1 and rat 3 are shown in figure 9.1. For rat 1 the channels 1-4, 7 and 9 were solely related to movements of the right hindlimb (green), whereas the rest of the channels were not only related to movements of the right hindlimb (yellow). For rat 3 the channels 2, 3 and 8 were solely related to movements of the right hindlimb, whereas the rest of the channels were either not only related to movements of the right hindlimb or the micro-stimulation did not elicit any reaction (red).

Figure 9.1. Results from the IC micro-stimulation applied on rat 1 and rat 3. Channels where only movements of the right hindlimb were observed are indicated with green. The values in the green circle represent the stimulation intensity in μA. The yellow color represent channels where not only movements related to the right hindlimb were observed. The red color represents channels where no reaction was observed (max stimulation intensity: 500 μA.)

The process of selecting channels of interest from the IC recordings was based on the calculated confidence limits (example see appendix E). For rat 1, the channels that exceeded the 95 % confidence interval in 3 out of 5 days were number 7 and 11, where channel 7 was the only one related to hindlimb movement. For rat 3, the channels that exceeded the 95 % confidence interval in 3 out of 5 days were number 6 and 8, where channel 8 was the only one related to hindlimb movement.

9.2 Gait duration and number of gait cycles

In table 9.1 the average duration for swing phase, stance phase and a complete gait cycle is listed for the different locomotor tasks. The average time duration for a gait cycle was 0.535 s (Swing phase 0.164 s and stance phase 0.359 s) from a total number of 3843 gait cycles for all tasks.

Table 9.1. Average gait duration and number of gait cycles obtained for each rat for the different tasks at treadmill velocity 29 cm/s, where *n* is the total number of gait cycles for the given task.

Task	n	Gait duration [s]	Swing duration [s]	Stance duration[s]
Rat 1				
Horizontal	911	0.490	0.155	0.335
Uphill	623	0.531	0.154	0.378
Initiation	138	0.413	0.138	0.275
End	276	0.515	0.175	0.340
Mean		**0.487**	**0.155**	**0.332**
Rat 3				
Horizontal	807	0.590	0.173	0.417
Uphill	698	0.582	0.175	0.407
Initiation	130	0.576	0.157	0.419
End	260	0.584	0.184	0.400
Mean		**0.583**	**0.172**	**0.412**
Overall	**3843**	**0.535**	**0.164**	**0.359**

9.3 Stability of the signals between days

To investigate the stability of the IC signals and the iEMG signals over the five recording days the correlation coefficient *r* was calculated (see appendix E). The coefficient was calculated for the iEMG activity for one muscle (BF) and the one IC channel related to hindlimb activity for each rat, respectively. In total 10 combinations were possible between the five days.

Stability for rat 1

The correlation coefficient for the recorded IC signals from channel 7 was in the range 0.12-0.78 with a mean of 0.47 ± 0.22 (mean ± standard deviation). The results show that the correlation of the IC signals was high ($r \geq 0.5$) in 4 out of 10 combinations of days. The correlation coefficient for the recorded EMG data for the BF muscle was in the range of 0.89-0.99 with a mean of 0.96 ± 0.03. Thus, the EMG signals were stable over the five recording days.

Stability for rat 3

The correlation coefficient for the recorded IC signals for channel 8 was in the range 0.04-0.89 with a mean of 0.59 ± 0.29. The correlation coefficient revealed a high correlation ($r \geq 0.5$) in 7 out of 10 combinations of days. For the recorded EMG data the correlation coefficient for the BF muscle was in the range of 0.87-0.99 with a mean of 0.95 ± 0.04. Similar to rat 1 the results show a high stability for the EMG signals over all five recording days.

9.4 Horizontal locomotion

Comparison between horizontal locomotion and steady recordings

In order to verify that the neural firing rate in M1 increased during locomotion IC signals from three recordings days were compared. A paired two-sample t-test was performed between recordings from horizontal locomotion and steady control recordings were the rat was at rest (see appendix E). The test showed that the firing rate between horizontal locomotion and steady recordings was significantly different for both rats for three different days, meaning that the firing rate of neurons in the motor cortex was significantly higher during locomotion compared to when the rat was not moving.

Rat 1 - Horizontal locomotion

Figure 9.2 shows the results for rat 1 during horizontal locomotion. The angle of the heel, the firing rate of one IC channel and the EMG amplitude of BF and VL is presented. Blue lines indicate the average of the single days while the red line indicates the overall average. The magnitude of the mean heel angle was in the range 30°-115°. The mean firing (spikes/s) rate for channel 7 revealed a peak around the touch down of the foot. The mean EMG amplitude of both muscles was low during the swing phase and increased steeply at the time before the touch down (at 32 % of gait cycle duration) while VL is activated before BF. The EMG activity of the BF increased until the maximum was reached shortly after the touch down (at ≈ 35 % of gait cycle duration). Afterwards it decreased slowly until the end of the stance phase with a temporary plateau between 55 % - 75 %. The EMG activity of the VL started to increase after the lift off and continued through out the stance phase until the maximum was reached at around 75 % of gait cycle duration, followed by a strong drop in amplitude. The magnitude of the EMG signals was in the range of 0.04-1.8 mV.

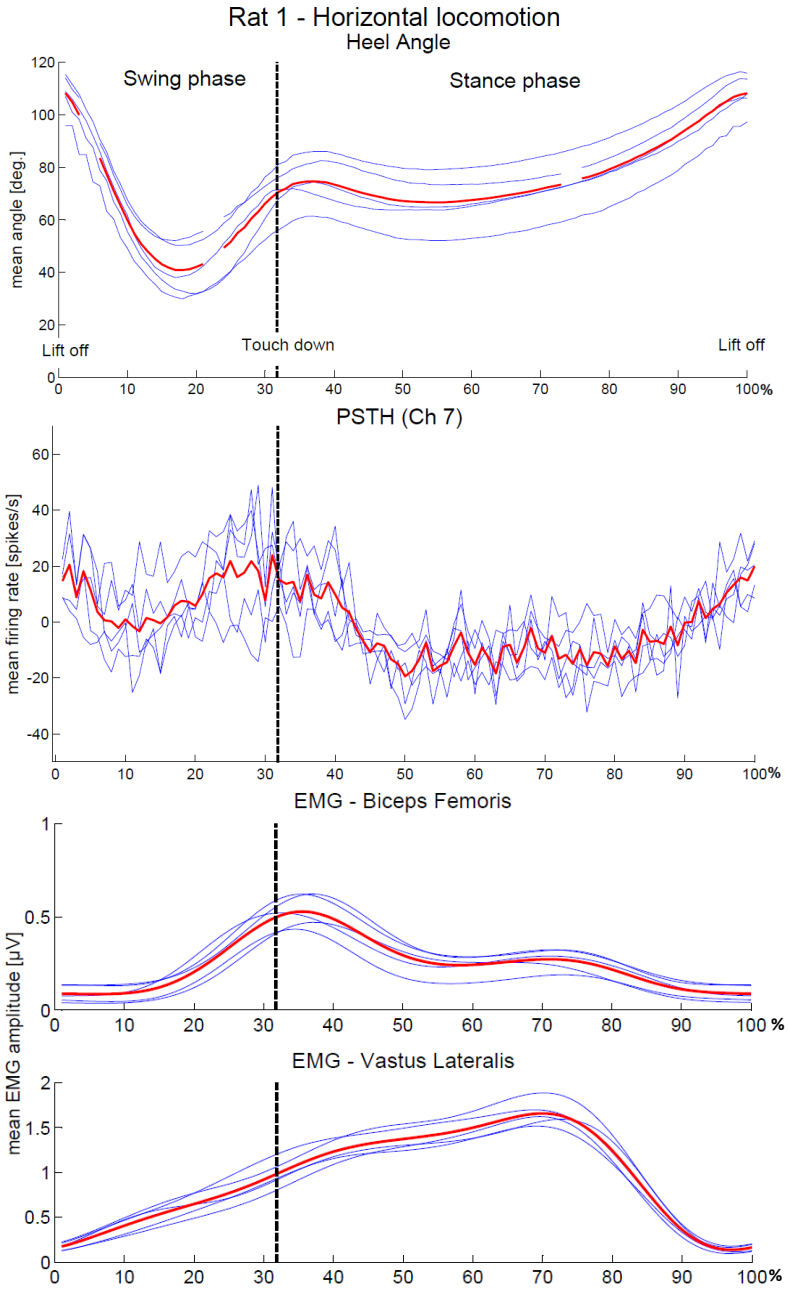

Figure 9.2. Results for rat 1 from horizontal locomotion. Shown are the mean kinematic angle of the heel, the mean firing rate (spikes/s) of channel 7 and EMG of BF and VL. All plots are in percentage of gait duration. The blue lines indicate the mean for each of the five recording days while the red line is the mean of all recording days (911 gait cycles). The dashed horizontal line indicates the touch down of the foot (32 %).

Rat 3 - Horizontal locomotion

Figure 9.3 shows the results for rat 3 during horizontal locomotion. The magnitude of the mean heel angle was in the range of about 40°-120°. The mean firing rate for channel 8 revealed the highest amplitude around the touch down of the right foot (at 29 % of gait cycle duration). The course of EMG activity of the BF and the VL was similar to rat 1. However, the amplitude of VL

increased later in rat 3, just before the touch down. The magnitude of EMG activity for both muscles was in the range of 0.01-0.16 mV, which was significantly lower compared to the range of the EMG amplitude of rat 1 ($\approx 1/10$).

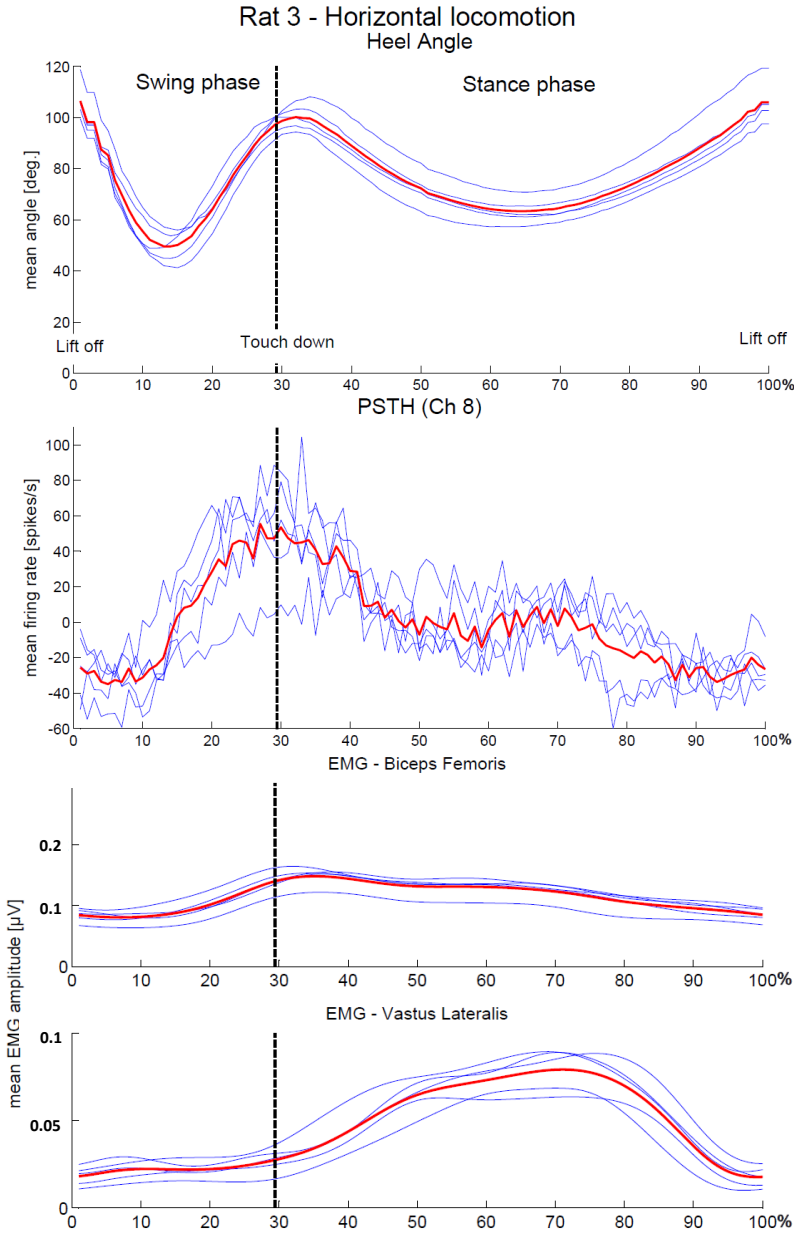

Figure 9.3. Results for rat 3 from horizontal locomotion. Shown are the mean kinematic angle of the heel, the mean firing rate (spikes/s) of channel 8 and EMG of BF and VL. All plots are in percentage of gait duration. The blue lines indicate the mean for each of the five recording days while the red line is the mean of all the five recording days (807 gait cycles). The dashed horizontal lines indicate the touch down of the foot (29 %). Note the small EMG amplitude for both BF and VL.

9.5 Uphill locomotion

Rat 1 - Uphill locomotion

Figure 9.4 shows the results for rat 1 during uphill locomotion. The magnitude of the EMG signals was in the range of 0.06-2.1 mV.

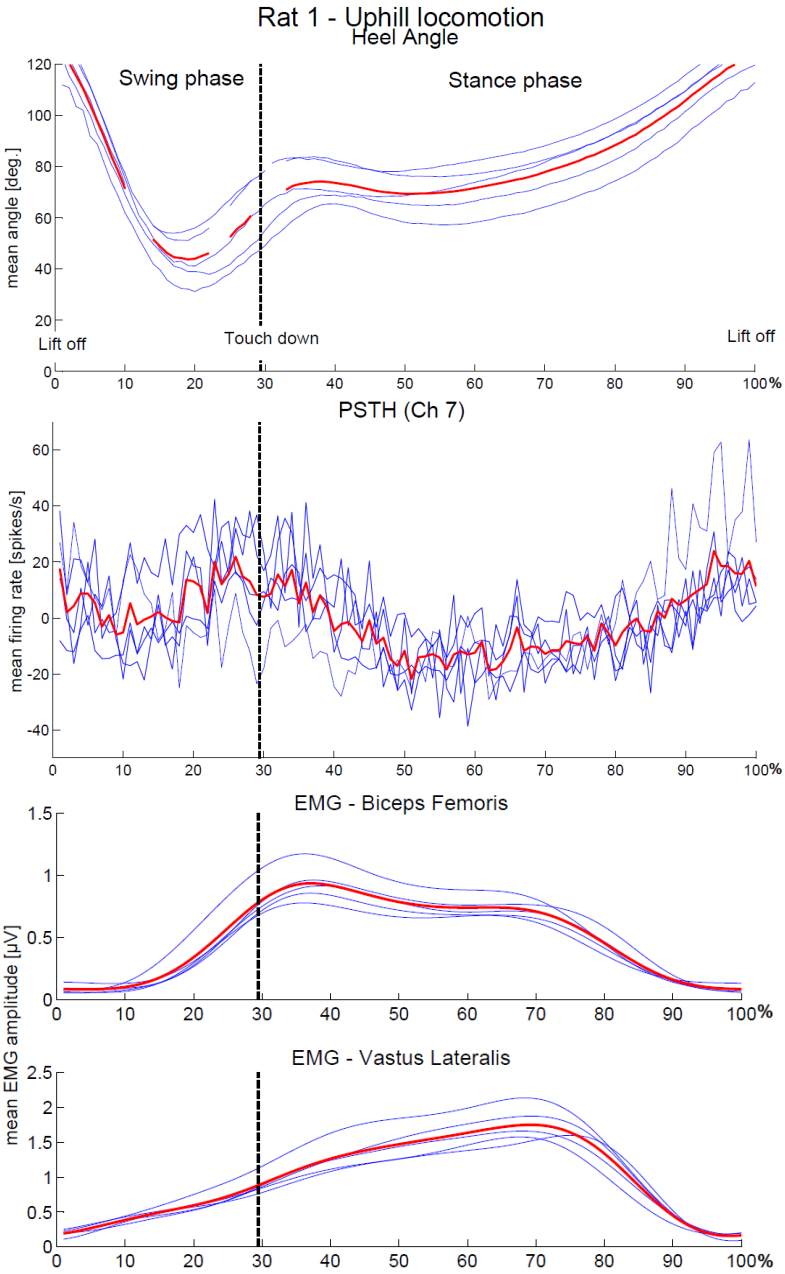

Figure 9.4. Results for rat 1 from uphill locomotion. Shown are the mean kinematic angle of the heel, the mean firing rate (spikes/s) of channel 7 and EMG of BF and VL. All plots are in percentage of gait duration. The blue lines indicate the mean for each of the five recording days while the red line is the mean of all recording days (623 gait cycles). The dashed horizontal line indicates the touch down of the foot (29 %).

Rat 3 - Uphill locomotion

Figure 9.5 shows the results for rat 3 during uphill locomotion. The magnitude of the EMG signals was in the range of 0.01-0.27 mV.

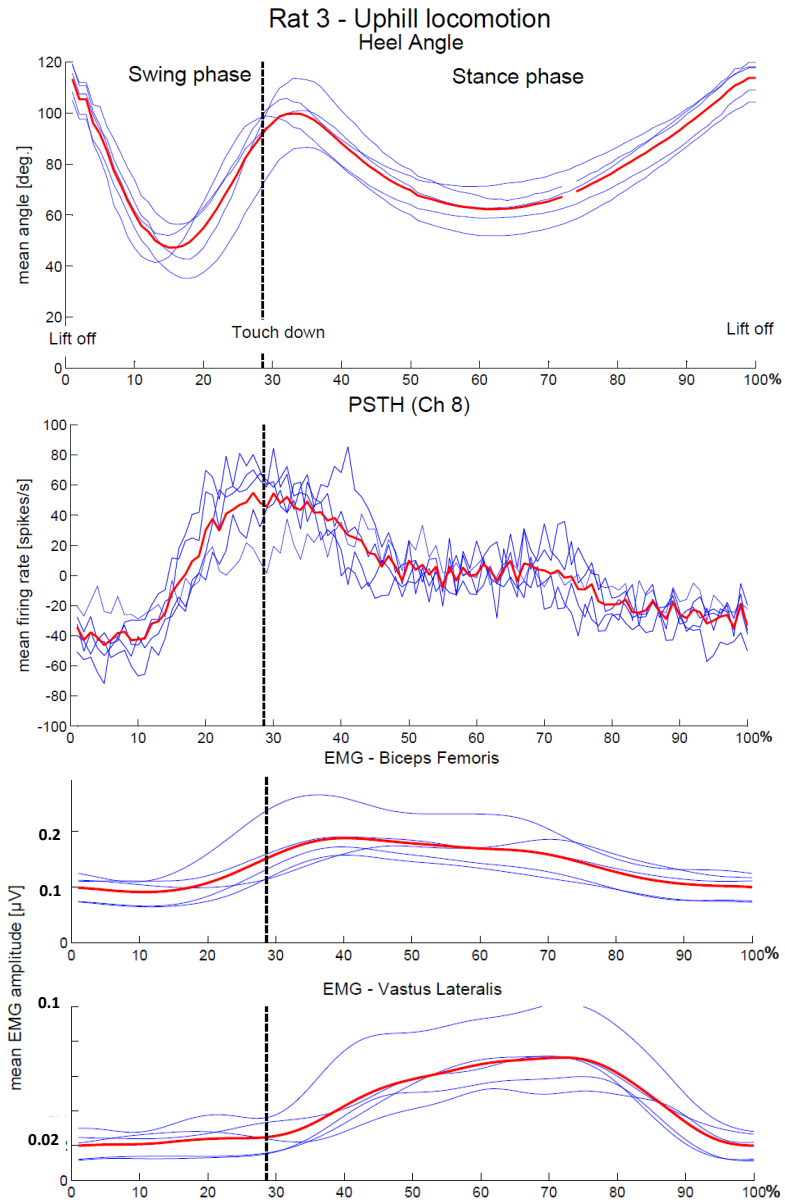

Figure 9.5. Results for rat 3 from uphill locomotion. Shown are the mean kinematic angle of the heel, the mean firing rate (spikes/s) of channel 8 and EMG of BF and VL. All plots are in percentage of gait duration. The blue lines indicate the mean for each of the five recording days while the red line is the mean of all the five recording days (698 gait cycles). The dashed horizontal lines indicate the touch down of the foot (28 %). Note the small EMG amplitude for both BF and VL.

9.6 Comparison between horizontal and uphill locomotion

Rat 1 - Horizontal versus uphill locomotion

Figure 9.6 shows the results for rat 1 when comparing horizontal and uphill locomotion as average over all days. The kinematic angles and the firing rate show a similar shape for the two different locomotor tasks. Comparing the area enclosed from the graphs which represent the firing rates a smaller area is enclosed for uphill locomotion equalling approximately 92.5 % of the area for horizontal locomotion. Significant difference ($p < 0.05$) was observed for the EMG amplitude for BF between the horizontal and uphill locomotion. During uphill locomotion the EMG activity in BF was approximately as twice as big compared to horizontal locomotion ($p < 0.05$). However, there was no significant difference in EMG activity for the VL during horizontal and uphill locomotion.

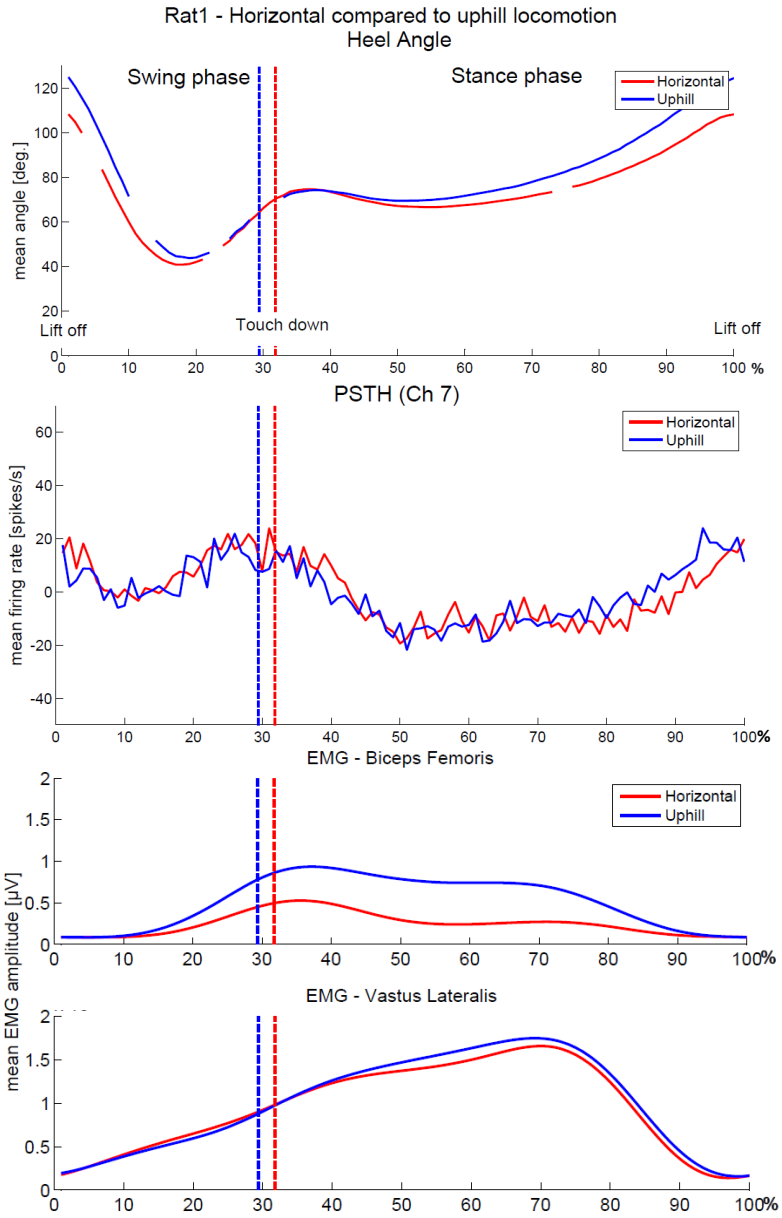

Figure 9.6. Comparison of the results for rat 1 from horizontal (red line - 911 gait cycles) and uphill locomotion (blue line - 623 gait cycles). Shown are the mean kinematic angle of the heel, the mean firing rate (spikes/s) of channel 7 and EMG of BF and VL. All plots are in percentage of gait duration. The vertical dashed lines indicate the touch down of the foot.

Rat 3 - Horizontal versus uphill locomotion

Figure 9.7 shows the results for rat 3 when comparing horizontal and uphill locomotion as average over all days. As in rat 1 the kinematic angles and the firing rate show a similar shape for the two different locomotor tasks. Comparing the area enclosed from the graphs which represent the firing rates a bigger area is enclosed for uphill locomotion equalling approximately 110 % of the area for horizontal locomotion. The EMG amplitude for BF was twice as big for uphill locomotion compared to horizontal locomotion and therefore significantly different.

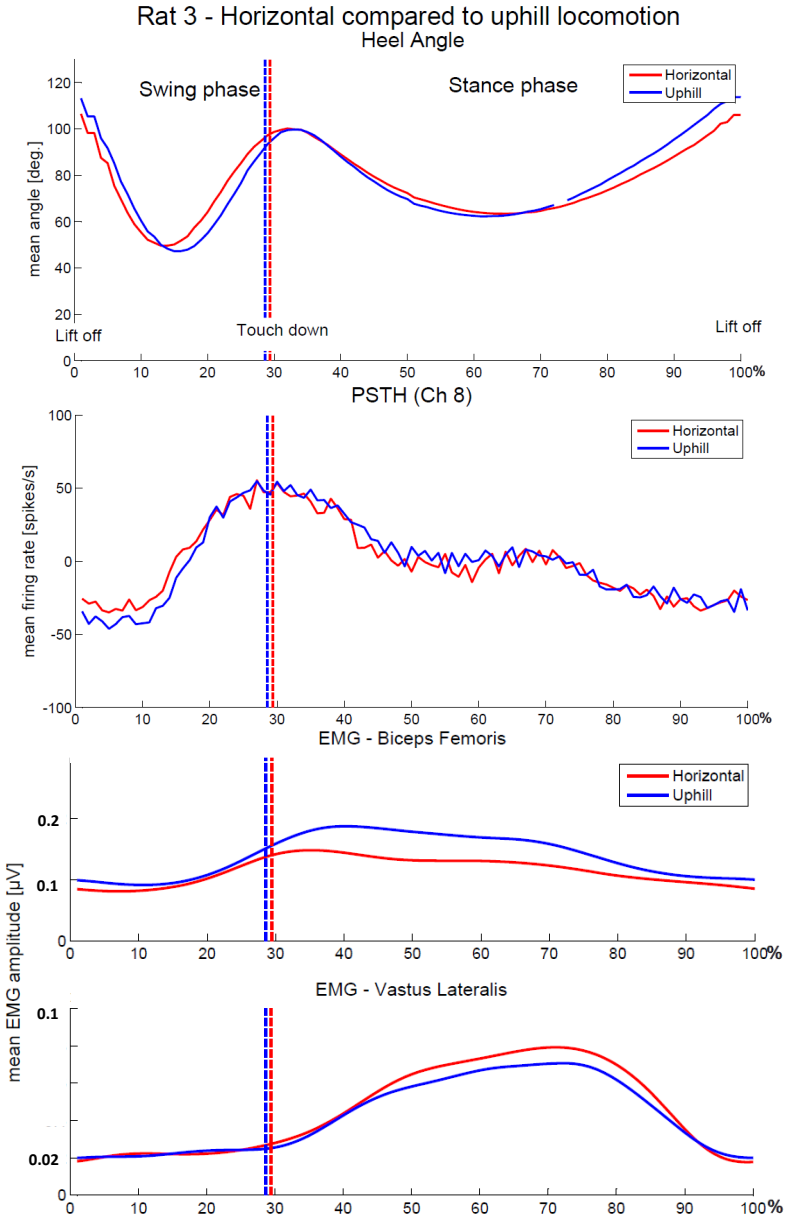

Figure 9.7. Comparison of the results for rat 3 from horizontal (red line - 807 gait cycles) and uphill locomotion (blue line - 698 gait cycles). Shown are the mean kinematic angle of the heel, the mean firing rate (spikes/s) of channel 8 and EMG of BF and VL. All plots are in percentage of gait duration. The vertical lines indicate the touch down of the foot for each task.

9.7 Initiation and ending phase of locomotion

Initiation phase of locomotion

For the investigation of the initiation phase of locomotion only the first step was analysed after the treadmill was started. The mean firing rate of 138 initial steps from rat 1 were compared to the mean firing rate during continuous horizontal locomotion (911 gait cycles, same rat). Results are shown in figure 9.8. Both graph show a similar course (r = 0.68) whereby the enclosed area from the graph that represents initiation of locomotion is only half (≈ 51 %) of

the area enclosed by the graph from the horizontal locomotion.

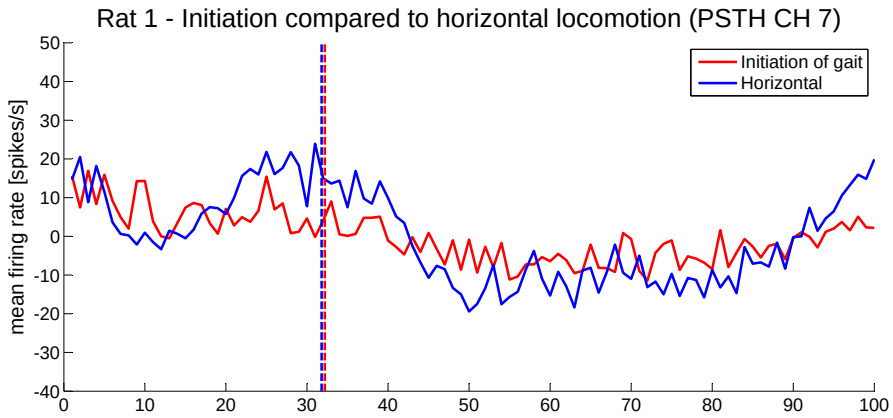

Figure 9.8. Results for rat 1 from the analysis of the initial step (138 gait cycles, red line) compared to horizontal locomotion (911 gait cycles, Blue line) obtained over five days, respectively. Shown are the mean firing rate (spikes/s) of channel 7 plotted in percentage of gait duration. The vertical lines indicate the touch down of the foot for each task.

Figure 9.9 shows the mean firing rate of 130 initial steps from rat 3, compared to the mean firing rate during continuous horizontal locomotion (807 gait cycles, same rat). Both graph have a similar course (r = 0.67) but the amplitude is significantly different. The graph representing initiation of locomotion encloses only 30 % of the area from horizontal locomotion.

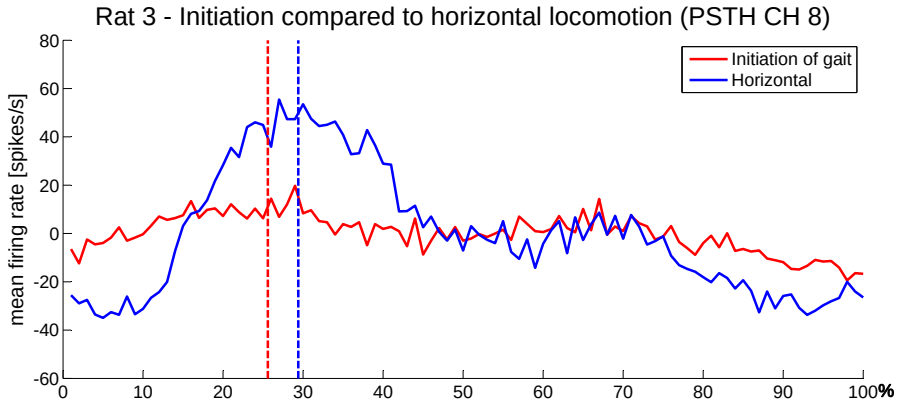

Figure 9.9. Results for rat 3 from the analysis of the first steps (130 gait cycles, red line) compared to horizontal locomotion (807 gait cycles, blue line) obtained over five days, respectively. Shown are the mean firing rate (spikes/s) of channel 8 plotted in percentage of gait duration. The vertical lines indicate the touch down of the foot for each task.

Ending phase of locomotion

For the investigation of the ending phase of locomotion the last two gait cycles were analysed before the treadmill was stopped. For rat 1 the mean firing rate of 276 gait cycles, obtained over the five recording days were analysed and compared to continuously horizontal locomotion (807 gait cycles). Results are shown in figure 9.10. Both graph show a similar course (r = 0.78)

whereby the enclosed area from the graph that represents the ending phase of locomotion is ≈ 21 % bigger than the area enclosed by the graph from the horizontal locomotion.

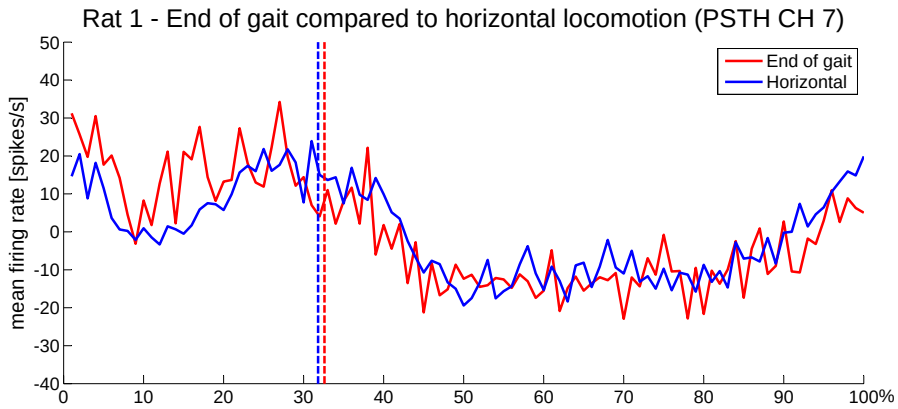

Figure 9.10. Results for rat 1 from the analysis of the last two gait cycles before locomotion ended (276 gait cycles, red line) compared to horizontal locomotion (911 gait cycles, blue line). Shown are the mean firing rate (spikes/s) of channel 7 plotted in percentage of gait duration whereby the The vertical lines indicate the touch down of the foot for each task.

Figure 9.11 shows the mean firing rate for the last two gait cycles before the treadmill was stopped (260 gait cycles) for rat 3, compared to continuously horizontal locomotion (807 gait cycles). Both graph have a similar course ($r = 0.94$) whereby the enclosed area from the graph that represents the ending phase of locomotion equals only 85 % of the area enclosed by the graph from the horizontal locomotion.

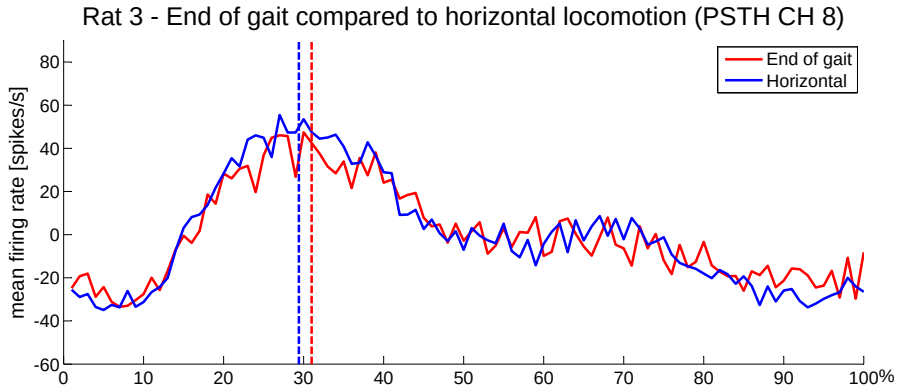

Figure 9.11. Results for rat 3 from the analysis of the last two gait cycles before locomotion ended (260 gait cycles, red line) compared to horizontal locomotion (807 gait cycles, blue line). Shown are the mean firing rate (spikes/s) of channel 8 plotted in percentage of gait duration. The vertical lines indicate the touch down of the foot for each task.

9.8 Encoding of gait in M1

The comparison between horizontal locomotion and steady recordings has shown that the motor cortex is activated during locomotion (see section 9.4). To further investigate how the motor cortex encodes information about gait control, IC channels related to hindlimb activity

were correlated with kinematic angles and muscle activity, respectively. In order to do so, one part of the gait cycle (10 % - 40 %) of the IC signal was correlated to another part of the gait cycle (20 % - 50%) of the kinematics and muscle activity, respectively. The results are listed in table 9.2.

Table 9.2. Overview of the correlation (r) between the IC signal and the kinematics or muscle activity.

Task	**Rat 1**	**Rat 3**
IC versus kinematics		
Heel angle	0.88	0.50
Toe angle	0.50	0.84
IC versus EMG		
BF	0.75	0.93
VL	0.69	0.61

PART III

Synthesis

Discussion 10

10.1 Methodological choices

Number of rats

Five out of ten trained rats were chosen for electrode implantation. Considering the limited time frame for the project, we chose the five rate that performed best on the treadmill after the given training period. Three out of the five operated rats were rejected in the course of the study due to various problems. One of the rejected rats was not able to perform locomotion on the treadmill with the implanted electrodes, which could be due to damages in the brain or the muscles obtained from the surgical procedure. In the case of another rat several video recordings were corrupted, meaning that a steady picture was shown while the frame number continuously increased, making it difficult to apply automatic tracking and detect the events of interest in the gait cycle. The third rat showed only very few changes of activity in the EMG recordings which might be caused by a misplacement of the implanted EMG wires. Finally, the results from only two rats are presented in this study. Clearly, a higher number of animals would be advantageous in order to validate the findings and conclude statistically valid outcomes.

Intra-cortical surgery

The implementation site for the micro-wire electrode array was chosen based on two different mapping studies [Fonoff et al. 2009, Neafsey et al. 1986]. By applying micro stimulations to the different channels it was possible to document to which areas within the topographical map of the motor cortex each channel of the electrode implant corresponded to. The results from this revealed a low number of channels related to the hindlimb. Only 3 and 6 channels were found to be related to hindlimb, which was below our expectations. Of the found channels only 1 out of 16 channels in rat 1 and 3 were selected for further investigation, because of low cortical activity in the other channels related to the hindlimb.
Although the corresponding channels were found in the upper half of the electrode array the pattern was not the same for both rats. This could be due to variability in the surgical procedure or physiological differences. The brain structure of the rat seems to be not as consistent as in humans, which corresponds to the study by Neafsey et al. [1986] concluding that the internal organisation of the pattern of movement varies significantly between animals. Further, the small size of the rats brain makes it difficult to place the electrode at the same spot for the different rats. Another reason for low correspondence of channels to hindlimb activity could

have been a mistake in the evaluation procedure when the micro stimulations were applied. The animal was sometimes very anxious during the procedure making it difficult to observe a reaction because the hindlimb muscles were not completely relaxed. Finally, the quality of the electrode could also have played a role because it was known that the distance between the micro-wires varied from electrode to electrode.
In order to gain more knowledge about the location of the electrode in the motor cortex a histology of the brain could have been assessed to compare and verify the placement of the implant. However, this method can only be applied after the electrode is already implanted. A possibility of verifying the placement before implanting the electrode could be the accomplishment of a mapping study during the surgery just before the implantation of the IC electrode [Neafsey et al. 1986].

Intra-muscular surgery

The used method for measuring iEMG was chosen due to the minimal influence on the range of leg movement and the stability in signal transmission for over two weeks after the time of implantation [Pearson et al. 2005]. The joint angles measured in this study were stable over the five recording days and lay in the same range reported in previous studies [Gillis & Biewener 2001, Thota et al. 2005, Gruner et al. 1980]. However, in order to determine the influence of the implant more accurately a control video recording could have been obtained from each animal prior to the surgical procedure and compared to rats kinematics after the surgery.
The results of the iEMG data showed a big difference in the amplitude between the two rats which most likely is caused by a variation in the placement of the iEMG leads in the muscle. The small anatomy of the rats hindlimb and the fact that the VL is positioned under the BF make it difficult for the surgeon to locate the intended muscle and place the leads in the same depth for the different animals. A dissection could have been accomplished after the experiment was carried out to verify the position and condition of the iEMG electrodes. The encapsulation process of the implant, which describes the enclosing of a foreign body in fibrous sheaths also affects the amplitude. Over time the amplitude decreases due to an increase in resistance [Reichert 2007]. However, this development was not observed in this study.
Finally, the manufacturing process of the electrodes (variation in length of the removed Teflon insulation) might also be a factor which influences the magnitudes of the measured muscle activity.

Evaluation of experimental tasks

For some of the rats a change in the behaviour was observed after the surgery, which included strong reaction to human contact making the handling during the experimental tasks difficult. This might indicate that the surgery had a painful and stressful impact on the animals and/or that they were still in pain 2-3 days after the surgery when the recording of data started. The challenge in choosing the experimental tasks and the corresponding treadmill velocity was obtaining a stable walking pattern, and a high number of events at the same time. During the experimental procedure it was observed that the animals had difficulties in accomplishing the experimental tasks of protocol. It might be that the chosen treadmill speed (29 cm/s) was set too high as well as the number of sessions and tasks per day. Although, no fatigue phenomenon was observed when the protocol was tested prior the surgical procedure. As a consequence the rats had to be given more time to rest between the tasks and in the worst case recording

sessions had to be postponed to another day. A drawback of postponing recordings sessions was that the threshold for the IC recording had to be adjusted again and was therefore not exactly the same. The different threshold levels might have influenced the results whereby the actual effect is unknown. Reducing the number of tasks for each day and/ or the treadmill velocity could have eliminated this problem. The protocol of the experimental tasks was not randomised meaning that the influence of fatigue was observed only in some of the tasks. This might have biased the results as well.

Tracking and event detection

The event detection was based on video recordings using distinguishable landmarks to detect the events of interest in the gait cycles and remove erroneous data. The event detection could have been improved by adding more features for verification of the properties of the single gait cycles, for example dividing the step cycle into the multiple subphases F, E_1, E_2 and E_3 mentioned by Kandel et al. [2000]. If more was known about the properties of the gait cycle more accurate exclusion criteria could have been implemented.
A permanent marker was used to indicate the location for the reflective markers stuck on the hindlimb. However, the dark color vanished already after only one day leading to minimal variations in the placement of the reflective markers between the days. This could partly explain the change in the joint angles observed between days. The reliability of the reflective marker position could have been improved by skin tattooing the rat with permanent ink as done in the study by Thota et al. [2005], thereby allowing identical marker placement over longitudinal studies.

10.2 Results

IC recordings

The results from the IC recordings show a significant increase of the neural firing rate in the M1 during locomotion compared to steady control recordings where the rats were at rest. The results support the view that the motor cortex plays an important role in controlling the muscle activity during locomotion [Armstrong 1986, Drew 1988, Drew et al. 2002]. The course of the firing rate appears to be stable over the five recording days for the channels related to hindlimb movement. In one rat the correlation coefficient was high ($r \geq 0.5$) in 7 out of 10 combinations of days. In the other rat the correlation was high ($r \geq 0.5$) in 4 out of 10 combinations of days. The stability of the signals supports the reliability of the results and is important regarding the development of for example a BCI walking assistant [Wolpaw et al. 2006]. The mean firing rate from the channels related to hindlimb from both rat 1 and 3 showed a peak just before the foot touch down (beginning of stance phase) in all the experimental tasks. This could indicate that the M1 prepares the hindlimb to support the weight of the foot touch down and through out the stance phase.

iEMG

This study shows a relationship between kinematics and iEMG of the VL and the BF during treadmill locomotion. The results suggest a major function of VL during the stance phase of the gait cycle. The EMG activity of VL started to increase in the end of the swing phase and

reached a significantly higher level during the stance phase. The results are in agreement with other studies in which the muscle is described as a primary extensor of the knee which also supports the weight of the animal during stance [Gillis & Biewener 2001, Schumann et al. 2006]. In contrast, the EMG activity of BF started to increase in the early phase of the stance phase and revealed a lower amplitude, but a more continuous activation pattern than VL. Our observations correlate with other studies on rodents by Thota et al. [2005] and Schumann et al. [2006] and show that the BF is important in stabilizing the hindlimb during touch down and through out the stance phase. Both muscles had in common a low activity during the swing phase. The stability of the EMG was very high ($r > 0.9$) over the five recording days for both rats with a mean correlation coefficient of 0.96 for rat 1 and 0.95 for rat 3.

Comparison between uphill and horizontal locomotion

The mean firing rate for uphill and horizontal locomotion showed similar shape demonstrating continuity between the curves for both rats. However, no significant difference was found in the firing rate during inclined locomotion. Therefore the project hypothesis needs to be rejected concerning an expected increase of the neural firing rate in M1 during inclined locomotion. Our results are in agreement with findings of former studies by Armstrong & Drew [1984] and Armstrong [1986] who found only very modest changes in mean rate or peak rate during uphill locomotion at 10° of inclination. Even so in this study an inclination angle of 15° was used the steeper slope did not have an effect on the amplitude of IC signals as assumed in the project hypothesis.
A remarkable increase in EMG amplitude was found for BF during uphill locomotion compared to horizontal locomotion. This correlates with studies by Armstrong & Drew [1984] and Armstrong [1986] who observed that inclined locomotion had little effect on step duration but almost doubled the amplitudes of flexor and extensor muscles.

Initiation and ending of gait

The mean firing rate for the initiation of locomotion (first step after treadmill belt was started) showed a high correlation for both rats and no increase in firing rate was found in contrast to horizontal locomotion. On the contrary, the firing rate appears to be shallower, particularly for rat 3. An explanation for this could be the low number of analysed gait cycles (138 and 130 gait cycles) collected for the initiation of locomotion. This gives the data an uncertainty compared to horizontal locomotion (911 and 807 gait cycles), where almost ten times more gait cycles were collected. The variation in gait cycle duration for the initial steps was also not accounted, because this would result in an even lower number of analysed gait cycles (< 100) making the calculated PSTH less valid. Therefore a higher number of gait cycles with similar duration needs to be collected for the initiation phase.
The mean firing rate for the end of locomotion (last two steps after the treadmill belt was stopped) showed similar shape demonstrating continuity between the curves with high correlation for both rats and no increase was found in the firing rate. The number of gait cycles for the end of locomotion was twice as high (276 and 260 gait cycles) as for the initiation. This could explain the higher correlation and similar shape in the curves compared to the initiation of locomotion. Overall results in this study found no increase in the cortical cell discharge in the M1 in rats during the initiation and ending phase of locomotion, meaning the null hypothesis has to be rejected.

Encoding of gait control in M1

Even though no increased firing rate for M1 was found between the different locomotor tasks, a high correlation was found between IC signals (10%-40% of gait cycle duration) compared to kinematics and muscle activity (20%-50% of gait cycle duration). The 10 % difference in gait cycle duration between the two correlated windows equals a delay in time of approximately 50-100 ms. This period might indicate the time shift between the sending of a motor command from the M1 until it elicits an activation of the target muscle. However, the encoding of muscle activation in M1 seems to be a complex problem and a higher number of IC channels is needed to validate that we have sampled muscle activation commands. Besides, a higher number of channels may also reveal temporal dynamics between neural populations in the hindlimb area.

Future perspective

The limited time frame of the project did not allow us to analysis the complete amount of the recorded data. Besides uphill locomotion another task of the experimental protocol implied downhill locomotion. The analysis of this data might give an indication how the M1 is activated during downhill locomotion which would be from interest for future work in that field of animal studies. Further, development of the study could be to focus on the possibility of observing dynamical processes in the M1 corresponding to muscle activation. In order to do so more rats and IC channels related to hindlimb movement are needed. This could be realized for example by a mapping study of M1 for the individual animals before the implantation of the IC electrode. Since gait is realized by synergies of several different muscles it might be also necessary to implant iEMG electrodes in other muscles additionally to the ones investigated in this study (BF and VL). Our results together with future research provide basis for a better understanding about the neural activity and muscle activity in the motor cortex. A future approach could imply the use of recorded IC signals in order to develop a predicting model of the muscle activation in the hindlimb.

Conclusion 11

Motor disorders are affecting millions of people worldwide, depriving the ability of producing controlled movements. In particular motor disorders affecting walking are of great interest, yet being a complex problem to solve. One approach is to create a BCI system to restore functionality in persons with motor disorders. To address the problem of restoring walking the investigation of processes in the motor system under normal conditions provides a fertile ground for future research in BCI systems. The use of IC recordings has the advantage of studying changes in neural activity inside the cortex over a longer period of time. The aim of the study was to investigate the role of the M1 in the initiation and ending phase of gait and the influence of slope during locomotion in healthy rats.

Ten Sprague-Dawley rats were trained to walk on a horizontal and inclined treadmill with a velocity of 29 cm/s and five animals were chosen for implantation. A 16 channel micro-wire electrode array was chronically implanted in the hindlimb region of the M1 and a 4 channel intramuscular micro-wire EMG electrode was implanted in the muscles VL and BF of the right hindlimb. IC signals and iEMG data were recorded simultaneously with high-speed videography over five days while the rat performed locomotion on a horizontal and inclined treadmill. The PSTH was calculated in percentage of gait duration prior to the kinematic events foot lift off and foot touch down in order to analyse the IC recordings.

Of the five implanted rats the results from two rats were analysed. Three rats were rejected for further analysis because the recorded data from two animals was partly unusable and the third rat was physically not able to accomplish the experimental tasks. For the two remaining rats the electrode position was verified by IC micro-stimulations whereby 6 channels (rat 1) and 3 channels (rat 3) were identified to be related to hindlimb activity. From the identified channels, one from each rat showed significant modulation related to hindlimb movement and was chosen for further analysis. The results obtained in this study showed that the neural firing rate and EMG curves appeared to be stable over the five recording days. The results from the IC recordings showed an significant increase ($p < 0.05$) in the firing rate of neurons in the hindlimb region of the M1 during locomotion compared to steady control recordings where the rats were at rest. The mean cortical cell discharge for all locomotor tasks showed a similar shape demonstrating continuity between the curves for both rats, however no increase was found in the neural firing rate between the different tasks. The EMG amplitude increased significantly in the BF muscle during the inclined locomotion task compared to horizontal locomotion.

In conclusion, our study suggests that the M1 does not play a major role in the initiation and ending phase of locomotion and during inclined locomotion. Therefore the project hypothesis needs to be rejected. However, the recorded synchronized data allows a temporal correlation of IC signals, EMG and kinematic parameters. Interrelationships of EMG activity and IC activity with the corresponding kinematics might indicate a quantitative assessment of certain phases in the gait cycle. It was shown that the EMG activity of VL and BF during treadmill locomotion could be precisely characterised whereby the different functions of both muscles during horizontal and inclined locomotion were revealed.
To our knowledge, this is the first study combining IC and iEMG recordings in rats to investigate the role of the M1 for different locomotor tasks. The applied method is a unique combination which permits the identification of IC and intramuscular co-ordination with respect to the gait cycle during locomotion. In summary our study is a good basis for future locomotion studies on rats and expands our knowledge about neural activity in relation to muscle activity in the motor cortex during gait.

Bibliography

M. Abeles (1982). 'Quantification, smoothing, and confidence limits for single-units' histograms'. Journal of Neuroscience Methods **5**:317–325.

R. M. Alexander (1984). 'Walking and Running'. American Scientist **7**2:348–354.

D. Armstrong & T. Drew (1984). 'Discharges of pyramidal tract and other motor cortical neurones during locomotion in the cat'. Journal of Physiology **3**46:471–495.

D. M. Armstrong (1986). 'Supraspinal contributions to the initiation and control of locomotion in the cat'. Neurobiology **2**6:273–361.

H. Aurlien, et al. (2004). 'EEG background activity described by a large computerized database'. Clinical Neurophysiology **1**15:665–673.

M. Bahr (2006). Brain Repair: Advances in Experimental Medicine and Biology. Springer.

I. Basler (2005). BASLER A600f USER'S MANUAL. Basler Inc.

D. Becker, et al. (2003). 'Restoring function after spinal cord injury'. The Neurologist. **9**(1):pp. 1–15.

N. Birbaumer (2006). 'Breaking the silence: Brain–computer interfaces (BCI) for communication and motor control'. Psychophysiology **4**3:517–532.

M. Boudreau & A. Smith (2001). 'Activity in rostral motor cortex in response to predictable force-pulse perturbations in a precision grip task'. Journal of Neurophysiology **8**6:1079–1085.

T. Brown (1911). 'The intrinsic factors in the act of progression in the mammal'. Proceedings of the Royal Society of London **8**4:308–319.

T. Carew (1985). Principles of Neural Science, chap. Posture and locomotion, pp. 478–486. New York: Elsevier/ North-Holland.

R. B. Chiasson (1994). Laboratory Anatomy of the White Rat. McGraw Hill.

M. M. Churchland, et al. (2007). 'Techniques for extracting single-trial activity patterns from large-scale neural recordings'. Current Opinion in Neurobiology **1**7:609–618.

K. A. Clarke & A. J. Parker (1986). 'A quantitative study of normal locomotion in the rat'. Physiology & Behavior **V**olume 38, Issue 3:345–351.

M. R. DeLong & T. Wichmann (2007). 'Circuits and circuit disorders of the basal ganglia'. Archives of neurology **6**4:20–24.

A. Despopoulos & S. Silbernagl (2003). Color Atlas of Physiology. Thieme.

T. Drew (1988). 'Motor cortical cell discharge during voluntary gait modification'. Brain Research **4**57:181–187.

T. Drew, et al. (2002). 'Contributions of the motorcortex to the control of the hindlimbs during locomotion in the cat'. Brain Research Reviews **4**0:178–191.

N. A. Fitzsimmons, et al. (2009). 'Extracting kinematic parameters for monkey bipedal walking from cortical neuronal ensemble activity'. Frontiers in Integrative Neuroscience **3**:1–19.

E. T. Fonoff, et al. (2009). 'Functional mapping of the motor cortex of the rat using transdural electrical stimulation'. Behavioural Brain Research **2**02:138–141.

H. Forssberg, et al. (1975). 'Phase dependent reflex reversal during walking in chronic spinal cats'. Brain Research **8**5:103–107.

C. R. Freed & B. K. Yamamoto (1985). 'Regional brain dopamine metabolism: A marker for the speed, deirection, and posture of moving animals'. Scienc **2**29:62–65.

A. Georgopoulos, et al. (1983). 'Spatial coding of movement: a hypothesis concerning the coding movement direction by motor cortical populations'. Experimental Brain Research **7**:327–336.

G. B. Gillis & A. A. Biewener (2001). 'Hindlimb muscle function in relation to speed and gait: in vivo patterns of strain and activation in a hip and knee extensor of the rat (Rattus norvegicus)'. The Journal of Experimental Biology **2**04:2717–2731.

Y. Giovanni & M. Lamarche (1985). 'A reappraisal of rat motor cortex organization by intracortical microstimulation'. Brain Research **3**44:49–61.

J. Gruner, et al. (1980). 'Effects of arrested cerebellar development on locomotion in the rat'. Experimental Brain Research **4**0:361–373.

A. C. Guyton & J. E. Hall (2005). Textbook of Medical Physiology. Saunders/Elsevier, 11 edn.

D. F. P. Hamers, et al. (2006). 'CatWalk-Assisted Gait Analysis in the Assessment of Spinal Cord Injury'. Journal of Neurotrauma **2**3:537–548.

S. Hattori, et al. (1994). 'Striatal dopamine turnover during treadmill running in the rat: relation to the speed of running'. Brain Research Bulletin **3**5:41–49.

L. Hochberg, et al. (2006). 'Neuronal ensemble control of prosthetic devices by a human with tetraplegia'. Nature **4**22:164–171.

D. Humphrey (1968). 'Representation of movements and muscles within the primate precentral motor cortex: Historical and current perspectives'. Federation Proceedings **4**5:2687–2699.

D. J. Jaanis & J. R. Wolpaw (2008). 'Brain-computer interfaces in neurological rehabilitation'. The Lancet Neurology **7**, Issue 11:1032 – 1043.

K. Jahn, et al. (2008). 'Supraspinallocomotorcontrol in quadrupeds and humans'. Progress in Brain Research **1**71:353–362.

W. Jensen, et al. (2006). 'A method for monitoring intra-cortical motor cortex responses in an animal model of ischemic stroke'. Engineering in Medicine and Biology Society, 2006. EMBS '06. 28th Annual International Conference of the IEEE pp. 1201–1203.

W. Jensen & P. J. Rousche (2005). 'Movement Discrimination Based On Rat Primary Motor Cortex Responses'. Neural Engineering, 2005. Conference Proceedings. 2nd International IEEE EMBS Conference on pp. 559–562.

J. John W. Clark & M. R. Neuman (1998). Medical Instrumentation - Application and Design. Wiley, 3rd edn.

S. Kakei, et al. (1999). 'Muscle and movement representations in the primary motor cortex.'. Science **2**85:2136–2139.

J. Kalat (1980). Biological Psychology. Belmont, CA: Wadsworth.

E. R. Kandel, et al. (2000). Principles of Neural Science. Mcgraw-Hill Professional, 4th edn.

A. Karayannidou, et al. (2009). 'Activity of pyramidal tract neurons in the cat during standing and walking on an inclined plane'. Journal of Physiology **5**87:3795–3811.

P. Kennedy & R. Bakay (1998). 'Restoration of neural output from a paralyzed patient by a direct brain connection.'. Neuroreport **9**(8):1707–1711.

B. Kolb & R. Tees (1990). The Cerebral Cortex of the Rat Cambridge. MIT Press.

M. A. Lebedev & M. A. Nicolelis (2006). 'Brain-machine interfaces: past, present and future'. Trends in Neuroscience **2**9:536–546.

M. LeDoux (2005). Animal models of movement disorders. Elsevier. Chapter A5 - Assessment of Movement Disorders in Rodents.

K. E. Misulis & T. C. Head (2003). Essentials of Clinical Neurophysiology. Butterworth-Heinemann, 3 edn.

T. Moritani, et al. (2004). Basic physiology and biophysics of the EMG signal generation, chap. 1, pp. 1–25. Wiley Interscience.

M. Morrow & L. Miller (2003). 'Prediction of muscle activity by populations of sequentially recorded primary motor cortex neurons'. Journal of Neurophysiology **8**9:2279–2288.

J. Muthuswamy, et al. (2005). 'An array of microactuated microelectrodes for monitoring single-neuronal activity in rodents'. IEEE Transactions on Biomedical Engineering **5**2:1470–1477.

L. Nashner, et al. (1979). 'Organization of rapid responses to postural and locomotor-like perturbations of standing man'. Experimental Brain Research **3**6:463–476.

L. M. Nashner & G. McColluma (1985). 'The organization of human postural movements: A formal basis and experimental synthesis'. Behavioral and Brain Sciences **8**:135–150.

E. Neafsey, et al. (1986). 'The organization of the rat motor cortex: a microstimulation mapping study'. Brain Research Reviews **1**:77–96.

M. Neumann, et al. (2009). 'Assessing gait impairment following experimental traumatic brain injury in mice'. Journal of Neuroscience Methods **1**76:34–44.

R. J. Nudo (2007). 'Postinfarct Cortical Plasticity an Behavioral Recovery'. Stroke **3**8:840–845.

P. Patil, et al. (2004). 'Ensemble recordings of human subcortical neurons as a source of motor control signals for a brain-machine interface'. Neurosurgery **5**5:27–35.

K. Pearson, et al. (2005). 'A new electrode configuration for recording electromyographic activity in behaving mice'. Journal of Neuroscience Methods **1**48:36–42.

R. Porter & R. Lemon (1993). Corticospinal function and voluntary movement. Oxford.

W. M. Reichert (2007). Indwelling Neural Implants. CRC Press, 1 edn.

G. Reina, et al. (2001). 'On the relationship between joint angular velocity and motor cortical discharge during reaching'. Journal of Neurophysiology **8**5:2576–2589.

D. A. Rosenbaum (1991). Human Motor Control. Academic Press, Inc.

J. C. Sanchez & J. C. Principe (2007). Brain–Machine Interface Engineering. Morgan & Claypool.

H. C. Scholle, et al. (2005). 'A surface EMG multi-electrode technique for characterizing muscle activation patterns in mice during treadmill locomotion'. Journal of Neuroscience Methods **1**46:174–182.

N. P. Schumann, et al. (2006). 'Treadmill locomotion in normal mice - Step related multi-channel EMG profiles of thigh muscles'. Pathophysiology **1**3:245–255.

L. Sergio & J. Kalaska (1997). 'Systematic changes in directional tuning of motor cortex cell activity with hand location in the workspace during generation of static isometric forces in constant spatial directions'. Journal of Neurophysiology **7**8:1170–1174.

S. C. S. Sherrington (1906). Integrative action of the nervous system. New York: Scribner.

M. Shik, et al. (1966). 'Control of walking and running by means of electric stimulation of the mid-brain'. Biophysics **1**1:756–765.

H. Shimazaki & S. Shinomoto (2007). 'A method for selecting the bin size of a time histogram'. Neural Computation MIT press **1**9:1503–1527.

E. Taub & A. Berman (1968). The neurophysiology of spatially oriented behaviour, chap. Movement and learning in the absence of sensory feedback, pp. 173–192. Homewood, IL: Dorsey.

D. M. Taylor, et al. (2002). 'Direct cortical control of 3D neuroprosthetic devices'. Science **2**96(5574):1829–1832.

N. I. Technology (2012). 'CatWalk XT'. `http://www.noldus.com/animal-behavior-research/products/catwalk`.

A. Thota, et al. (2005). 'Neuromechanical control of locomotion in the rat'. Journal of Neurotrauma **2**2:442–465.

T. Tucker-Davis Technologies Inc (2012). TDT System 3 Manual. Tucker-Davis Technologies Inc,. http://www.tdt.com/.

I. Q. Whishaw (2003). 'Did a change in sensory control of skilled movements stimulate the evolution of the primate frontal cortex?'. Behavioural Brain Research **1**46:31–41.

WHO (2006). Neurological disorders - public health challenges. World Health Organization.

W. Widajewicz, et al. (1994). 'Motor Cortical Activity Voluntary Gait Modifications in the Cat. II. Cells Related to the Hindlimbs'. Journal of Neurophysiology **7**2:2070–2089.

J. Wolpaw, et al. (2002). 'Brain-computer interfaces for communication and control'. Clinical Neurophysiology **1**13:767–791.

J. R. Wolpaw, et al. (2006). 'BCI Meeting 2005-Workshop on Signals and Recording Methods'. IEEE Transactions on Neural Systems and Rehabilitation Engineering **1**4:138–141.

PART

Appendix

Manufacturing and design of intra-cortical electrodes A

The following chapter explains in detail the manufacturing of the IC electrodes used in this project. The electrode consists of a 4x4 micro-wire electrode array developed for implementation in the motor cortex of the rat.

List of material

The following materials were used to create each IC-electrode:

- Two board-to-board sockets, with 2x4 rows, row pitch of 2 mm (Harwin M22-7140442)
- PFA-Coated Tungsten wire (Diameter: 0.1 mm bare, 0.05 mm coated, Catalog number: 795500), 16 wires of 50 mm of length
- Components for making cold-curing resins prosthetics (Heraeus Kulzer Paladur)
- Ground wire(Cooner AS631, diameter 0.26 mm)
- Soldering iron
- Super-glue

Equipment used

The following equipment were used to producing the IC-electrode:

- Microscope
- Lighter
- Tape
- Wire wrapping tool
- Solder
- 16 crocodile clamps
- Graph paper
- Aluminium foil
- Needle (0.30 mm x 30 mm)
- Micro-scissor
- Branson 200 Ultra Sound Cleaner

Design

An illustration of the design of the electrode is shown in figure A.1.

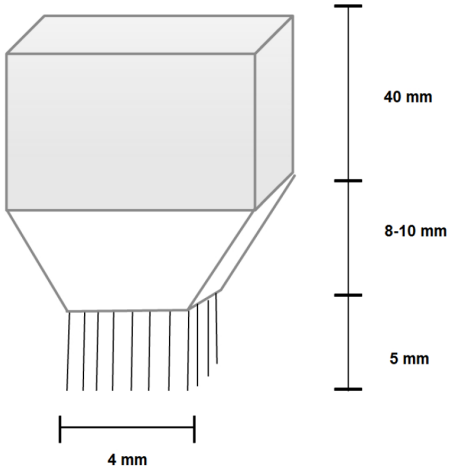

Figure A.1. Design of the 16 array IC electrode.

Procedure

Preparation of the wires

- Use yellow paper as an underlay for better view.
- Cut the Tungsten wire in 16 pieces of 50 mm in length.
- Use the candle to remove the insulation on both ends of the wire. The insulation must be removed for approximately 5-10 mm.
- Clean the ends of the wires with distilled water.

Soldering wires on the socket

- Solder the 16 Tungsten wires onto each of the two socket pins (8 on each socket) using the microscope.
- Check the connection for all wires with a multimeter.
- Check solder joint mechanically by pulling it slightly with a tweezer.
- Glue the two sockets together using super glue and place them in a stand with a crocodile clamp.

Fixation of the wires

- Place the board-to-board socket over an aluminium model in order to shape the electrode, see picture.
- Cover the mould with transparent tape and puncture holes in the foil of the 4x4 grid with a half millimetre between the dots using a needle.
- Pull each wire through the wholes corresponding to their position and fixate each wire with a crocodile clamp on the other end to hold the wire straight and in place.

- After finishing the first eight wires from one socket position a piece of paper as seen in figure A.2 to separate the wires from each socket (better overview)

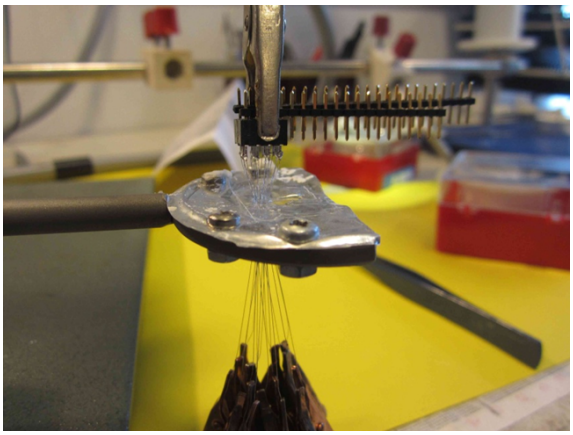

Figure A.2. 16 micro-wires used in the IC electrode array.

Coating wires with prosthetic material

- Plug two additional sockets (dummy connector) on top of the IC electrode.
- Prepare the prosthetics material by mixing the Paladur powder component with the Paladur liquid component in the proper ratio mix until it reaches a suitable thickness.
- Apply the prosthetics material around the soldering and the wires at a distance of approximately one centimeter until the bottom and the wires are completely covered.
- Lift the socket carefully so that there is a space of about 20 to 25 mm between socket and mould and glue two pieces (around 20 mm) of a toothpick on two sides of the electrode in order to stabilize the wires after it is taking out of the holder.
- Apply prosthetic material on the end and remove redundant material with a scalpel and cut of the wires on the other end of the mould.

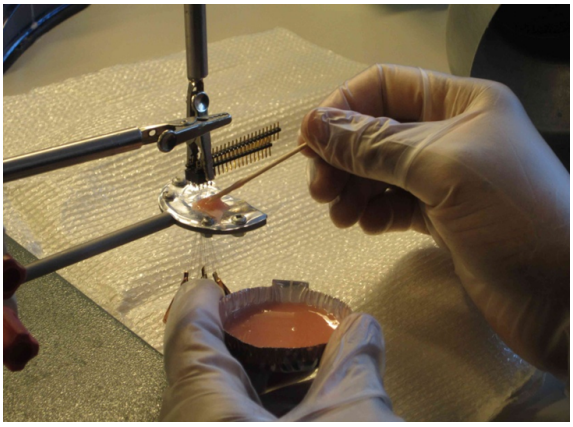

Figure A.3. Dental acrylic is applied on the IC electrode to cover the micro-wires.

Finishing the electrode and Laser cutting

- A laser is used to cut the wires so the wires will have a length of 5 mm from the prosthetics material.
- After the laser cutting the position of the wires can be tangled and to fix this they have to be manually straightened using the microscope.
- If necessary remove redundant dental acrylic at the side of the electrode using a dremel. It is important that the electrode has a cone shape in the end.
- Clean the wires for 20 minutes with ultrasound using the Branson 200 Ultra Sound Cleaner which is filled with distilled water.

Manufacturing and design of intramuscular EMG electrodes

B

List of material

The following materials were used to create iEMG electrode.

- 7-stranded Teflon coated annealed stainless steel wire (A-M systems, Catalog Number 793200) Diameter: Bare: 0.003 in. Coated: 0.14 mm (0.0055 in)
- Ground wire (Cooner AS631, diameter 0.26 mm)
- Board-to-board socket, with 2x4 rows, row pitch of 2 mm (Harwin M22-7140442)
- Components for making cold-curing resins prosthetics (Heraeus Kulzer Paladur)

Equipment used

The following equipment were used to producing the IC-electrode.

- Microscope
- Scalpel
- Ruler
- Scissor
- Laboratory stand with crocodile clamp
- Soldering iron

Design of EMG electrode

The electrode design is based on a study by Pearson et al. [2005]. The electrodes were made using seven-stranded Teflon coated annealed stainless steel wire (A-M systems, Catalog Number 793200). The diameter of the wire was 0.0762 mm bare and 0.1397 mm coated. The electrode design is shown in figure B.1.

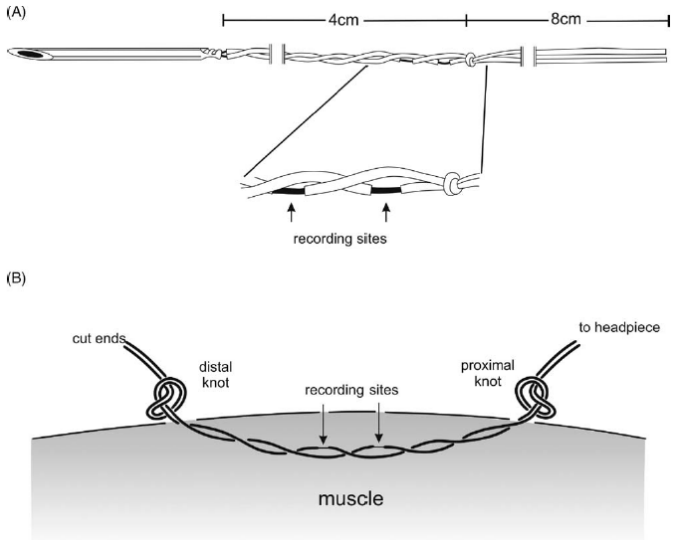

Figure B.1. Design and method of the intramuscular EMG electrode. [Pearson et al. 2005]

Procedure

Preparation of the wires

- Cut two pieces of stainless steel wires with a length of 68 cm.
- Fold wire in the middle so each electrode has the length of 34 cm.
- With both wires make 3 knots with two left-handed overhand knots followed by a right-handed overhand knot after 28 cm (Figure B.2 below).

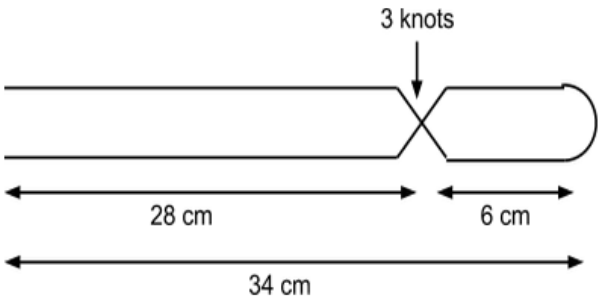

Figure B.2. Schematic drawing of the length of the EMG electrode and positioning of the knot.

De-isolation of wires

- Use scalpel to remove 1 mm of isolation at the loop. Isolation is removed 2 mm after the knot on one side of the loop and on the other side the isolation is removed 5 mm after the knot (Figure B.3 below).
- At the ends of the wires use the scalpel to remove approximately 2 mm of isolation.

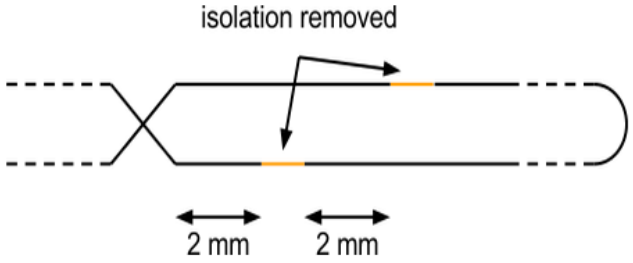

Figure B.3. Schematic drawing of locations where the Teflon insulation was removed on the EMG electrode.

Preparation of ground wires

- Cut two pieces of stainless steel wires with a length of approximately 5 cm and 10 cm.
- Use scalpel to remove approximately 2 mm of isolation at both ends of each wire.

Soldering

- Fixate socket in a vice so that the socket are exposed horizontally to one side of the vice.
- Use a laboratory stand with an horizontally attached crocodile clamp to align one end of an electrode wire to the first pin of the socket in the vice.
- Use fine solder tip and special solder to solder wires to the socket.
- Pin layout - Electrode wire 1 Pin 1 and 2. Electrode wire 2 Pin 3 and 4. GND 1 Pin 5. GND 2 Pin 8.
- Check connections by measuring at the Pins of the female side of the socket and the corresponding wire(s).

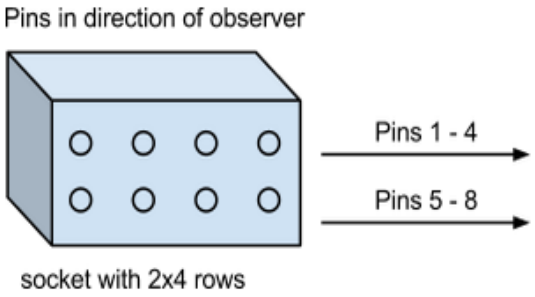

Figure B.4. Schematic drawing of the pin layout on the EMG electrode.

Coating with dental acrylic

- Plug an additional 2x4 rows socket on top of the existing socket (important to avoid dental acrylic coming in the connector holes).
- Let the extra socket sit on top of the connector to avoid dental acrylic getting in the connector when implanting the electrode.

- Apply dental acrylic at the soldering side of the socket and make sure that wires are completely covered with dental acrylic at the not insulated part.
- Pay attention that the socket does not grow in it's dimension (except for the depth), i.e. avoid dental acrylic on the side of the socket.

Place markers

- Round up one corner of the socket at Pin 1 by using a solder iron.
- Fixate a piece of wire Tungsten wire (approximately 4 cm) at the loop of the wire connected to Pin 1 and 2.

Final check

- Try out if an additionally socket can be easily put in and removed again.
- Check connections by measuring at the Pins of the female side of the socket and the corresponding wire(s).
- Place additional socket on top of the iEMG electrode socket.
- Pack finished electrode in green surgery bag, weld shut the bag.

Materials and surgery tools

C

The following materials and surgery tools were used to perform the surgical procedure (see figure C.1.

Figure C.1. Steam sterilized surgery tools and materials used for the surgical procedure.

Surgery materials

- 2 tables with chairs (one for sterile material, one for non-sterile material)
- 2 sterile fields for the table
- Microscope
- Stereotaxic frame
- Masks
- Hats
- Shaver
- Anaesthesia (Hypnorm/Dormicum and sterile water)
- Local anesthetic (Lidocaine)
- Vaseline
- Iodine sponge

- Components for making cold-curing resins prosthetics (Heraeus Kulzer Paladur, Germany)

Sterilized materials

- 3 pairs of gloves for surgeon
- 5 towels
- Gauze
- T-shirt to cover microscope
- Syringe
- Absorbable haemostatic gelatin sponge (Spongostan TM)
- 2 sutures of size 4.0 or 5.0
- 2 scalpels
- Saline
- Surgical glue (LiquiBand Surgical S)

Surgery tools (steam sterilized)

- 3 Aluminium trays
- Cotton sticks
- Rubber bands
- 6 Clamps (curved)
- 6 Rongeurs (for opening the skull)
- Surgical spreader
- 3 forceps
- Drill
- Needle
- Ruler
- Tissue forceps
- Long forceps
- Blunt scissors
- Delicate scissors
- Scissors
- Trocar
- 2 bone screws with ground wires and 2 without wires
- IC electrode (sterilized with gamma emission)
- EMG electrode (sterilized with gamma emission)

Treadmill velocity test D

The velocity of the treadmill was calculated as a function of the input voltage to the treadmill engine running the 1 meter belt of the treadmill. To obtain the velocity of 29 cm/s for the treadmill, the input voltage had to be calculated and changed. In order to assess the velocity-voltage relationship recordings were made of the time the treadmill belt needed to complete three full turns for 10 V, 11 V and 12 V. The results from the test are shown in table D.1 and the setup is shown in D.1.

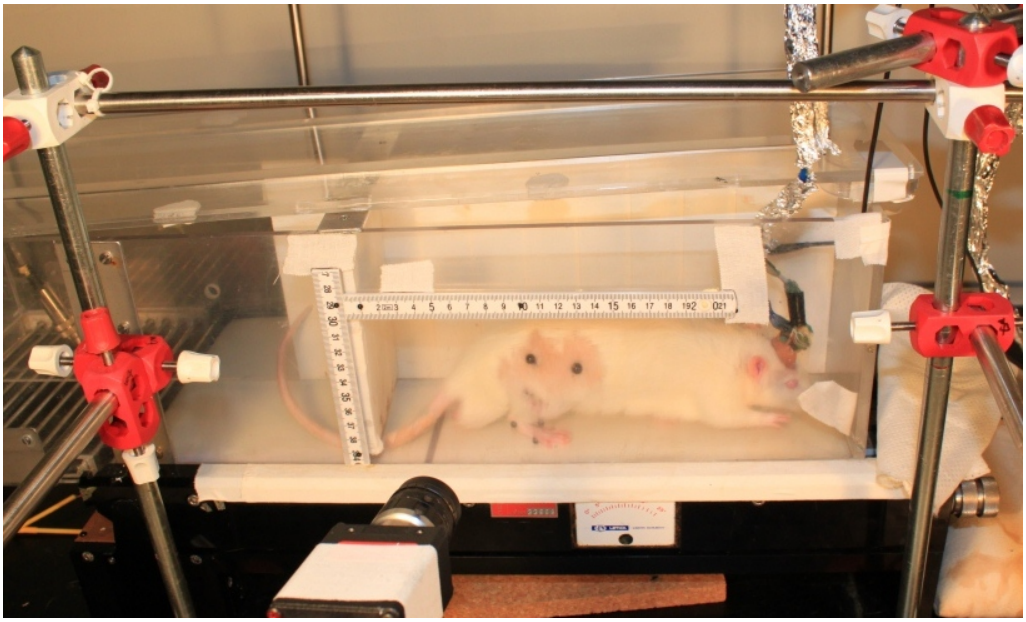

Figure D.1. Setup of the velocity test for the treadmill.

Calculated resistor values in Ω to obtain a velocity of 29 cm/s for the treadmill for the different tasks:

- **Horizontal** = 15 Ω
- **Uphill** = 22 Ω
- **Downhill** = 13 Ω

Table D.1. Results from the treadmill velocity test. Each recording represents the time of three full turns of the treadmill belt in s.

	Recording 1	**Recording 2**	**Recording 3**	**Average**	**Velocity (m/s)**
Horizontal					
12V	8.94	8.98	9.1	3.00	33.31
11 V	9.87	9.9	9.8	3.29	30.44
10 V	11.07	11.12	11.16	3.71	26.99
Uphill					
12V	8.5	8.41	8.74	2.85	35.09
11 V	9.32	9.45	9.36	3.13	31.99
10 V	10.41	10.3	10.27	3.44	29.05
Downhill					
12V	9.41	9.47	9.47	3.15	31.75
11 V	10.45	10.53	10.46	3.49	28.63
10 V	11.74	11.83	11.8	3.93	25.45

Supplemental Results E

Stability of the IC signals and EMG between days

To investigate the stability of the IC signals and the EMG signals over the five recording days the correlation coefficient (r) was calculated. The coefficient was calculated for the BF muscle and the channel related to hindlimb movement for each rat, respectively.

Stability for rat 1

The correlation coefficient for the recorded IC signals for channel 7 between the different recording days for rat 1 are listed in table E.1.

Table E.1. Correlation coefficient (r) for channel 7 over the five recording days for rat 1.

Day	**1**	**2**	**3**	**4**	**5**
1	•	0.395	0.150	0.122	0.458
2	0.395	•	0.779	0.473	0.735
3	0.150	0.779	•	0.514	0.591
4	0.122	0.472	0.514	•	0.307
5	0.458	0.735	0.591	0.307	•

The correlation coefficient for the recorded EMG data for the BF muscle between the different recording days for rat 1 are listed in table E.2.

Table E.2. Correlation coefficient (r) for the EMG data from BF over the five recording days for rat 1.

Day	**1**	**2**	**3**	**4**	**5**
1	•	0.993	0.967	0.928	0.976
2	0.993	•	0.987	0.959	0.963
3	0.967	0.987	•	0.974	0.911
4	0.928	0.959	0.974	•	0.889
5	0.976	0.963	0.911	0.889	•

Stability for rat 3

The correlation coefficient for the recorded IC signals for channel 8 between the different recording days for rat 3 are listed in table E.3.

Table E.3. Correlation coefficient (r) for Channel 8 over the five recording days for rat 3.

Day	1	2	3	4	5
1	•	0.426	0.589	0.042	0.171
2	0.426	•	0.864	0.752	0.791
3	0.589	0.864	•	0.628	0.732
4	0.042	0.752	0.628	•	0.889
5	0.172	0.791	0.733	0.889	•

The correlation coefficient for the recorded EMG data for the BF muscle between the different recording days for rat 3 are listed in table E.4.

Table E.4. Correlation coefficient (r) for the EMG data from BF over the five recording days for rat 3.

Day	1	2	3	4	5
1	•	0.975	0.989	0.879	0.958
2	0.975	•	0.974	0.943	0.980
3	0.989	0.974	•	0.867	0.952
4	0.879	0.944	0.867	•	0.967
5	0.958	0.981	0.952	0.967	•

Comparison between horizontal locomotion and steady recordings

In order to verify that the firing rate in the M1 was higher during locomotion a paired two-sample t-test was performed between horizontal locomotion and steady control recordings from both rats, see table E.5.

Table E.5. Results from the paired two-sample t-tests for the neural firing rate between horizontal locomotion and steady recordings from rat 1 and 3, where n is the total number of gait cycles for the given day.

Day	Rat 1	Rat 3
Day 1	P = 2.69e-06 (n=53)	P = 2.799e-15 (n=48)
Day 2	P = 1.54e-06 (n=54)	P = 1.244e-33 (n=45)
Day 3	P = 7.19e-04 (n=51)	P = 2.349e-43 (n=45)

PSTH plots with confidence limits

On figure E.1 all 16 channels are plotted for one day with confidence limits.

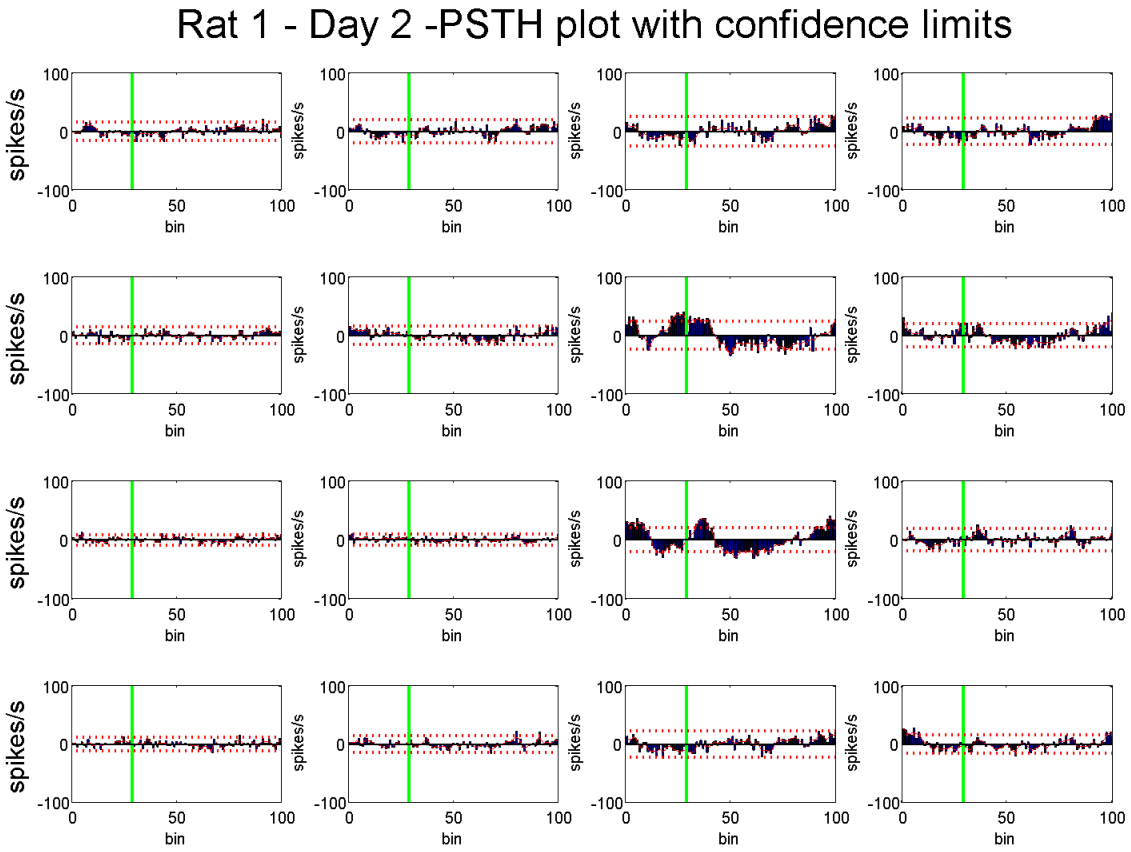

Figure E.1. Results for rat 1 from horizontal locomotion. Shown are the mean firing rate (spikes/s) of all 16 channels. The PSTH are in percentage of gait duration. The blue bins indicate the mean firing for day 2 while the red graph is the smoothed mean (207 gait cycles). The 95% confidence interval is indicated by the two vertical red dashed lines. The horizontal green line indicates the touch down of the foot

On figure E.2 all 16 channels are plotted for one day with confidence limits.

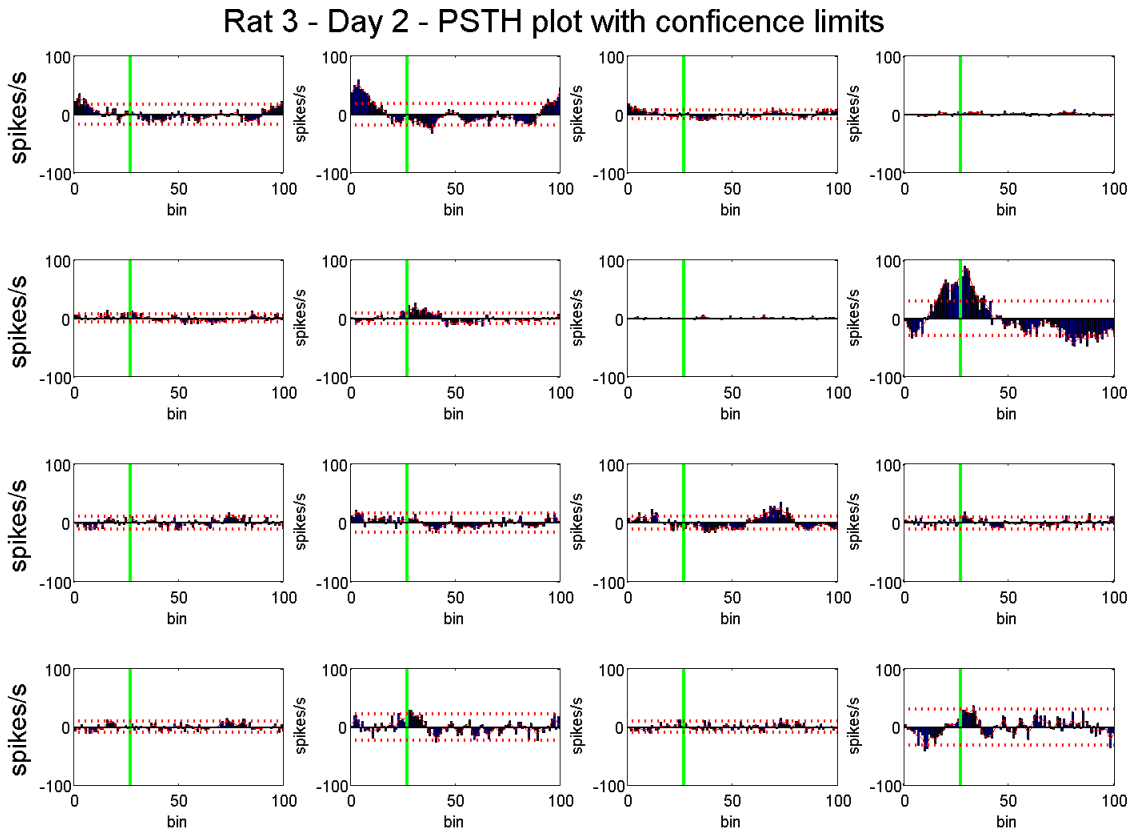

Figure E.2. Results for rat 3 from horizontal locomotion. Shown are the mean firing rate (spikes/s) of all 16 channels. The PSTH are in percentage of gait duration. The blue bins indicate the mean firing for day 3 while the red graph is the smoothed mean (161 gait cycles). The 95% confidence interval is indicated by the two vertical red dashed lines. The horizontal green line indicates the touch down of the foot.